Gizem ARGIN — CALCINED CLAYS AS SUPPLEMENTARY CEMENTING MATERIALS FOR SUSTAINABLE CONCRETE — AGU 2019

CALCINED CLAYS AS SUPPLEMENTARY CEMENTING MATERIALS FOR SUSTAINABLE CONCRETE

A THESIS
SUBMITTED TO THE DEPARTMENT OF SUSTAINABLE URBAN INFRASTRUCTURE ENGINEERING
AND THE GRADUATE SCHOOL OF ENGINEERING AND SCIENCE
OF ABDULLAH GUL UNIVERSITY
IN PARTIAL FULFILLMENT OF THE REQUIREMENTS
FOR THE DEGREE OF
M.Sc.

By
Gizem ARGIN
December 2019

CALCINED CLAYS AS SUPPLEMENTARY CEMENTING MATERIALS FOR SUSTAINABLE CONCRETE

A THESIS
SUBMITTED TO THE DEPARTMENT OF SUSTAINABLE URBAN INFRASTRUCTURE ENGINEERING
AND THE GRADUATE SCHOOL OF ENGINEERING AND SCIENCE OF ABDULLAH GUL UNIVERSITY
IN PARTIAL FULFILLMENT OF THE REQUIREMENTS
FOR THE DEGREE OF
M.Sc.

By
Gizem ARGIN
December 2019

SCIENTIFIC ETHICS COMPLIANCE

I hereby declare that all information in this document has been obtained in accordance with academic rules and ethical conduct. I also declare that, as required by these rules and conduct, I have fully cited and referenced all materials and results that are not original to this work.

Name-Surname: Gizem ARGIN

Signature :

REGULATORY COMPLIANCE

M.Sc. thesis titled Calcined Clays as Supplementary Cementing Materials for Sustainable Concrete has been prepared in accordance with the Thesis Writing Guidelines of the Abdullah Gül University, Graduate School of Engineering & Science.

Prepared By

Gizem ARGIN

Advisor

Assoc. Prof. Burak UZAL

Head of the Sustainable Urban Infrastructure Engineering Program

Assoc. Prof. Burak UZAL

ACCEPTANCE AND APPROVAL

M.Sc. thesis titled Calcined Clays as Supplementary Cementing Materials for Sustainable Concrete and prepared by Gizem ARGIN has been accepted by the jury in the Sustainable Urban Infrastructure Engineering Graduate Program at Abdullah Gül University, Graduate School of Engineering & Science.

24 /12 / 2019

JURY:

Advisor: Assoc. Prof. Burak UZAL

Member: Prof. Cengiz Duran ATİŞ

Member: Prof. Mustafa ŞAHMARAN

APPROVAL:

The acceptance of this M.Sc. thesis has been approved by the decision of the Abdullah Gül University, Graduate School of Engineering & Science, Executive Board dated ….. /….. / …….. and numbered ……..……. .

…….. /…….. / ……..

(Date)

Graduate School Dean

Prof. İrfan ALAN

ABSTRACT

CALCINED CLAYS AS SUPPLEMENTARY CEMENTING MATERIALS FOR SUSTAINABLE CONCRETE

Gizem ARGIN

MSc. in Sustainable Urban Infrastructure Engineering Department

Supervisor: Assoc. Prof. Burak UZAL

December 2019

The Portland cement, which is used as a binder material in concrete, has an important share for CO_2 emission worldwide. For this purpose, supplementary cementing materials are used to be substituted with Portland cement in specific amounts. The usage of industrial by-products such as fly ash, silica fume, and slag as supplementary cementing materials seems advantageous. However, potential in availability of good quality by-products in a local scale have led to the search for feasible alternatives to these materials.

The aim of this study is to evaluate the clay samples obtained from two different deposits in Turkey after calcination in terms of their use as supplementary cementing material. Chemical, mineralogical and thermal characterization of clay samples were made before and after calcination at various temperatures. Pozzolanic activity and reaction kinetics of the clay samples were evaluated with and without limestone addition by thermal analysis and isothermal calorimetry, respectively. Water requirement and strength activity index of calcined clays selected depending on their pozzolanic activity were also determined.

The pozzolanic activity of clay containing a relatively higher amount of kaolinite mineral was determined to be higher. Clays calcined at 700 ºC showed the highest pozzolanic and strength activity whereas a calcination temperature of 1100 ºC results in a relatively lower activity. The limestone addition improved the pozzolanic activity, and the heat evolution during hydration. As BET surface area increased, the water requirement for calcined clay also increased.

Keywords: calcined clay, , isothermal calorimetry, supplementary cementing materials, Portland cement, pozzolanic activity, sustainable concrete

ÖZET

SÜRDÜRÜLEBİLİR BETON İÇİN İLAVE BAĞLAYICI MALZEME OLARAK KALSİNE KİLLER

Gizem ARGIN

Sürdürülebilir Kentsel Altyapı Mühendisliği Bölümü Yüksek Lisans

Tez Yöneticisi: Doç. Dr. Burak UZAL

Aralık 2019

Betonda bağlayıcı olarak kullanılan Portland çimentosu dünya genelinde CO_2 salınımında önemli bir paya sahiptir. Bunun için çimento ile belli miktarlarda ikame edilecek ilave bağlayıcı malzemeler kullanılmaktadır. Uçucu kül, silis dumanı ve cüruf gibi endüstriyel yan ürünlerin ilave bağlayıcı malzeme olarak kullanımı avantajlı gözükmektedir. Ancak, yerel ölçekte iyi kalitede yan ürünlerin bulunmaması, bu malzemelerin alternatifini bulmak konusunda arayışa sebep olmuştur.

Bu çalışmanın amacı, Türkiye'de iki farklı rezervden temin edilen kil örneklerini kalsinasyon sonrası ilave bağlayıcı malzeme olarak kullanımları açısından değerlendirmektir. Kil örneklerinin kimyasal, mineralojik ve termal karakterizasyonları çeşitli sıcaklıklarda kalsinasyon öncesi ve sonrasında gerçekleştirilmiştir. Kil numunelerinin puzolanik aktivitesi ve reaksiyon kinetiği, kireçtaşı tozu ilavesi ve kireçtaşı ilavesi olmadan, sırasıyla termal analiz ve izotermal kalorimetre ile değerlendirilmiştir. Ayrıca puzolanik aktivitelerine bağlı olarak seçilen kalsine killerin su ihtiyacı ve dayanım aktivite indeksi de belirlenmiştir.

Görece daha yüksek miktarda kaolinit minerali içeren kilin puzolanik aktivitesinin daha yüksek olduğu tespit edilmiştir. 700 ºC'de kalsine edilen killer en yüksek puzolanik ve dayanım aktivitesini gösterirken 1100 ºC gibi bir kalsinasyon sıcaklığı nispeten daha düşük bir aktivite ile sonuçlanmıştır. Kireçtaşı ilavesi, puzolanik aktiviteyi ve hidratasyon sırasında ısı çıkarımını iyileştirmiştir. BET yüzey alanı arttıkça kalsine killerin su ihtiyacı da artmıştır.

Anahtar kelimeler: kalsine kil, izotermal kalorimetre, ilave bağlayıcı malzemeler, Portland çimentosu, puzolanik aktivite, sürdürülebilir beton

Acknowledgements

Firstly, I would like to thank my research advisor Associate Professor Burak UZAL. His office was always open whenever I had a problem or needed advice about my research. Especially, I am so grateful for his endless support and wise advice on my career plans.

I would like to express my gratitude to the Niğtaş company for their contributions to my thesis.

I am so grateful to my dear friends Rukiye Nur KAÇMAZ, Çağatay KOÇER and Refika Sultan DOĞAN who always support me and share our wonderful times. I have had one of the most fun and quality times of my life with them in the last two years.

I am particularly grateful to my husband Can ARGIN, who makes invaluable contributions to my life and has the most significant share in every success I have achieved so far.

Finally, I must express my deep gratitude to my dear family for providing me with endless support and continuous encouragement. Nothing would have been possible without them.

Table of Contents

List of Figures

List of Tables

To my lovely sister

Chapter 1

1 Introduction

1.1 General

Destruction of forests, carbonate degradation, and fossil fuel usage are the three primary sources of anthropogenic carbon dioxide emissions. Portland cement is the major source of emissions from carbonate degradation. After World War II, cement production increased rapidly throughout the world. Today, concrete and cement industries are responsible for 8% of total CO_2 emissions in the world [1]. Figure 1.1.1 shows the increase in worldwide production over the years [2].

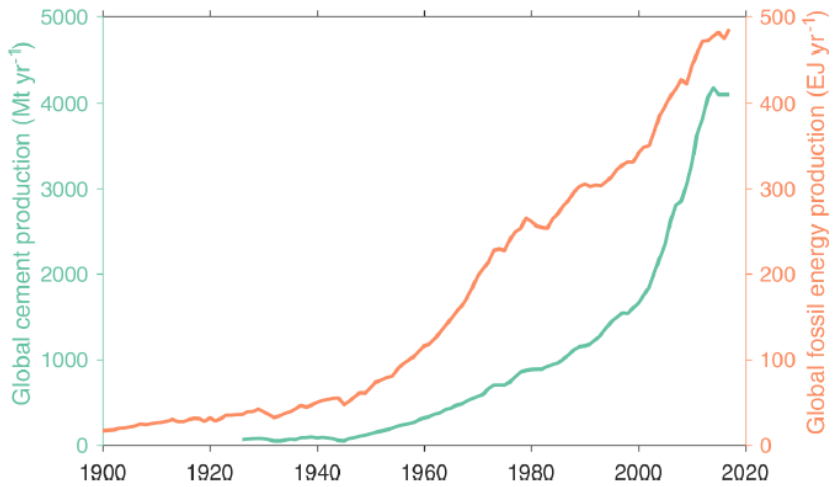

Figure 1.1.1 Global production of cement and energy [2]

An estimated 4 million tons of cement was produced in 2018. As shown in Figure 1.1.2, 2018, Turkey ranks fourth in the world in the production of cement [3]

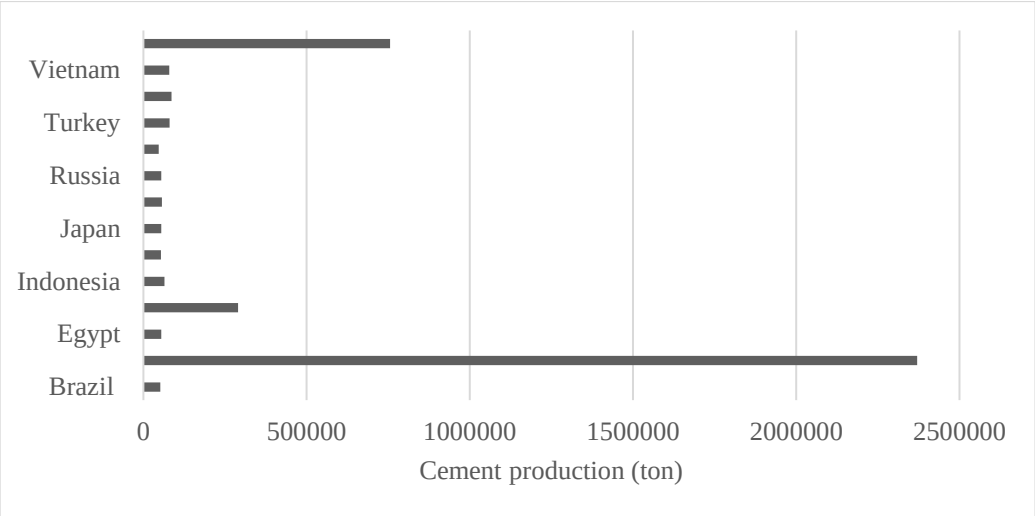

Figure 1.1.2 World cement production [3]

When we take all of these into account, it shows that decreasing the amount of Portland cement production is a way to reduce CO_2 emissions. Due to adverse environmental impacts around the world, there is an increasing interest in supplementary cementing materials [4]. In addition to its environmentally positive effect, generally the use of supplementary cementing materials (SCMs) has a positive impact against sulphate-chloride attack, alkali-aggregate reaction, and it provides low permeability [5].

Although fly ash, blast furnace slag, silica fume are effective alternatives SCMs, their future is in danger because of their availability and low quality [6].

The availability problems of SCMs, which are expected to increase further in the future, leads to the search for alternative materials. Figure 1.1.3 summarizes the availability of SCMs frequently used worldwide. Since clays are one of the most common and abundant minerals in the world and they have a high pozzolanic activity after the calcination, calcined clays have high potential as SCMs [7]. During the calcination of clays, less energy is used compared to Portland cement production. Since, Portland cement production takes place at 1400° C, while the temperature range at which clays undergo dehydroxylation and amorphous phase are formed 600-850° C [8].

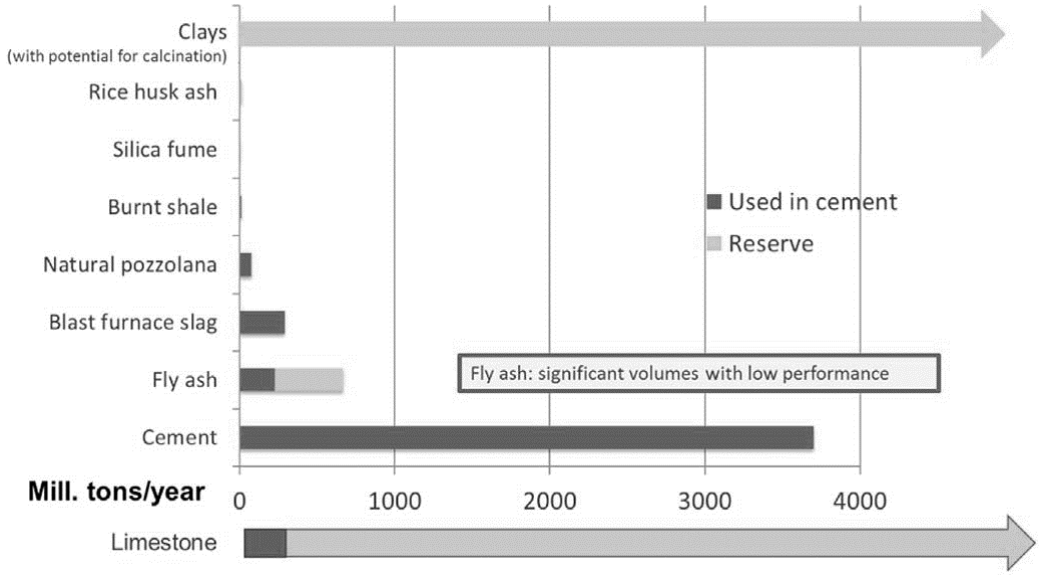

Figure 1.1.3 Availability of SCMs [7]

1.2 Objectives and Scope

The objective of the study is to investigate the potential of clays from two different deposits in Turkey for use as SCMs. One of the main ideas of the study is that clays are calcined at lower temperatures when compared to Portland cement, making it a good alternative to improve the sustainability of concrete. First aim of the study to show that low-quality clays are suitable for use in cementitious systems. Second aim is to observe the effects of different chemical composition, calcination temperatures, and limestone powder addition on their reactivity in cementitious system.

Firstly, the characterization of clay samples obtained from Balıkesir/Düvertepe and Niğde/Hacıabdullah regions were performed. X-ray fluorescence (XRF), thermogravimetric analysis (TGA), and X-ray diffraction (XRD) methods were used to characterize the samples for chemical composition, thermal behaviour and mineralogical characterization, respectively.

Both clay samples were ground for an equal grinding time to obtain fine powders. Next step was to calcine the samples at various temperatures. The calcination temperatures were determined according to the results of the TGA as 400 ºC, 520 ºC, 700 ºC and 1150 ºC. In accordance with XRD patterns of raw and calcined clays, how different temperatures change the mineralogical characterization was observed and compared.

In order to evaluate the pozzolanic activity, lime-calcined clay pastes were prepared, and cured at 50 ºC for the ages of 3, 7, and 28 days, then analysed by TGA. Calcium hydroxide consumption was calculated according to thermal analysis results. Afterward, the same experiment was carried out by adding limestone powder to lime-calcined clay pastes. Pozzolanic activity of both clay samples were evaluated comparatively before and after calcination as well as absence and presence of limestone powder addition. In addition, isothermal calorimetry tests were performed to observe the effect of raw and calcined clays on hydration kinetics of Portland cement. The heat flows of the reference sample (prepared by Portland cement only), pastes containing Portland cement-calcined clay and Portland cement-calcined clay-limestone powder were compared.

Finally, the water requirement and strength activity index (SAI) tests according to ASTM C311 were performed on the calcined clays selected depending on their pozzolanic activity for the cases with and without limestone powder addition.

Chapter 2

2 Literature Review

2.1 Introduction

In this chapter, the literature review related to the use of calcined clays as supplementary cementing materials (SCMs) in cementitious systems is presented. Firstly, the general structure of the Portland cement, the hydration mechanism, and environmental impact are discussed in order to understand the use of SCMs for sustainable concrete better. Subsequently, general information about SCMs is given. In addition, the calcined clays and pozzolanic activity of the calcined clays are explained in detail. Finally, the background and literature review of the calcined clay limestone cement system, an innovative approach for the Portland cement sector, is described.

2.2 Portland Cement

Cement can be defined as a hydraulic construction material which becomes the binder due to the hydration reaction that occurs when mixed with water. Portland Cement, which is the most widely used type in concrete production, is obtained from limestone and clay as the main raw material. As a first step in the production of Portland cement, clay and limestone are mixed in definite proportions and burning in a rotary kiln at 1400° C; the resulting product is a clinker. Afterward, clinker is grinding together with some gypsum (3-5%), and Portland cement is produced. The reason for the addition of gypsum is to adjust the setting time and to prevent flash setting [9].

The Portland cement, which was patented by Joseph Aspdin in 1824, has developed over the years and has taken its present form. The developments occurring since the emergence of Portland cement are summarized in Figure 2.2.1 [10].

1820	✓ Portland cement was found by J. Aspdin
1840	✓ W. Aspdin, son of J. Aspdin, established production facility in Northfleet
1860	✓ J. Grant applied tensile strength testing for cement
1880	✓ Rotary kiln started to be used ASTM (C9) standard was published
1900	✓ Portland Cement is started to be marketed in paper bags
1940	✓ The first electrostatic precipitator was established in Portland cement production
1960	✓ X-ray fluorescence (XRF), a rapid method for chemical analysis, was introduced
1980	✓ Portland cement grinding process was started by high efficiency separators
2000-…	✓ Horizontal Portland cement mill and multi-stage combustion were developed Measures have been taken for CO_2 emissions

Figure 2.2.1 Milestones in Portland cement production

2.2.1 Chemical and Compound Composition of Portland Cement

Raw materials used to provide calcium silicate, the main constituent of Portland cement, must contain appropriate proportions of calcium and silica. Limestone calcium, clays, and shales are raw materials used as silica sources. Clays also contain alumina, iron, and alkalis, which has a positive effect on the formation of calcium silicates at low temperatures. Hence, if the main raw materials do not contain enough Al_2O_3 and Fe_2O_3, iron and bauxite may be added to the mixture. Homogenization of the raw mixture by some processes such as crushing, grinding, and mixing before heat treatment is very important for producing the clinker in the desired composition [11]. The contents of the two raw materials used during clinker production and the four main oxides formed during production are given in Figure 2.2.1.1 [10]. The chemical reactions during the heat treatment in the rotary kiln are summarized below:

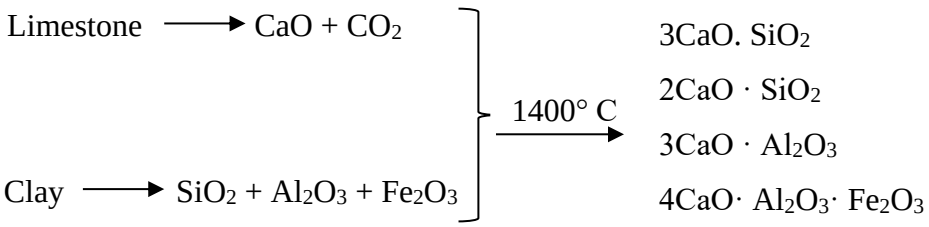

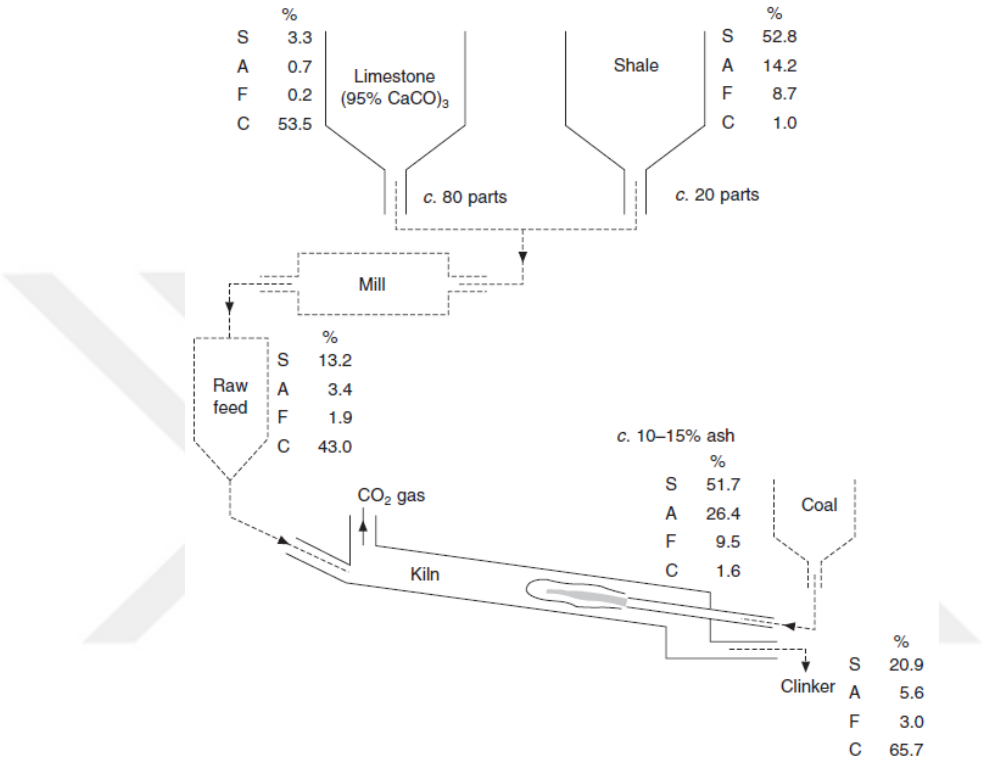

Figure 2.2.1.1 Clinker production analysis (S: SiO_2, A: Al_2O_3, F: Fe_2O_3, C: CaO) [10]

In the Portland cement industry, the compound composition is found by the calculation method developed by the chemist Robert Herman Bogue. The main compounds in the ordinary Portland cement are given in Table 2.2.1.1. The oxide contents of ordinary Portland cement are listed in Table 2.2.1.2 [9].

Table 2.2.1.1 Main compound of ordinary Portland cement [9]

Compound	Abbreviations	Weight, %
$3CaO.\ SiO_2$	C_3S	50
$2CaO \cdot SiO_2$	C_2S	25
$3CaO \cdot Al_2O_3$	C_3A	12
$4CaO \cdot Al_2O_3 \cdot Fe_2O_3$	C_4AF	8

Table 2.2.1.2 Typical chemical composition of ordinary Portland cement [9]

Oxide	Abbreviations	Content, %
SiO_2	S	21.0
Al_2O_3	A	6.1
Fe_2O_3	F	2.6
MgO	M	2.6
CaO	C	64.6
K_2O	K	0.6
Na_2O	N	0.3
SO_3	$\bar{S}$	2.03

2.2.2 Hydration of Portland Cement

Cement has not binding properties unless it meets water. Since cement chemically reacts with water and starts to show hardening properties. This process is generally referred to as hydration of cement [11].

The Portland cement compound C_3S and C_2S react with water to produce C-S-H gel, the main component that provides strength. Table 2.2.2.1 summarizes these hydration mechanisms. Approximately 50% of C_3S reacts within 3 days and 80% reacts at the end of 28 days. C_2S shows no significant reaction for up to 14 days. Also, C_3S reacts much faster than C_2S [10].

Table 2.2.2.1 Calcium silicates hydration [10]

Compound	Reaction Rate	Reaction Products
C_3S	Medium	C-S-H gel
		CH (Calcium Hydroxide)
C_2S	Slow	C-S-H gel
		Small amount of CH (Calcium Hydroxide)

C_3A and C_4AF also react from the moment of contact with water, but their hydration mechanisms are somewhat more complex due to the reaction between them and the gypsum. Table 2.2.2.2 summarizes these hydration mechanisms. If there is no soluble $CaSO_4$, C_3A reacts quickly, and forming C_2AH_8, C_4AH_{19} phases. However, the reaction rate of C_3A is slowed down when gypsum is added. The formation of ettringite as a protective layer on the surface of C_3A crystals slows the reaction rate of C_3A.This reaction can be summarized as follows:

C_3A + dissolved Ca^{+2} +dissolved SO_4^{2-} + water = ettringite

After depletion of the gypsum, C_3A reacts with ettringites to form a hydrated calcium monosulfate. This reaction can be summarized as follows:

$C_3A.\ C\bar{S}.\ 2C_3A.\ 4H = 3(C_3A.\ C\bar{S}.\ 12H)$

If the ettringite is depleted, the remaining C_3A forms the calcium alumina hydrated compounds (C_4AH_{19}). In C_4AF, it performs the same reactions as C_3A at a slower rate [10].

Table 2.2.2.2 Aluminates hydration [10]

Compound	Available $CaSO_4$	Reaction Rate	Reaction Products
C_3A	No	Very fast	C_2AH_8, C_4AH_{19} convert to C_2AH_6
C_3A	Yes	Initially fast	Ettringite reacts to monosulfate
C_4AF	No	Changeable according to Al/Fe ratio	$C_2(A, F)H_8$, $C_4(A, F)H_x$ convert to $C_3(A, F)H_6$
C_4AF	Yes	Changeable but generally slow	Iron substituted ettringite and monosulfate

Portland cement hydration has a rather complicated mechanism. Figure 2.2.2.1 is explained in a simplified way to make this process easier to understand. In Portland cement hydration, gypsum ($CaSO_4$) dissolves rapidly first. This dissolving is particularly crucial to avoid the flash setting properties of the C_3A. Limiting the setting time is a critical task depending on the features of the clinker. For shorter setting time, the free lime level must be high and the cement should be finer [10].

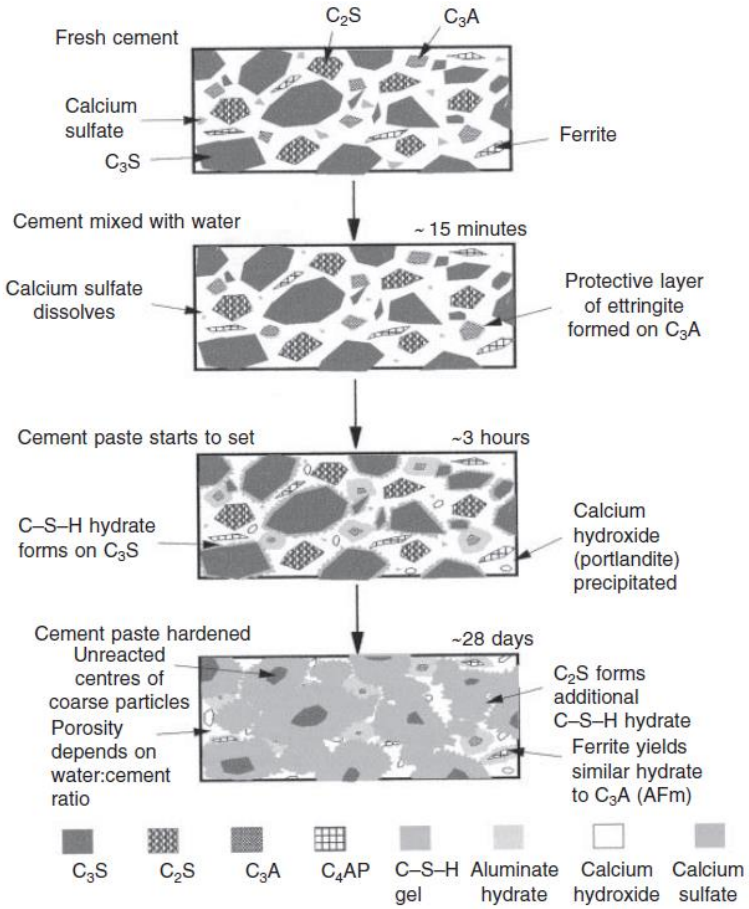

Figure 2.2.2.1 Hydration of Portland cement paste [10]

According to the hydration properties of the main components of Portland cement mentioned in Table 2.2.2.3, it is possible to create suitable cement contents for the intended use [11]. According to ASTM C150, there are ten different types of cement with different properties, such as low hydration temperature, sulphate resistance, early high strength [12].

Table 2.2.2.3 Hydration characteristics of Portland cement major compounds[11]

Property	C_3S	C_2S	C_3A	C_4AF
Heat of Hydration	High	Low	Very high	Medium
Contribution to strength				
Early days	High	Low	Low	Low
Ultimate	High	High	Low	Low

2.2.3 Environmental Impact of Portland Cement

From 74% to 80% of the total CO_2 emission of concrete, are due to Portland cement. In raw material, which emits the highest amount of CO_2 after the Portland cement in concrete production, it is coarse aggregates that emit CO_2 in the range of 13%-20%. The use of different SCMs has been shown to reduce CO_2 emissions by 13%-22% [13].

Worldwide, 20% of CO_2 emissions are from industrial sectors (not including the energy sector). Approximately 52% of this ratio comes from the Portland cement production sector. As shown in Figure 2.2.3.1, Portland cement production in general consists of three main processes: raw material preparation, clinker production in a rotary kiln, and finally grinding process. According to these processes, CO_2 emission in Portland cement production can be divided into two parts: direct and indirect. Direct emission is caused by fossil fuel consumption and limestone calcination, making up 90% of total emissions. The remaining 10% is indirect emission from electricity consumption [14].

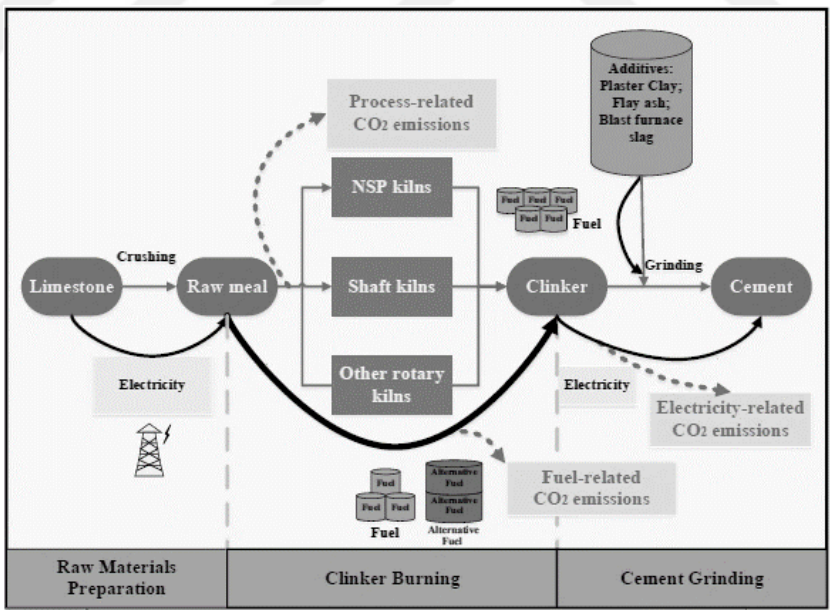

Figure 2.2.3.1 Portland cement manufacturing process [14]

Three different methods can be applied to reduce CO_2 emissions in Portland cement production. The first one is to apply processes such as preheating to increase the energy efficiency of the rotary kiln. And second way is to replace the fuels used with low

carbon fuels. Finally, reducing the clinker ratio using SCMs reduces CO_2 emissions [15].

2.3 Supplementary Cementing Materials

Supplementary cementing materials are used in the concrete industry as cement substitutes worldwide. SCMs can generally be defined as materials that contribute to the properties of concrete when used with Portland cement showing pozzolanic or hydraulic properties. Even though the features of SCMs are different from each other, the properties of reacting with the products formed by Portland cement hydration are common. Granulated blast furnace slag, which is one of the SCMs, exhibits hydraulic properties of its own, but reactions are accelerated when used with cement. Some fly ashes (Class C) show both pozzolanic and hydraulic properties. For using SCMs efficiently, it is necessary to know the behaviour of each type of SCM when used in cementitious systems [16].

Especially Roman and Greece civilization frequently used natural pozzolans, primarily volcanic ash, and built structures beyond time. The Greeks produced binding materials from lime and volcanic ash mixtures on the island of Santorini in 600 B.C [16]. The Pantheon temple, which is still standing today, is one of the most important historical buildings showing the Romans' skill in concrete use [17].

The name pozzolan comes from a source of volcanic ash in the village of Pozzouli near Italy. The most important of the natural pozzolans are trass, which is extracted from the Rhenish Valley in Germany. Since these pozzolans have very superior properties, are called trass in many countries [16].

The pozzolan-lime mixtures were changed to Portland cement-natural pozzolan with the presence of the Portland cement. The first significant project in which slag-lime cement was used was the Paris subway, which was built in 1889. The first major use of natural pozzolans with Portland cement is an aqueduct built-in 1910 in Los Angeles. Slag-Portland cement mortar was used in the Empire State Building, which was built in 1930 and is still one of the most important symbols of New York. As a result of the studies carried out at the University of Berkeley, fly ash was first used in the Hungry Horse Dam in Montana, whose construction began in 1948. Although work on silica fume

started in the mid-1900s, it was not used in a large project until 1971. The first use in the United States was a retrofitting study at the Kinzua Dam. In 1983, silica fume was used in ready-mixed concrete for the first time in Canada. Silica fume was used in Toronto in 1986 to meet the need for high-strength concrete at Scotia plaza [16].

2.3.1 Types and Classification of Supplementary Cementing Materials

SCMs can be classified into two main categories: natural and artificial pozzolans. For natural pozzolans, it is challenging to make a single and precise classification. The mineralogical structure of natural pozzolans is quite different due to their geological formations. One of the classifications for natural pozzolans is structured according to the origin of pozzolans, as shown in figure 2.3.1.1. Another classification is based on the main lime reactive component present in natural pozzolans. These four categories are volcanic tuff, unaltered volcanic glass, calcined clay or shale, and raw or calcined opaline silica [5].

Artificial pozzolans may also be referred to as by-product pozzolans [18]. The most known and used artificial pozzolans are: thermal power plant by-product fly ash, silicon-based industrial plant by-product silica fume, metal industry by-product slag, agricultural by-product rice husk ash [5].

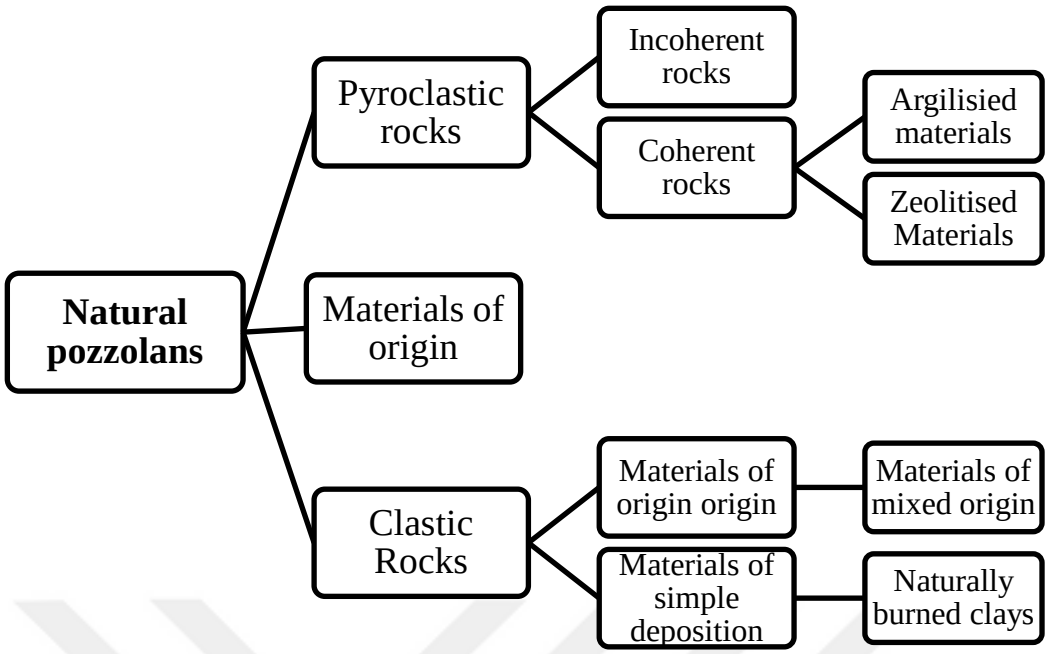

Figure 2.3.1.1 Classification of natural pozzolans [5]

According to ASTM C618, coal fly ash and raw or calcined natural pozzolans are examined in three main categories. The chemical and physical requirements of this classification are given in Table 2.3.1.1 and Table 2.3.1.2. In this classification; class N refers to raw or calcined natural pozzolans, Class F refers to fly ash with pozzolanic properties, and Class C refers to fly ash with both pozzolanic and cementitious properties [19].

Table 2.3.1.1 Chemical requirements [19]

	Class N	**Class F**	**Class C**
$SiO_2+Al_2O_3+Fe_2O_3$ (min, %)	70	50	50
CaO	Report only	18 max	>18
SO_3 (max, %)	4	5	5
Moisture content (max, %)	3	3	3
Loss on ignition (max, %)	10	6	6

Table 2.3.1.2 Physical requirements [19]

	Class N	Class F	Class C
Fineness (Amount retained when wet-sieved on 45 μm (No. 325) sieve, max, %)	34	34	34
Strength activity index			
With Portland cement, at 7 days, min, percent of control	75	75	75
With portland cement, at 28 days, min, percent of control	75	75	75
Water requirement, max, percent of control	115	105	105
Uniformity requirements:			
Density, max variation from average, %	5	5	5
Percent retained on 45-μm, max variation, percentage points from average	5	5	5

2.3.2 Pozzolanic Reaction

The active phases of pozzolan and their reaction with lime define pozzolanic activity. Pozzolanic activity is generally assessed by the determination of lime consumption or the amount of acid-soluble silica, alumina because it is difficult to detect active phases. The amount of amorphous phases is a critical factor for determining pozzolanic reactivity [5].

It is divided into three categories for the evaluation of pozzolanic activity: physical, mechanical, and chemical methods. In the physical method, the progression of lime uptake in Portland cement containing pozzolan can be monitored by the XRD technique. For mechanical method pozzolanic activity evaluation, the strength activity index test specified in ASTM 311 is performed. Finally, the chemical method measures the amount of silica, alumina, and iron, which are soluble as a result of pozzolanic activity, in acids or alkalis [20].

The pozzolanic reaction requires calcium hydroxide, a cement hydration product. The reaction of CH with silica present in pozzolans is given below [16]:

$$xCH + yS + zH \rightarrow CxSyHz$$

The x/y ratio in this reaction, the C / S ratio of C-S-H, is lower than the C/S ratio of hydrated Portland cement without pozzolan. This difference varies according to the age, type, and amount of pozzolans [16].

The pozzolanic activity depends on the amount of lime that pozzolans can react and the rate at which this reaction occurs. Both parameters are directly related to the quantity, and quality of the active phases. Due to the nonhomogeneous of the materials and the complex nature of the hydration process, there is no exact model for pozzolanic activity. However, it is possible to comment on the parameters affecting the amount of combined lime. These parameters can be sorted as follows [18]:

- the nature of active phases
- content of active phases
- SiO_2 content of active phases
- the lime/pozzolan ratio of the mix
- curing time
- specific surface area of pozzolan
- water/solid mix ratio
- temperature

The hydration products of the pozzolan-lime mixtures are very similar to the hydration products of Portland cement. Due to the similarity of their chemical compound, pozzolans generally produce the same aluminates and silicates. However, the amount of hydrated phases varies according to the pozzolan type [18]. The hydration products other than C-S-H gel from the reaction of pozzolans with CH are: strätlingite or gehlenite hydrate (C_2ASH_8) and hydrogarnet (C_3AH_6), calcium aluminate hydrate (C_4AH_{13}), ettringite ($C_3A{\cdot}3C\bar{S}{\cdot}H_{32}$), calcium monosulfoaluminate ($C_3A{\cdot}C\bar{S}{\cdot}H_{12}$), and calcium carboaluminate ($C_3A{\cdot}C\bar{C}{\cdot}H_{12}$) [16].

2.3.3 Calcined Clays and Pozzolanic Reactivity

Clay minerals are heat-treated, their crystal structure is degraded due to the combined loss of water. As a result, it undergoes chemical and structural changes. In this case, alumina and silica may exhibit pozzolanic properties while remaining in an unstable and

amorphous phase. The pozzolanic properties vary depending on the properties of the clay minerals and the calcination conditions. Clays generally exhibit pozzolanic properties when calcined at between 600 to 1000 °C [16].

Calcined clays contain active silica and alumina to react with calcium hydroxide, the Portland cement hydration product. The main reasons for the use of calcined clays in concrete are its availability, increasing durability, and the reduction of CO_2 emissions by replacing Portland cement. Due to calcination temperature and clay mineralogy, an increase in strength was observed. This increase is attributed to the filling effect and the acceleration of Portland cement hydration [21].

The best-known calcined clay is metakaolin with its high quality and pozzolanic activity. However, the removal of impurities in metakaolin production is a very complex and energy-consuming process. This feature increases the price of metakaolin and makes it difficult to use as SCMs. While the use of metakaolin makes more sense in industries such as paper, paint, and ceramics, it is a cost disadvantage for the concrete sector. Therefore, the use of lower quality calcined clays as SCM is a good alternative to reduce the cost of removing impurities [4].

High reactive aggregates were used in a reservoir built in the Amazon basin in the 1960s. However, no alkali-silica reaction was observed due to the PC-calcined clay blend used [21].

The changes in the mineralogical structure of kaolin calcined at different temperatures are given in Figure 2.3.3.1. Alunite and kaolinite peaks are found at 550 °C, while they are almost disappeared at 650 °C. Alunite shows $KAI(SO_4)_2$ at 650 °C and K and Al sulfates at 750 °C. Al_2O_3 released after 770 °C is slowly introduced into the mullite as γ-Al_2O_3 [22].

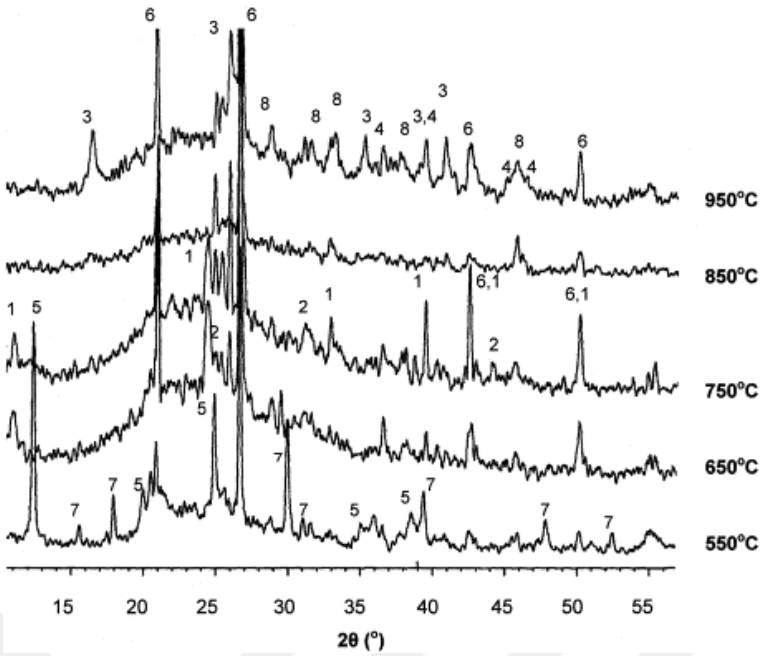

Figure 2.3.3.1 XRD patterns of kaolin treated at different temperatures (1: $KAl(SO_4)_2$, 2: $Al_2(SO_4)_3$, 3: mullite, 4: γ-Al_2O_3, 5: kaolinite, 6: quartz, 7: K-Alunite, 8:K_2SO_4) [22]

Amankwah et al. were used two different calcined clays with alumina contents of 14% and 18% in their studies. With these two samples; three different concrete mixtures were prepared in 25, 30, and 40 N/mm^2 grades. For all three classes, 7-day compressive strengths decreased by an average of 6%. However, 28-day compressive strength was higher than that of the control samples [23].

Taylor-Lange et al. investigated kaolinite-bentonite-containing clay mixtures that were calcined at 650, 830, and 930 °C. The samples contained about 35% weight kaolinite before calcination. While the 90-day strength of the mortars with metakaolin is approximately 50 MPa, the mortars prepared with calcined clays used in this study are 47 MPa. These results showed that kaolinite-bentonite mixed clays have the potential for use as SCM [4].

Garg and Skibsted studied the structural characterization of an interstratified illite/smectite clays. This clay type undergoes dehydroxylation between 600-900 °C, passes into the amorphous phase, and it shows pozzolanic properties. However, at higher temperatures, over 950 °C, it crystallizes to reduce pozzolanic activity [24].

Ng et al. studied a more innovative and different study that was conducted on calcined clays compared to other studies. Portland cement was substituted with calcined clay to improve the properties of aerogel containing mortars used for thermal insulation. As a result, it has been observed that thermal conductivity decreases while maintaining

strength. As the amount of substitution increased above 40 percent, smectite-containing clays were found to be better in reducing thermal conductivity than those containing kaolinite [25].

Suraneni and Weiss used isothermal calorimetry and thermal analysis methods to determine the pozzolanicity of different SCMs such as fly ash, calcined clay, ground granulated blast furnace slag, silica fume, and limestone. As shown in Figure 2.3.3.2, the amount of CH consumption determined by thermogravimetric analysis was calculated. Figure 2.3.3.3 shows the cumulative heat release of different SCMs. Calcined clay and silica fume are shown up to 180-200 h. Because after these hours the calorimetric signal was almost at the same level as the baseline. Calcined clay showed the largest heat release and limestone showed the smallest heat release. While quartz was expected to be inert, some of it dissolved due to the temperature (50 °C) of the test, and the solution (0.5 M KOH) used. Calcined clay and silica fume complete 90% of the heat release in the first 48 hours in terms of reaction kinetics and shows a rapid reaction. The four different fly ash (F1, F2, F3, F4) and slag (S1, S2, S3, S4) tested in this study show similar heat release. The difference between the two calcined clays (CC1 and CC2) is thought to be due to the difference in mean particle size and alumina content. In silica fume, SF2 (undensified) showed more heat release than SF1 (densified). This result showed that the procedure used to disperse densified silica fume was unsuitable (Figure 2.3.3.4). [26].

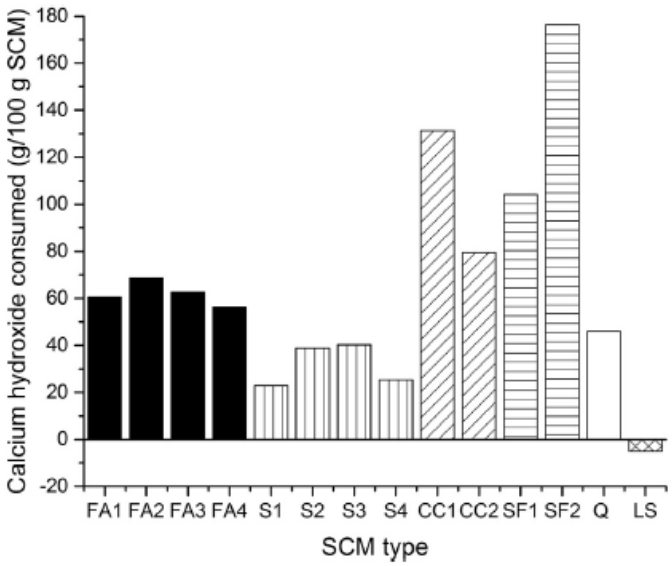

Figure 2.3.3.2 CH consumption of different SCMs [26]

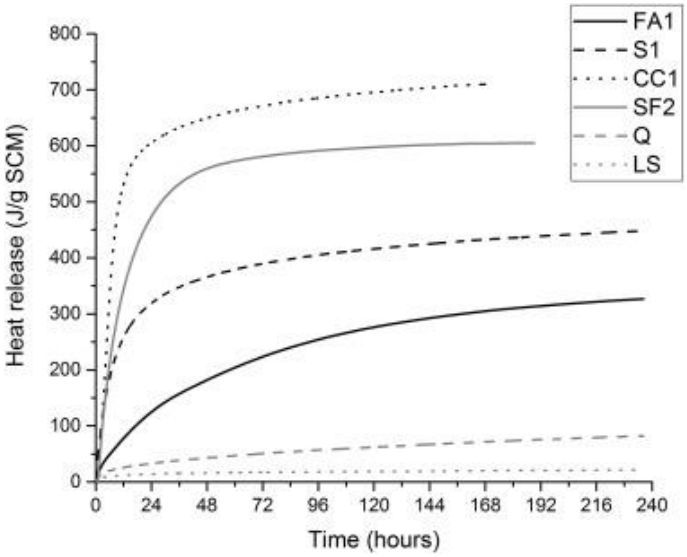

Figure 2.3.3.3 Heat release for different SCMs addition to that of quartz and limestone [26]

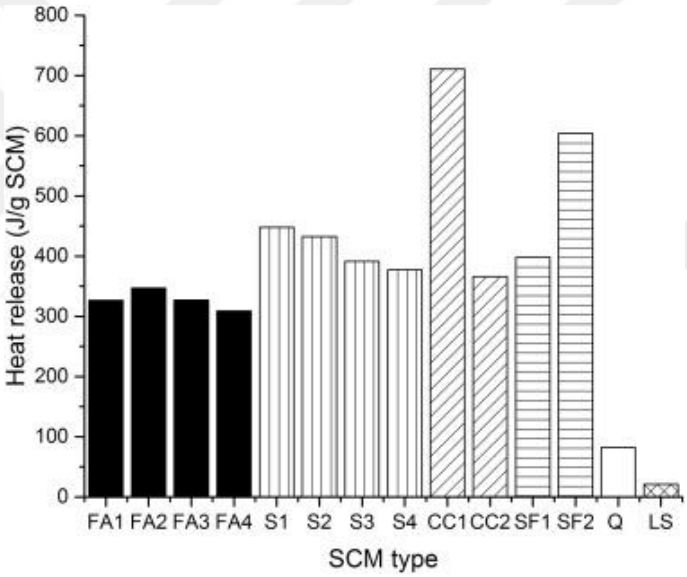

Figure 2.3.3.4 Heat release at 240 h [26]

Msinjili et al. compared two illitic clays, two low-grade kaolinitic clays with respect to strength development, CH consumption, hydrated phase formation and heat release. As a result of this study, it is understood that for complete dehydroxylation of illitic clays, higher temperature is required than kaolinitic clays. The particles of illitic clays with high iron content are sintered at high calcination temperatures. This sintering reduces surface area and pozzolanic activity. Nevertheless, illitic clays with low iron content may be an alternative as SCM when calcined at the optimum calcination temperature [27].

2.3.4 Clay Minerals

Clays and clay minerals, origin belong to the group of phyllosilicate, which comes from the Greek phyllon: leaf and Latin silic: flint. The classification of these silicates is shown in Figure 2.3.4.1 [28].

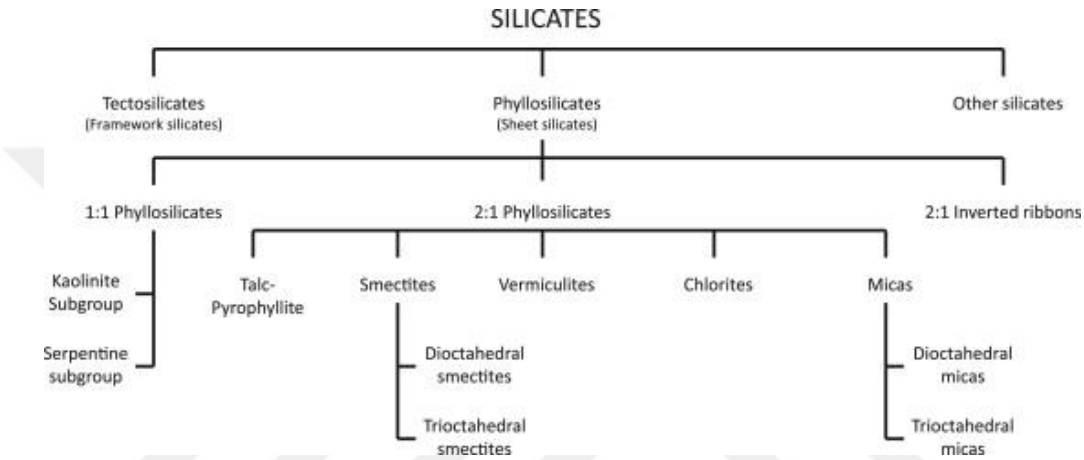

Figure 2.3.4.1 Classification of silicates with the main subgroups of clays [28]

Calcination of kaolinitic clays at temperatures ranging from 500 to 800 °C results in metakaolin with high pozzolanic activity. In clinker production, CO_2 is released as a result of limestone decarbonation, but water is released instead of CO_2 during dehydroxylation of kaolinitic clays [29]. Kaolinitic calcined clays are suitable for use in concrete with their advantages such as increasing compressive and flexural strength, reduced permeability and potential for efflorescence, increasing durability and resistance to chemical attack [30].

Raw kaolinite-containing clay sample is calcined, the following reactions take place, respectively [31]:

$$H_2O(l, \text{bound}) \xrightarrow{100^\circ C} H_2O(g)$$

$$Al_2O_3.2SiO_2.2H_2O(\text{kaolinite}) \xrightarrow{450-700^\circ C} Al_2O_3.2SiO_2(\text{metakaolinite}) + 2H_2O(g)$$

$$2(Al_2O_3.2SiO)_2 \xrightarrow{925-1050^\circ C} 2Al_2O_3.3SiO_2(\text{spinel}) + SiO_2(\text{silica, amorphous})$$

$$3(2Al_2O_3.3SiO_2) \xrightarrow{\geq 1050^{\circ}C} 2(3Al_2O_3.2SiO_2)(\text{mullite}) + 5SiO_2(\text{silica, amorphous})$$

$$SiO_2(\text{silica, amorphous}) \xrightarrow{\geq 1200^{\circ}C} SiO_2(\text{cristobalite})$$

The structures of kaolinite, illite and montmorllinite clay minerals are presented in Figure 2.3.4.2. Kaolinite consists of silica and alumina plates, and these plates are connected very strongly, because kaolin clay is very stable. Illite has layers made from two silica plates and one alumina plate. However, illite contains potassium ions between each layer; this characteristic makes the structure of the clay stronger than montmorillonite. Montmorillonite has layers made from two silica plates and one alumina plate. Because there is a very weak bond between the layers, large quantities of water can easily enter the structure.This event causes the swelling of such clay. In the DTG curves of Figure 2.3.4.3, evaporation of the water absorbed between 30-200 °C is observed. In this temperature range, more water is released montmorillonite, due to the water between the layers. Removal of OH groups in clay minerals occurs between 400-800 °C. The size of the peaks depends on the amount of OH groups present in the structure of the minerals. The peak of kaolinite mineral is higher because it contains more OH groups than other minerals. The shape and range of the peaks vary depending on the particle size distribution, and crystallinity. In addition, the DTG curves of calcined clays show how effective the calcination process is for dehydroxylation. It is understood that the dehydroxylation of kaolinite was completed at 600 °C, while illite did not complete dehydroxylation at 600 °C. It was observed that the peak size did not change after the calcination of montmorillonite at 600 °C. This shows that dehydroxylation occurs between 600-800 °C [32].

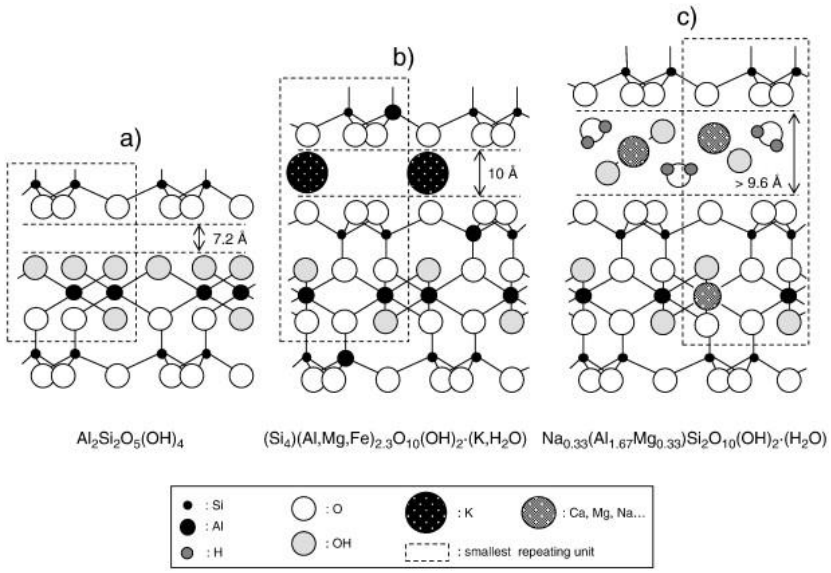

Figure 2.3.4.2 Structures of kaolinite (a), illite (b) and montmorillonite (c) [32]

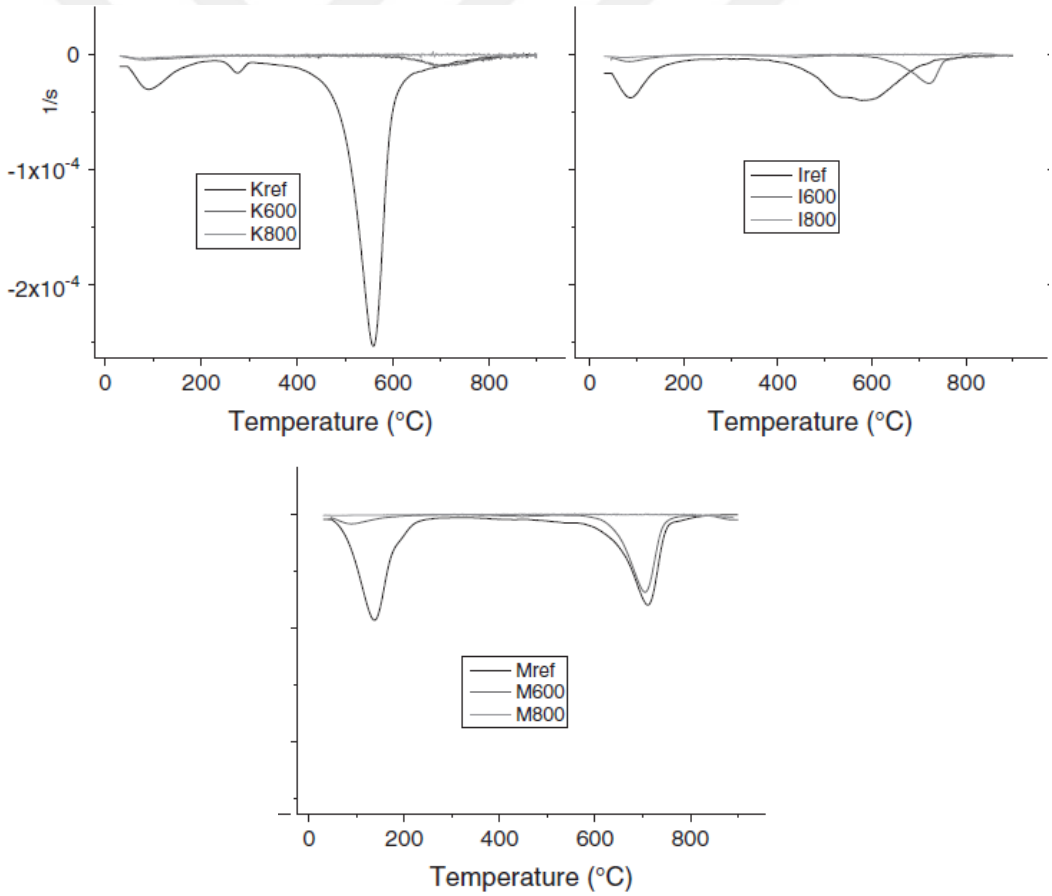

Figure 2.3.4.3 DTG curves of raw and calcined clay minerals [32]

25, 50, 75% kaolinitic clay was replaced with illitic clay and thermal analysis were performed. As shown in Figure 2.3.4.4, the loss of water increased as the amount of

kaolinite increased. The reason for this is that the kaolinite mineral contains more water than illite [33] .

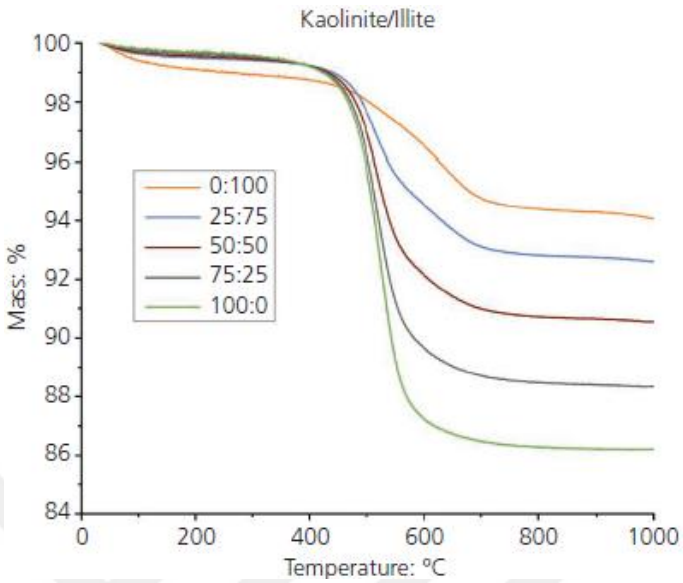

Figure 2.3.4.4 TGA curves of the mixes of kaolinitic and illitic clay [33]

Frias and Cabrera prepared pastes containing metakaolin and worked to establish a link between pore size distribution and degree of hydration. Cement was substituted with 0, 10, 15, 20, and 25% MK in the preparation of the pastes. The water/binder ratio was selected as 0.55. The development of the amount of calcium hydroxide over 360 days is shown in Figure 2.3.4.5. It was observed that the amount of CH increased until 3-7 days and then started to decrease according to MK content. The increase in CH amount was due to hydration of Portland cement, while the decrease was due to the pozzolanic reaction of MK. Correlations for total, capillary, and gel porosity were found to correlate the porosity and degree of hydration. When these results were compared, the best correlation coefficient was found in gel porosity [34].

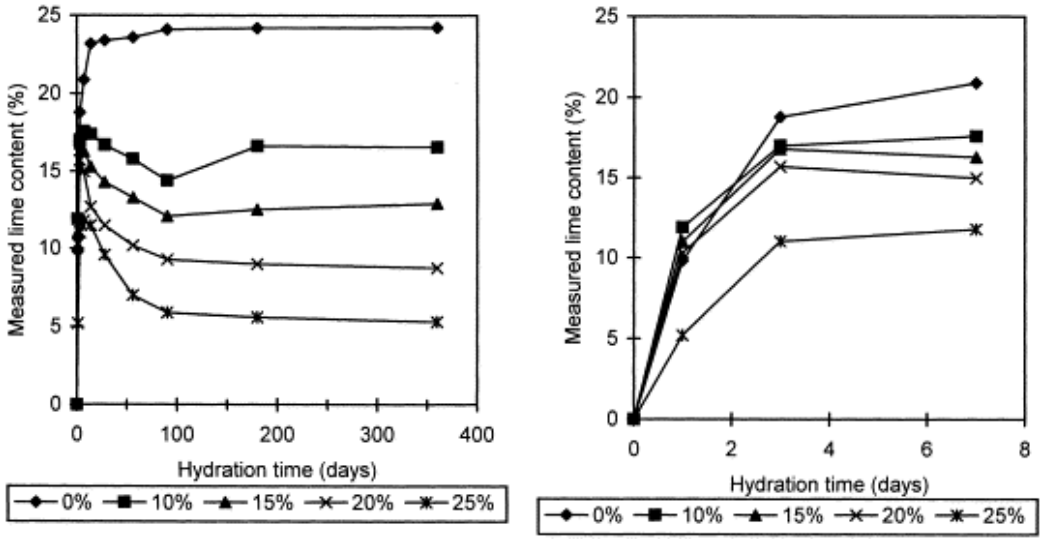

Figure 2.3.4.5 CH evolution with hydration time [34]

Tironi et al. studied on five different clay samples with kaolinite contents of 94, 76, 65, 48, and 16%, respectively. The pozzolanic activities and structural changes after calcination of the calcined clays at 700 °C were observed. 700 °C was found to be a suitable temperature for clays with a kaolinite content of over 45%. Clays with medium and high kaolinite content show a very good difference in specific surface area and pore size distribution after calcination. The compressive strength of blended cement, which was substituted by 30% with calcined clays with medium and high kaolinite content, was tested. As a result, it was found that this mortar was equal to or more than the 28-day compressive strength of the mortar made with Portland cement only [35].

Danner et al. investigated the use of two different clays containing kaolinite (Clay A) and calcareous montmorillonite (Clay B) as SCM in concrete. 20% of the cement was replaced with these calcined clays, and the compressive strength of the mortars increased by 10% for 28 days. Also, as shown in Figure 2.3.4.6, the effect of calcination at different temperatures on compressive strength was observed. In Clay B, glassy phases were observed as a result of coccoliths ($CaCO_3$) and montmorillonite reaction [36].

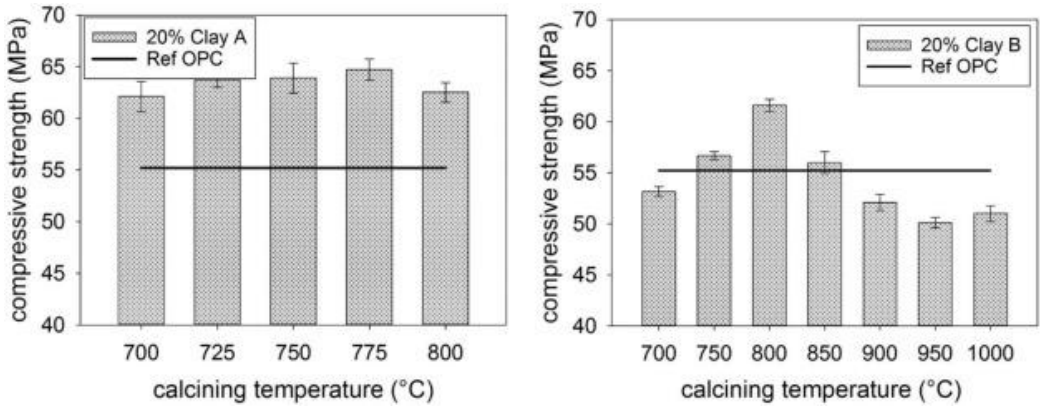

Figure 2.3.4.6 28-day compressive strength of mortars [36]

2.4 Limestone Calcined Clay Cements

Calcined clays are often used as supplementary cementing materials in concrete with the advantages it offers. In limestone calcined clay cement, the biggest innovation is the addition of limestone to the binder system. In the use of calcined clay alone, the rate of substitution is limited to 30%, especially due to the decrease in strength at an early age. When calcined clay and limestone are used together, the substitution rate increases up to 50%. In this way, the decrease in cement ratio makes a positive contribution to both environmental impact and cost [7, 37].

Antoni et al. investigated the combination of metakaolin and limestone as cement substitutes. It was observed that the addition of more than 5% limestone powder reacted with cement and had a positive effect. The limestone reaction produces calcium monocarboaluminate, and hemicarboaluminate and prevents the formation of monosulfoaluminate, which forms more ettringite. 2: 1 metakaolin and limestone were used in all blended samples. As shown in Figure 2.4.1, the PC substitution of the combination of metakaolin and limestone gave excellent results, especially at an early age. In all substitutions up to 45%, the 7 and 28-day compressive strength was higher than the reference sample prepared with PC. Even the 60% substitution shows 93% of the performance of the PC sample in 28 days. The evolution of CH for all blended and reference samples is given in Figure 2.4.2, normalized by the amount of PC in the paste. CH consumption was calculated by using mass balance calculations on TGA results. Limestone blend (L15) and quartz references (Ref15, Ref30, Ref45, Ref60) showed no

pozzolanic activity. 30% metakaolin (MK30) and all other blended samples showed significant CH consumption even as early as 1 day [37].

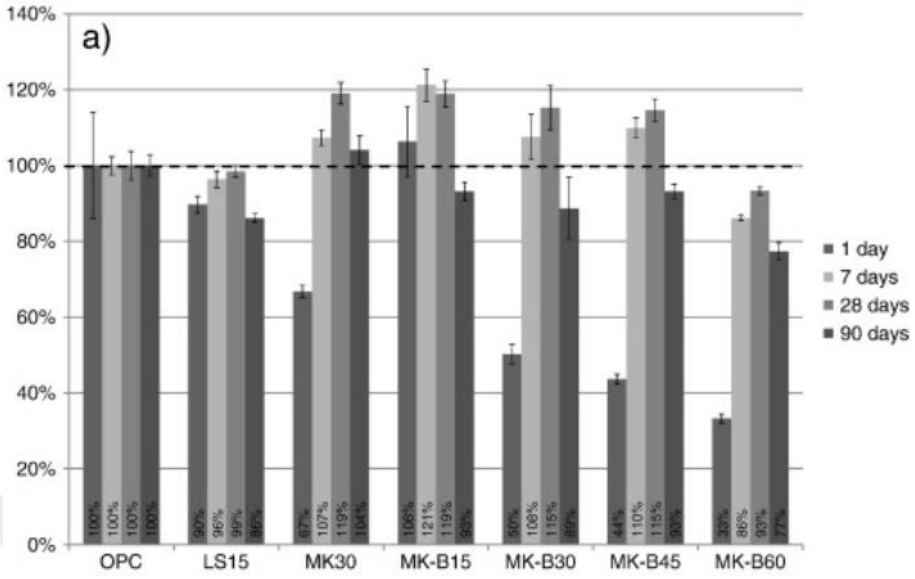

Figure 2.4.1 Compressive strength of blends normalized to the strength of pure PC [37]

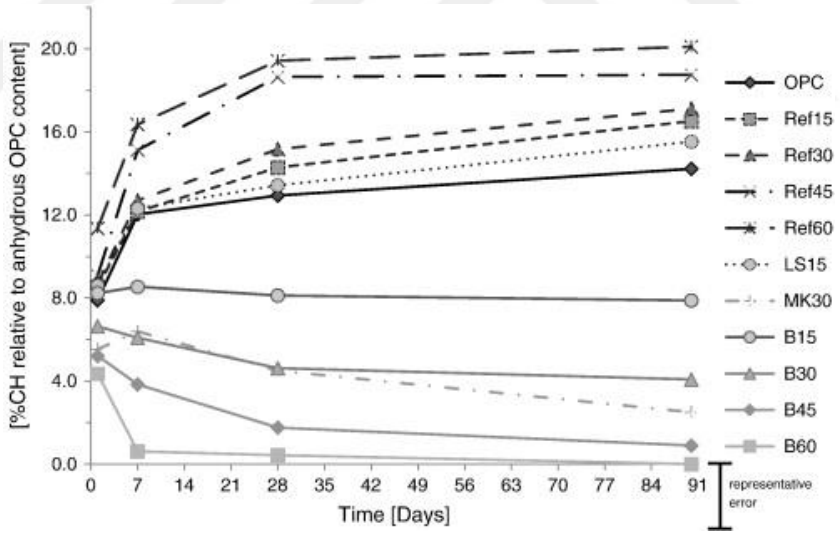

Figure 2.4.2 Evolution of the CH content [37]

Avet and Scrivener investigated how kaolinite content effects hydration in LC_3 systems. Accordingly, they used three different clays containing 0, 50, 90% kaolinite in 50% clinker (LC_3-50) mixture. The heat release that occurs at approximately 40 h is shown in Figure 2.4.3. Superplasticizer was added to the LC_3 systems so that the paste prepared by PC was close to the workability. Due to this additive, the dormant period starts later for LC_3-50 systems. As the amount of kaolinite increases, so does the need for

superplasticizer. In LC_3-50 systems, the silicate peak shows a higher slope and density. This shows that the hydration of C_3S developed for these systems by the filling effect of calcined clay and limestone. The density of the aluminate peak increases with the calcined kaolinite content. This increase in heat can be explained by the reaction of CH and kaolin, in addition to the filler effect [38].

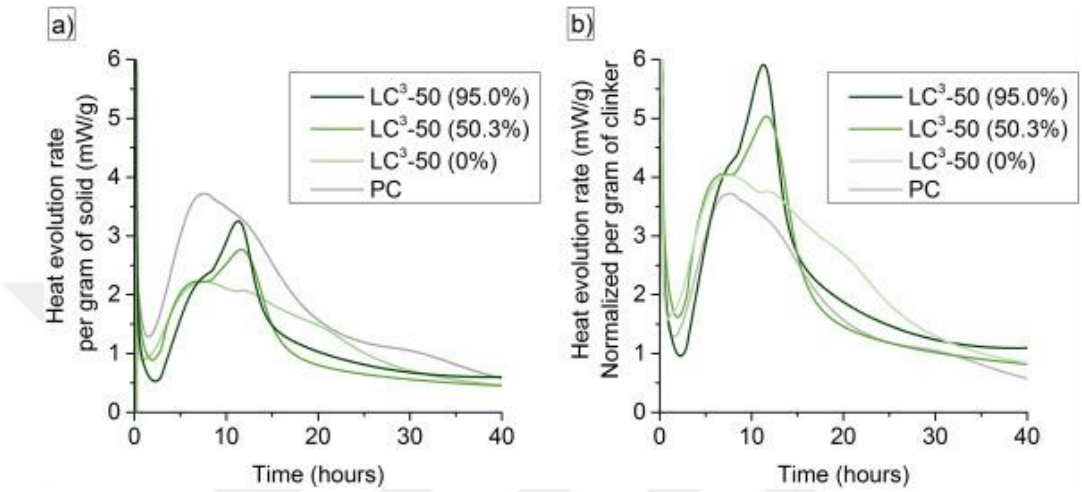

Figure 2.4.3 Heat release per gram of solid (a) and normalized per gram of clinker (b) [38]

Scrivener et al. investigated the main factors and properties affecting the limestone calcined clay cement system. One of the most important factors is the selection of suitable clay. Clays containing a minimum of 40% kaolinite give very close values to the 7-day strength of samples using Portland cement. Clays containing more than 60% kaolinite were found to have no additional advantage. Clays containing 40-50% kaolinite are better in terms of workability and improve chloride resistance. The 7 and 28-day hydration phases of PC and LC_3-50 are shown in Figure 2.4.4. In general, there is not large difference in phases. A higher amount of C-A-S-H phase was observed as the clinker content of Portland cement was higher [33].

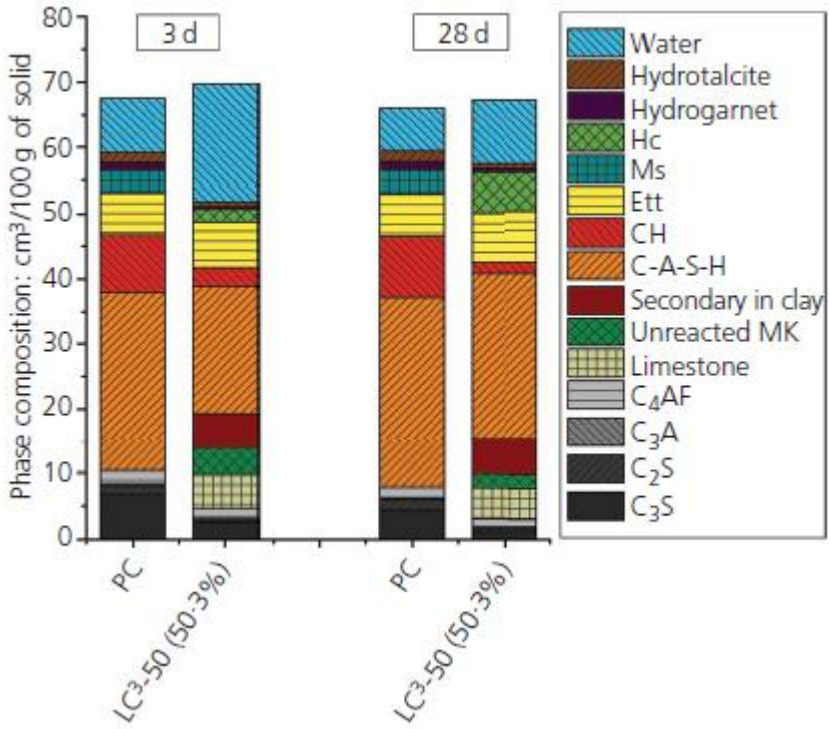

Figure 2.4.4 Hydration phases of PC and LC_3-50 (50.3% refer kaolinite content) [33]

Chapter 3

3 Experimental Study

The objective of the study was taken from the two different locations of Turkey clay samples were to observe the effect when used as SCMs for cementitious systems. The pozzolanic activity of two different samples calcined at different temperatures was determined. The effects of different temperatures and the addition of limestone powder on pozzolanic activity were investigated. For these objectives, the experimental study is planned as follows:

- Grinding of materials and making them ready for calcination
- XRD analysis to observe mineralogical changes
- Determination of calcium hydroxide consumption by thermal analysis in lime-calcined clay and lime-calcined clay-limestone powder pastes
- Isothermal calorimetry method for measuring the heat flow of pastes consisting of lime-calcined clay-limestone powder
- Performing the strength activity index test

In this section, experimental methods and materials used in the study are presented.

3.1 Materials

3.1.1 Portland Cement

CEM I 42,5R type Portland cement was obtained from Çimsa for use in the samples prepared for the strength activity index and isothermal calorimetry test. Chemical composition of the Portland cement is given in Table 3.1.1.1.

Table 3.1.1.1 Chemical composition of PC

Chemical Composition (%)	
CaO	62.94
SiO_2	17.78
Al_2O_3	4.59
Fe_2O_3	3.73
SO_3	4.87
MgO	2.41
Na_2O	1.08
K_2O	1.00
TiO_2	0.34
CuO	0.10
MnO	0.07
P_2O_5	0.07
Loss on ignition	1.00

3.1.2 Raw Clays

The clays were obtained from two different locations in Turkey, Balıkesir/Düvertepe (Clay 1) and Niğde/Hacıabdullah (Clay 2). Figure 3.1.2.1 and Figure 3.1.2.1 shows the raw state of the clays. According to the visual determination, Düvertepe clay looks more whitish, while clay brought from Hacıabdullah looks more greyish. Both raw clays are not suitable for use without grinding in terms of particle size.

Chemical composition of the raw clays was determined by X-ray fluorescence (XRF) technique. Major oxide compositions of the raw clays are given in Table 3.1.2.1. There was not much difference in chemical composition between the two raw clays. However, according to X-ray diffraction (XRD) analysis results shown in Figure 3.1.2.3 and Figure 3.1.2.4, it is understood that they are different from each other in terms of mineralogical structure. Kaolinite mineral was observed in both clay samples. Besides, quartz in the Clay 1 sample, and cristobalite in the Clay 2 sample were observed as an inert mineral. Also, in Clay 2, sanidine mineral which is a high temperature form of feldspar was found.

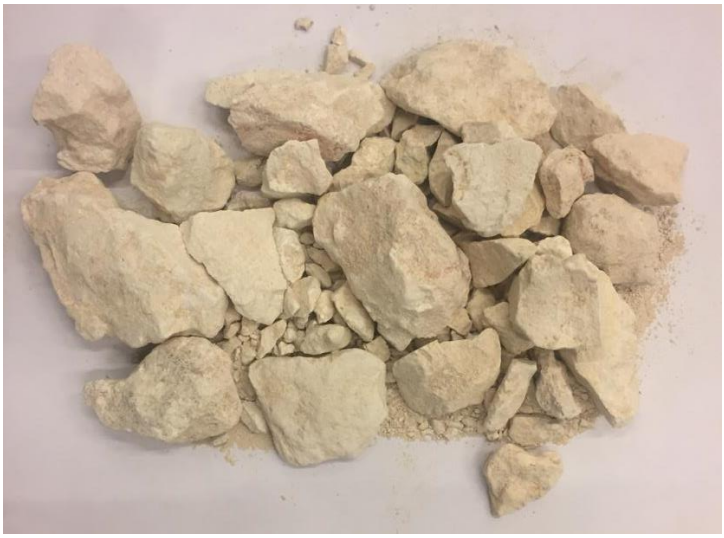

Figure 3.1.2.1 Düvertepe raw clay

Figure 3.1.2.2 Hacıabdullah raw clay

Table 3.1.2.1 Chemical composition of raw clays

Chemical Composition (%)	Clay 1	Clay 2
SiO_2	55.00	59.50
Al_2O_3	28.86	24.24
Fe_2O_3	0.80	2.94
CaO	0.31	0.83
MgO	0.07	0.54
TiO_2	0.97	0.88
SO_3	0.87	0.29
Na_2O	0.02	0.46
K_2O	0.20	1.09
Loss on ignition	11.72	9.30

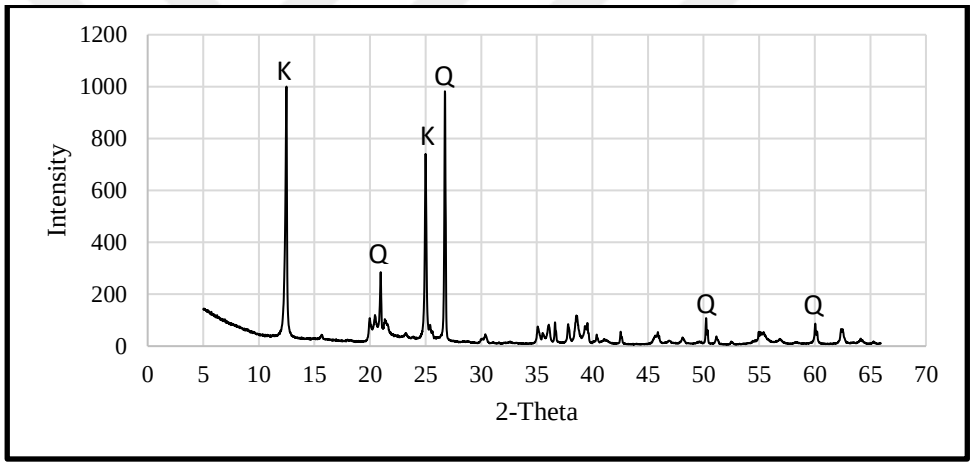

Figure 3.1.2.3 X-Ray diffraction patterns of Düvertepe (Clay 1) clays

(Q: Quartz, K: Kaolinite)

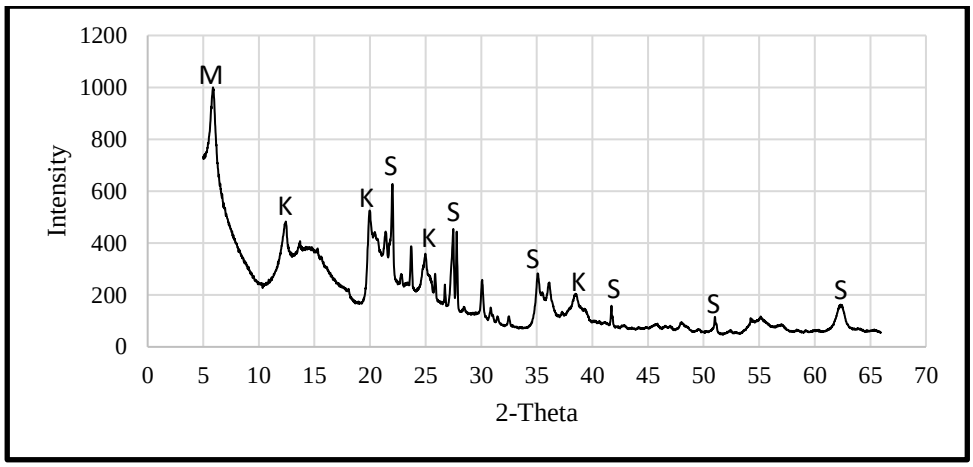

Figure 3.1.2.4 X-Ray diffraction patterns of Hacıabdullah (Clay 2) clays
(M: Montmorillonite, K: Kaolinite, S: Sanidine)

3.1.3 Hydrated Lime

In order to investigate the pozzolanic activities of calcined clays, a technical-grade $Ca(OH)_2$ was used. Pastes containing lime-calcined clay and lime-calcined clay-limestone powder were prepared with this $Ca(OH)_2$. Thermo-gravimetrical analysis was performed to determine the purity of $Ca(OH)_2$ used and it was found to contain 92% $Ca(OH)_2$.

3.1.4 Limestone Powder

Limestone powder was supplied from Niğtaş Company to see how limestone powder influences pozzolanic activity. The pastes containing lime-calcined clay-limestone powder for thermal analysis and prepared to measure heat flow in the isothermal calorimetry were prepared with this limestone powder. In addition, this limestone powder was used in the samples prepared in the strength activity index test. The thermo-gravimetrical analysis was performed to determine the purity of limestone powder, and it was found to contain 99% $CaCO_3$. The chemical composition and technical data of limestone powder are given in Table 3.1.4.1 and Table 3.1.4.2. The data regarding the particle size distribution of limestone powder are given in Table 3.1.4.3.

Table 3.1.4.1 Chemical composition of limestone powder

Chemical Composition (%)	
CaO	55.39
MgO	0.30
SiO_2	0.10
Fe_2O_3	0.04
LOI	43.96

Table 3.1.4.2 Technical data of limestone powder

Technical data	
Whiteness	> 98.30 (%)
Brightness	> 96.00 (%)
Moisture	< 0.3 (%)
pH	9 ± 0.5
Hardness	3 (Mohs)
Refractive index	1.57

Table 3.1.4.3 Particle size data of limestone powder

Particle size data	
Median particle size, D50	2.70 ± 0.20 (μ)
Max. particle size, D97	9.20 ± 0.80 (μ)
Particles below 2μ	41 ± 4 (%)
Specific surface area	3.2 ± 0.3 (m^2/cm^3)
Amount retained on 45 μm sieve	< 0.01 (%)

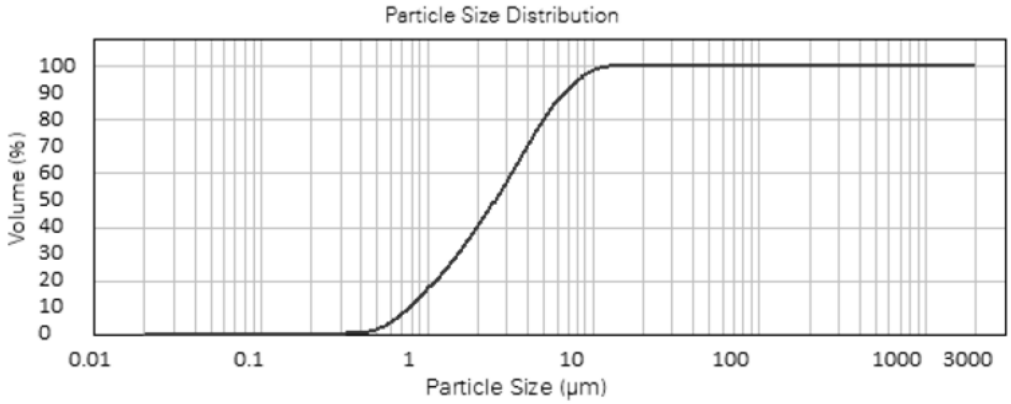

Figure 3.1.4.1 Particle size distribution of limestone powder

3.1.5 Water

In pastes prepared for thermal analysis and isothermal calorimetry experiments, distilled water was used to clearly observe pozzolanic activity. For the strength activity index test, potable tap water taken from the city water supply was used while preparing the sample.

3.1.6 Sand

Standard sand obtained from Limak Cement Company was used to prepare the sample for strength activity index test. The standard sand used is produced in accordance with TS EN 196-1 [39].

3.2 Experimental Methods

3.2.1 Grinding and Calcination of the Raw Clays

The clay samples used are not suitable for use with their raw material in terms of particle size. Therefore, the samples were ground for 45 minutes with a ball mill (Atom Teknik) at Erciyes University laboratory (Figure 3.2.1.1). The grinding samples were sieved through a 0.850 mm mesh screen, and the residue on the sieve was separated. Passing the sieves were calcined in a porcelain crucible. For calcination, the laboratory

muffle furnace (Protherm) shown in Figure 3.2.2 was used. Each sample was kept in the furnace at the specified temperature for 1 hour. These processes were performed in two clay samples, and the particle size distribution curve in Figure 3.2.1.3 was determined by laser diffraction method. After 45 minutes of grinding, Clay 1 was found to be finer than Clay 2.

BET surface area was determined by TAUM in Erciyes University. BET surface area of Clay 1 and Clay 2 are 8339 m^2/kg and 42180 m^2/kg, respectively.

Figure 3.2.1.1 Ball mill for grinding

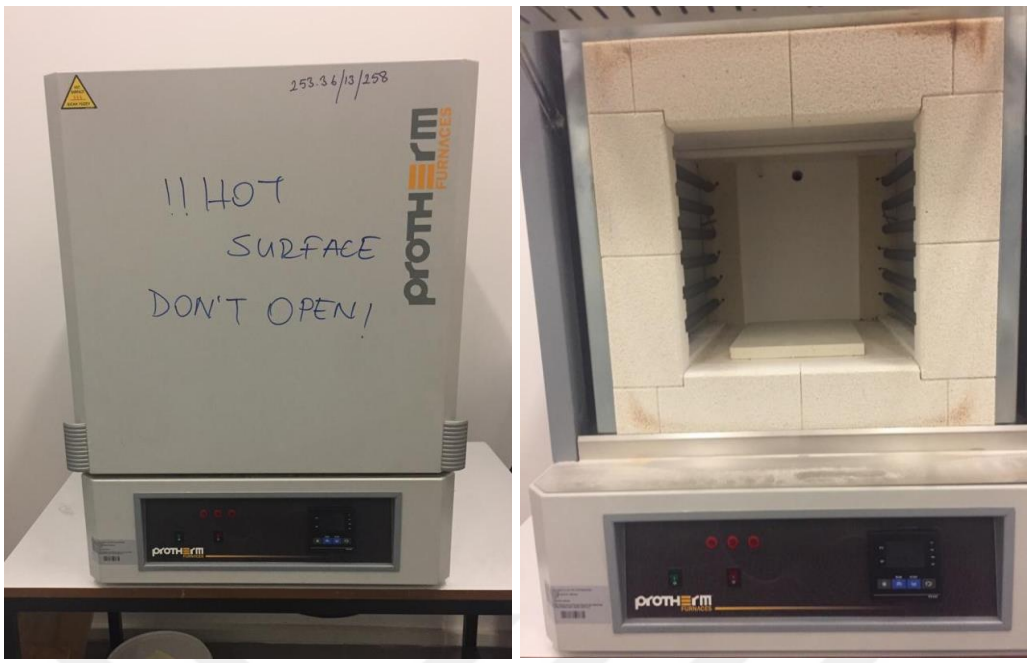

Figure 3.2.1.2 Laboratory muffle furnace for calcination

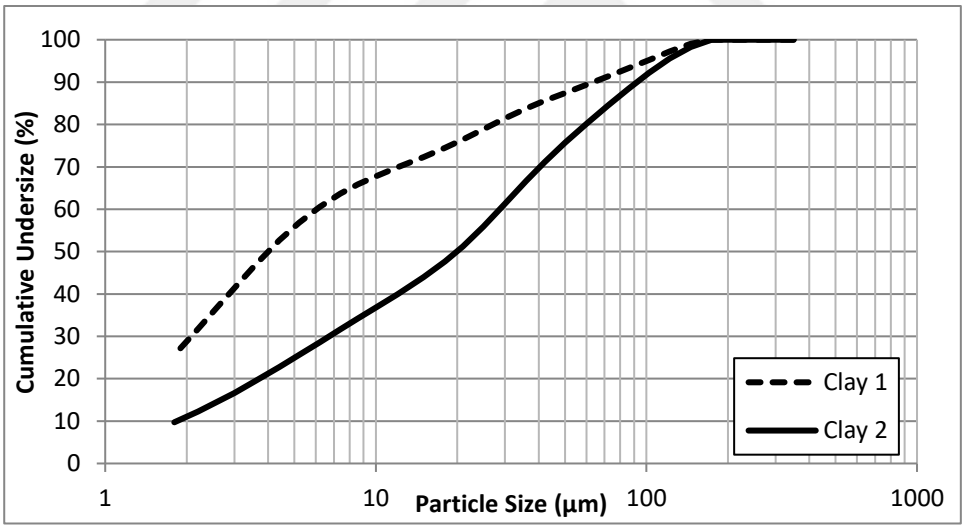

Figure 3.2.1.3 Particle size distribution curves

The samples calcined at three different temperatures are shown in Figure 3.2.1.4. Especially at 1150 ºC Clay 1 sample is seen to become quite white.

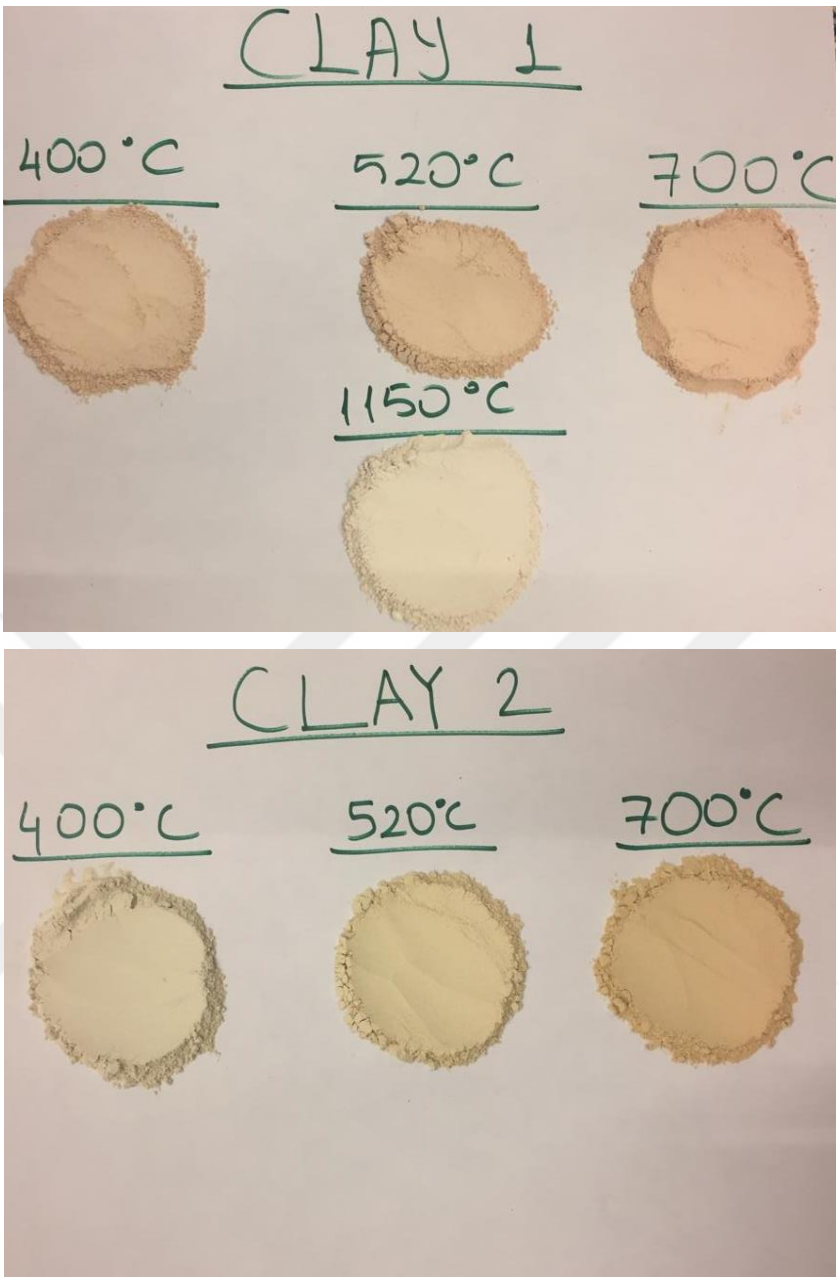

Figure 3.2.1.4 Calcined clays at different temperatures

3.2.2 XRD Analysis

Each substance in the crystal structure gives a certain pattern as a result of X-ray application. In this pattern, there are specific peaks for each mineral at certain positions (2θ Angle). The same crystals always form the same original peaks. In the pattern obtained from the crystal mixtures, each crystal produces its peaks independently of the other crystals. Therefore, the X-ray diffraction of pure minerals is like a fingerprint of that mineral. Thus, XRD is considered as the most direct and accurate analytical method

to determine the presence and absolute amounts of all minerals in a clay-rich rock (claystone, marl) [40].

The mineralogical analyses of the raw and calcined clays were carried out with X-ray diffraction instrument (Bruker/Siemens) at Abdullah Gül University Research laboratory (Figure 3.2.2.1). The samples were scanned between 5 and 65° 2θ with the detector. The step size per step was set to 0.02° 2θ.

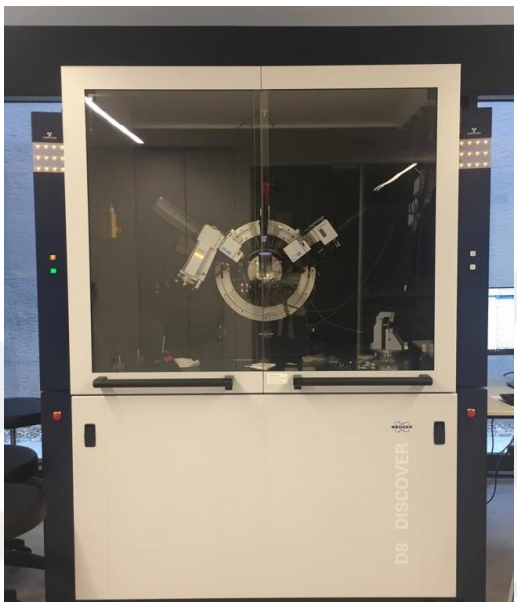

Figure 3.2.2.1 X-ray diffraction instrument

3.2.3 Thermal Analysis

The TGA instrument (Shimadzu) in Abdullah Gül University laboratory was used frequently during the study (Figure 3.2.3.1). The thermal analysis instrument was used at a heating rate of 10 °C/min for the temperature range from room temperature to 1000 °C.

Firstly, the temperature range at which raw clays occur dehydroxylation was examined by thermal analysis. Thus, calcination temperatures were determined. The temperatures selected according to the TGA plot shown in Figure 3.2.3.2 are 400 (beginning of dehydroxylation), 520 (middle of dehydroxylation), 700 °C (end of dehydroxylation). Afterward, thermal analysis was then performed for all calcined samples. The amount of kaolinite was calculated according to these thermal analyses. Dehydroxylation of kaolinite occurs between 400-700 °C. The amount of kaolinite with respect to weight

loss in this temperature range is calculated as follows. $M_{kaolinite}$ (258.16 g.mol^{-1}) and M_{water} (18.02 g.mol^{-1}) indicate the molecular weight of kaolinite and water. $wt\%_{kaol\text{-}OH}$ indicates mass loss during the dehydroxylation of kaolinite [38].

$$w\%_{kaolinite} = w\%_{kaol-OH}\frac{M_{kaolinite}}{2M_{water}}$$

Calcined kaolinite is defined as the difference of kaolinite between raw and calcined clays to only consider the part of kaolinite which was dehydroxylated during calcination. The amount of calcined kaolinite is calculated as shown below. After calcined, the amount of unreacted kaolinite should be normalized to the amount of water remaining from calcined clay. Because the total calcined clay mass is not the same as the raw clay mass due to the evaporation of water [38].

$$w\%_{calcined\ kaolinite} = w\%_{kaolinite} - w\%_{kaol-OH,calcined}\frac{M_{kaolinite}}{2M_{water}}\frac{100 - w\%_{kaol-OH,calcined}}{100}$$

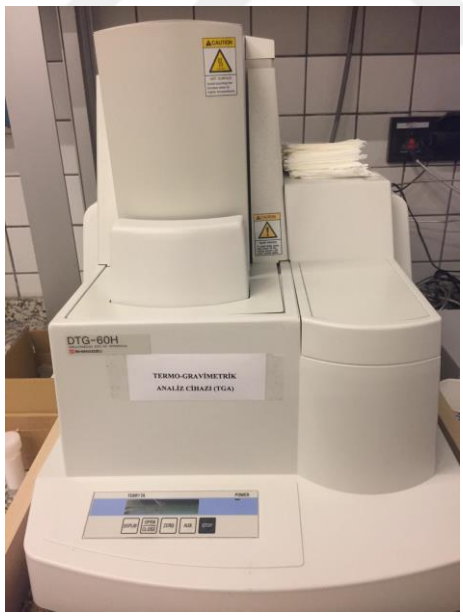

Figure 3.2.3.1 TGA instrument

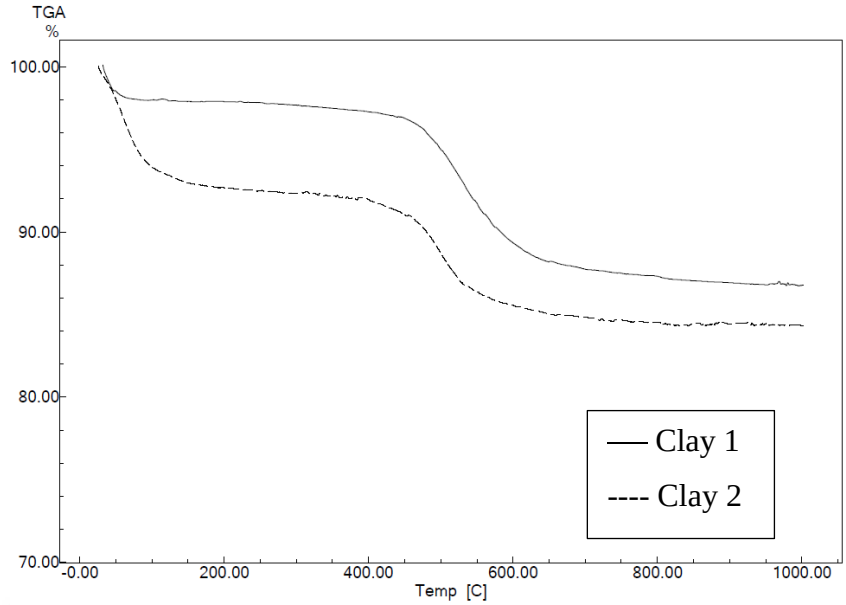

Figure 3.2.3.2 TGA plot of the raw clays

For the pozzolanic activity determination of calcined clays, lime-calcined clay pastes were prepared. A technical grade $Ca(OH)_2$ was used as lime. The lime-calcined clay ratio was 1:1, and the water-to-solid ratio was 0.55. Prepared pastes were stored in syringes in order to prevent contact with air (to protect carbonation), moisture loss, and cured at 50 °C to accelerate pozzolanic activity.

$Ca(OH)_2$ consumption of lime-calcined clay pastes was calculated by thermal analyses of 3,7, and 28-days for pozzolanic activity examining. The amount of CH in the pastes can be calculated by weight loss, starting at approximately 400 °C. A reaction occurs due to CH decomposition and evaporation of water. This reaction is calculated from the amount of CH and the evaporating water from the molar weight ratio.

First, the purity of the technical grade $Ca(OH)_2$ used was calculated over the TGA plot. The amount of CH initially presents in the lime-calcined clay paste was then calculated in percentages based on the original lime and ignited weight of the paste. For pastes of 3,7 and 28-days, the amount of free lime was calculated as a percentage based on the ignited weight of the paste. Finally, CH consumption was expressed as a percentage of the difference between the initial and final free lime quantities.

In addition, lime-calcined clay-limestone powder pastes were prepared to examine the effect of limestone powder on pozzolanic activity. The lime: calcined clay: limestone powder ratio was 1:1:0.22, and the water-to-solid ratio was 0.55. As a result of three different experiments, it was observed that adding 10% of solids (lime+ calcined clay+

limestone powder) limestone powder had the most positive effect on pozzolanic activity. Storage and curing conditions were preferred in the same way as lime-calcined clay pastes.

3.2.4 Isothermal Calorimetry

In this method, a calorimeter is used to measure the heat flow of the mixtures. The reference and sample are in an isolated container. The temperature in the container is kept constant by a thermostat whose temperature is controlled by a thermoelectric air heater or cooler. This means that all processes involving heat loss or heat gain take place at a constant temperature. Therefore, this method is called “isothermal calorimetry”. In cementitious systems, hydration kinetics, degree of hydration, and effects of additives can be interpreted by measuring heat flow. The hydration kinetics of cementitious mixtures were determined according to ASTM C1679 standard [41].

The isothermal calorimetry (TAM Air, TA Instruments) used in the study is in the Abdullah Gül University Research Laboratory (Figure 3.2.4.1). The instruments can be used to analyze up to 8 different samples at the same time. When placing the prepared samples into the instrument, the sample holders containing the reference samples must not be opened, because temperature fluctuations in the calorimeter affect the measurements and may cause serious noise to the output signal.

For each test, 35 g of material was mixed with the help of a spatula. Immediately after mixing, 7 g of material was transferred to the ampoules shown in Figure 3.2.4.2. 0.40 water/binder ratio in the preparation of paste used. These prepared samples are quickly placed in the sample holders of the isothermal calorimetry. Since the isothermal calorimeter effects the ambient temperature, it should be as fast as possible when performing experiments. Heat flow from the samples was recorded for 72 hours.

Figure 3.2.4.1 Isothermal calorimetry instruments

Figure 3.2.4.2 Isothermal calorimetry samples

3.2.5 Strength Activity Index Testing

Calcined clays were subjected to the necessary tests to determine the compliance with the strength activity index and water requirement values given in ASTM C618 standard [19]. Control and test mixtures were prepared according to ASTM C311. While the control mixture was prepared only with Portland cement, the test mixture was prepared 80% Portland cement and 20% tested samples (calcined clay and limestone powder). While the water/cement ratio of the control mixture was 0.485, the amount of water in the test mixtures was calculated to provide a ±5% flow [42]. The mixing ratios for the control and test mixture are given in Table 3.2.5.1.

Table 3.2.5.1 Mixing ratio for strength activity index testing mortars

Material	Control mixture (g)	PC-C Test mixture (g)	PC-C-LS Test mixture (g)
Portland cement	500	400	400
Calcined clay	-	100	80
Limestone powder	-	-	20
Standard sand	1375	1375	1375
Water	242	Variable by flow	Variable by flow

A laboratory mixer complying with the ASTM C305 standard was used in preparing the mortars. The mortar mixing procedure given in the same standard was followed. Firstly, all the water was placed in the mixing bowl, and the binder was added. Mixing at the slow speed for 30 s. All of the sand was added for 30 s while continuing to mix at slow speed. The mixer was then stopped and mixed at medium speed for an additional 30 s. After this step, the mixer was stopped again, and the mortar was allowed to stand for 90 s. During the first 15 s of this holding, the mortars remaining on the edge of the bowl were quickly collected. Finally, it was mixed at medium speed for a further 60 s [43].

After the mixing process was completed, the flow test was performed immediately. Shown in Figure 3.2.5.1, the flow table and accessory apparatus were used for this test [44]. The produced mixtures were subjected to flow table testing according to ASTM C1437 standard. The flow mold was placed in the center of the flow table. The mold was filled in half with mortar and tapped by 20 times with the help of tamper. The remaining part is filled, and the same tamp procedure is applied. The mortar on the surface of the mold is leveled to the same level with a trowel. Wait 1 minute before removing the mold and drop the table 25 times in 15 s. The diameter of the mortar is measured from 4 different places and the average of these four values [45].

Figure 3.2.5.1 Flow table and accessory apparatus

The casting process of the samples was carried out following ASTM C109. Samples were poured into 3-chamber steel cube molds of 50x50x50 mm. These molds were lubricated before casting the samples so that the samples would come out of the molds more easily and not be deformed. In order to compress the mixture well, the casting was made in two layers [46]. The samples were cured by placing a wet cloth on the molds to prevent water loss for 24 hours after pouring. After 24 hours, the samples removed from the molds were cured in the water at room temperature (Figure 3.2.5.2).

The casting process of the samples was carried out following ASTM C109. Samples were poured into 3-chamber steel cube molds of 50x50x50 mm. These molds were lubricated before casting the samples so that the samples would come out of the molds more easily and not be deformed. In order to compress the mixture well, the casting was made in two layers [46]. The samples were cured by placing a wet cloth on the molds to prevent water loss for 24 hours after pouring. After 24 hours, the samples removed from the molds were cured in the water at room temperature (Figure 3.2.5.2).

Figure 3.2.5.2 Curing of samples

7 and 28-day samples were used for the strength activity index test. For this test, the compressive strength of 6 samples from each mixture was determined, and these values were averaged. The testing machine, which is placed in the laboratory of Abdullah Gül University, was used for the experiment. The surfaces of the samples to be used in the test shall also be smooth in order to take the load from the pressure surfaces properly. The load rate was selected to be 500 N/s. The strength activity index (SAI) value was calculated as follows [42].

$$\text{SAI} = \frac{\text{average compressive strength of test mixture cubes, MPa}}{\text{average compressive strength of control mix cubes, MPa}}$$

Figure 3.2.5.3 Strength activity index test

Chapter 4

4 Results and Discussions

4.1 Chemical Composition of Calcined Clays

The pozzolans may contain large amounts of silica and alumina, as well as some amounts of iron oxide, calcium oxide, and alkalis. The pozzolanic materials must contain enough quantities of silica, alumina, and iron oxide to exhibit pozzolanic activity.

Table 4.1.1 and Table 4.1.2 shows the chemical composition change of Clay 1, and Clay 2, with respect to temperature. As calcination temperature increases, clays enrich in silica, alumina, and iron content. According to Table 4.1.1 and Table 4.1.2, it is seen that the amount of silica varies between 55% -62.47%, the amount of alumina varies between 24.9%-33.39%, and the amount of iron oxide varies between 0.8% and 1.96%. The amount of alkali does not exceed 2% for both samples. As the calcination temperature increases, the amount of sulphate decreases. The sulphate content decreases after decomposition of the alunite occurs. The decomposition of alunite occurs in two-stage, as shown below. As a result of the second endothermic reaction, 75% of the sulphate is loss [47].,

$$2KAl_3(SO_4)_2(OH)_6 \xrightarrow{480-620^{\circ}C} 2KAl(SO_4)_2 + 2Al_2O_3 + 6H_2O$$

$$2KAl(SO_4)_2 \xrightarrow{770-900^{\circ}C} K_2SO_4 + Al_2O_3 + 3SO_3$$

Although alunite has been decomposed at 900 °C, Kakali et al, presented that sulphate was still present in the samples calcined at 950 °C [22]. The thesis study supports that the sulphate is not completely lost. Calcination of Clay 1 at 1100 ° C, it is seen that the amount of sulphate decreased to 0.2. Loss on ignition (LOI) was determined according

to the results of thermal analysis. The percentage of weight loss from 105 °C to 1000 °C gives LOI.

According to ASTM C618 standard, the total amount of silica, alumina, and iron oxide should be a minimum of 70% in natural pozzolans. The amount of SO_3 should be a maximum of 4% [19]. Both clay samples meet these specifications as specified in the standard.

Table 4.1.1 Chemical composition of Clay 1

Chemical Composition (%)	**Clay 1 400 °C**	**Clay 1 520 °C**	**Clay 1 700 °C**	**Clay 1 1150 °C**
SiO_2	56.76	57.81	58.94	61.86
Al_2O_3	28.80	28.85	31.90	33.39
Fe_2O_3	0.65	0.79	0.92	1.03
CaO	0.26	0.26	0.42	0.48
MgO	0.06	0.06	0.06	0.07
TiO_2	0.92	1.04	1.11	1.23
SO_3	0.87	0.81	1.05	0.22
Na_2O	0.01	0.01	0.01	0.03
K_2O	0.20	0.20	0.21	0.24
Loss on ignition	11.5	9.88	4.03	0.16

Table 4.1.2 Chemical composition of Clay 2

Chemical Composition (%)	Clay 2 400 °C	Clay 2 520 °C	Clay 2 700 °C
SiO_2	61.10	59.80	62.47
Al_2O_3	24.90	25.30	25.54
Fe_2O_3	1.96	2.00	2.66
CaO	0.97	1.03	0.87
MgO	0.54	0.54	0.57
TiO_2	0.82	0.82	0.96
SO_3	0.37	0.53	0.56
Na_2O	0.02	0.02	0.56
K_2O	1.19	1.29	1.35
Loss on ignition	8.00	7.80	4.10

4.2 XRD Analysis of Calcined Clays

Precisely identifying clays is quite difficult. Because clay minerals are very fine-grained, they can be crystallized in various ways or combined with amorphous-glassy material [48].

Changes in the crystal structure were observed for both the raw and calcined states of the samples. XRD analysis of the Clay 1 sample from Balıkesir/Düvertepe region is shown in Figure 4.2.2. When the XRD patterns are examined, the minerals clearly identified for the Clay 1 sample are quartz and kaolinite. The 2θ value of the strongest peak of the quartz is 26.76º. If this peak occurs, the weaker peak position 2θ is automatically checked at 20.85º; because the weaker peak of the quartz occurs at position 2θ = 20.85º. The peaks of quartz shown in Table 4.2.1 were observed in all XRD patterns of Clay 1 [49]. Quartz is highly resistant to decomposition by the effect of temperature. Therefore, even in samples calcined at high temperatures, quartz peaks are clearly observed.

Usually, a peak around 7Å identifies chlorite or kaolinite minerals. It is necessary to look at the presence of 3.58Å peak for the kaolin group and 3.54Å peak for the chlorite group to separate these minerals [49]. As shown in Figure 4.2.1, a kaolinite peak of

3.58Å (2θ = 25.2º) was found in Clay 1. Thus, the accuracy of the kaolinite mineral in Clay 1 was proved. Also, the intensity of kaolinite peaks is reduced after the sample is calcined. The reason for this is that the crystal structure of kaolinite mineral changes as a result of decomposition between 450-600 ºC. Hence, in the sample calcined at 700 °C, the kaolinite peaks almost disappeared.

Table 4.2.1 Diffraction data of quartz [49]

Intensity	**2θ**	**d(Å)**	**Intensity**	**2θ**	**d(Å)**
22	20.80	4.270	4	45.83	1.979
100	26.67	3.342	14	50.18	1.818
8	36.57	2.457	4	54.91	1.672
8	39.49	2.282	2	55.38	1.659
4	40.32	2.237	9	60.00	1.541
6	42.50	2.128	1	64.04	1.453

In the sample calcined at 1150 ºC, kaolinite peaks disappeared completely. However, mullite peaks were observed in the sintered material as a result of high temperatures. At higher temperatures, it is expected that the intensity of the mullite peaks will increase as more sintering will occur [50].

Zhou et al. investigated the formation of mullite in the 1100-1500 ºC range from kaolin containing muscovite and quartz. The quartz in the kaolin content is very important in the formation of high alumina containing mullite. As the temperature increased, the intensity of the mullite peaks increased, and the peaks were observed more clearly [51] (Figure 4.2.1).

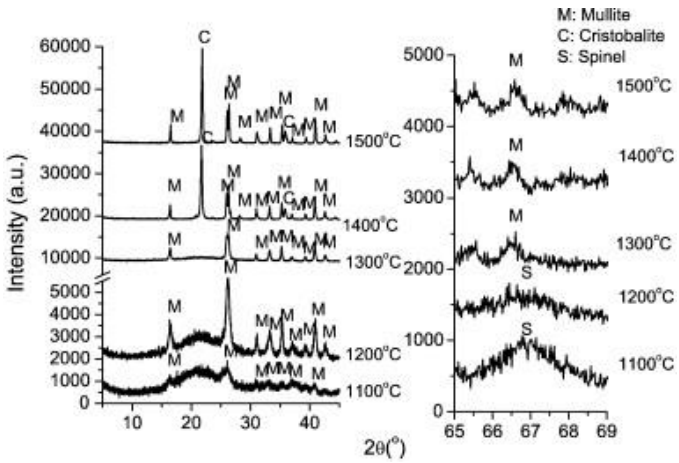

Figure 4.2.1 XRD pattern traces of sample calcined between 1100-1500 °C [51]

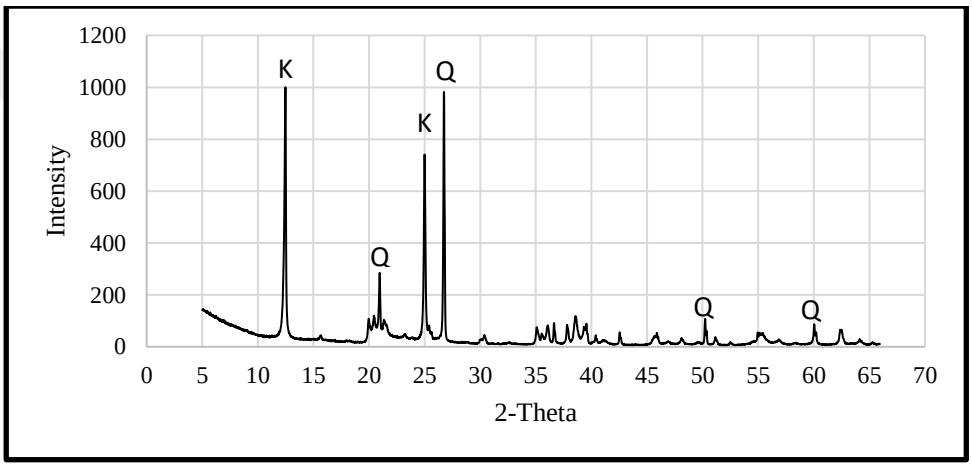

(a)

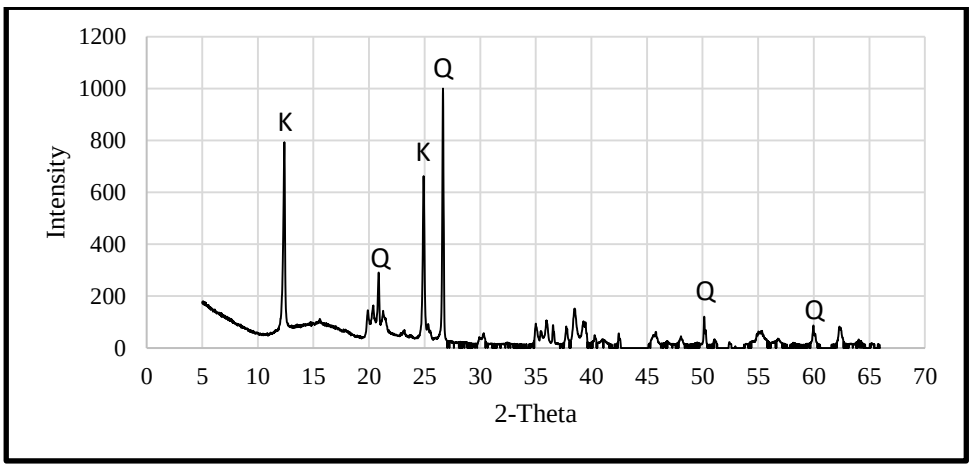

(b)

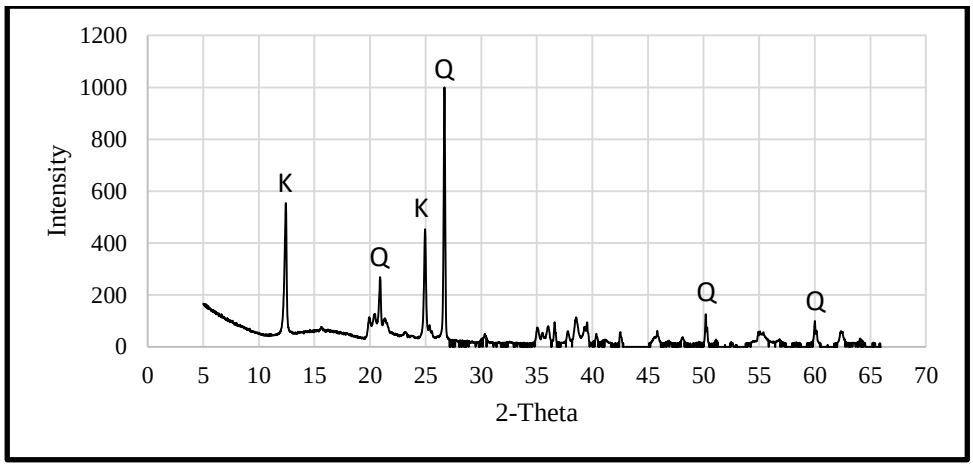

(c)

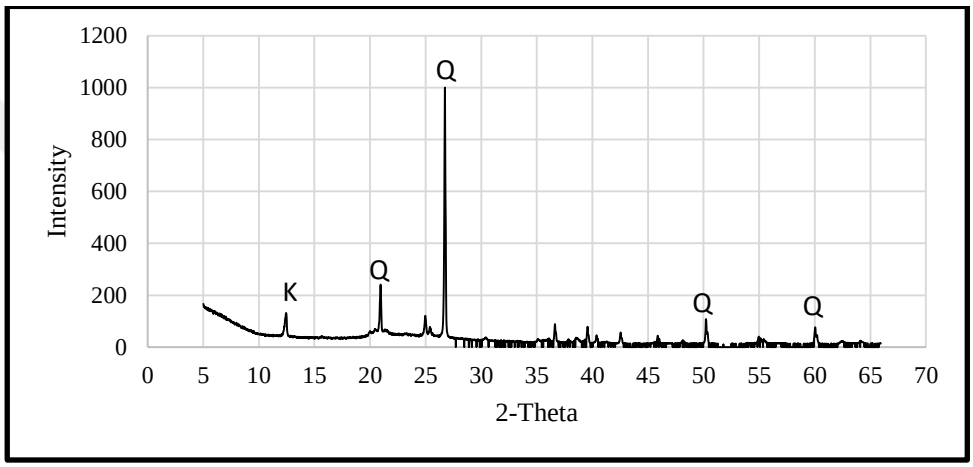

(d)

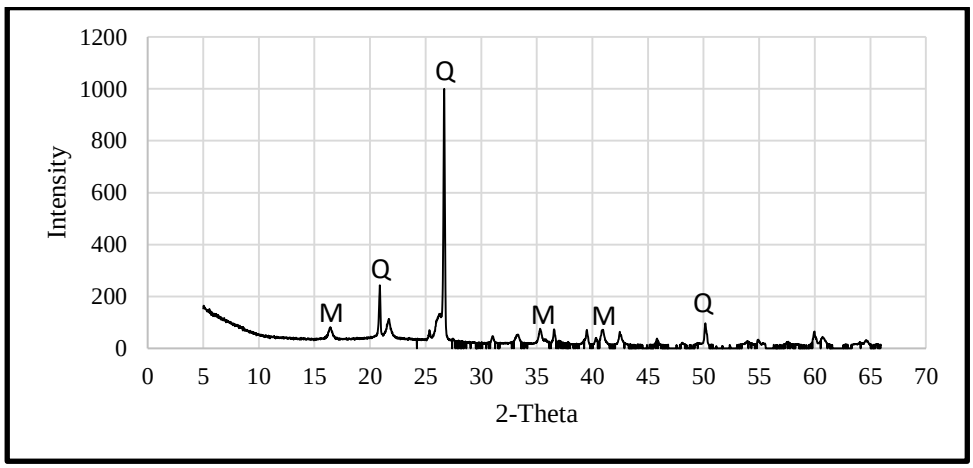

(e)

Figure 4.2.2 XRD pattern of samples (a) C1_raw, (b) C1_400 ºC, (c) C1_520 ºC, (d) C1_700 ºC and (e) C1_1150 ºC (Q: Quartz, K: Kaolinite, M: Mullite)

The first peak of the montmorillonite group is around 12.5-15Å. As shown in Figure 4.2.3, the montmorillonite peak of 15.2Å (2θ = 5.81º) was discovered in the raw Clay 2

sample. In the raw and 400-520 ºC, calcined form of Clay 2, kaolinite peaks were observed, as seen in Clay 1. As seen in Clay 1, kaolinite peaks disappeared in the sample calcined at 700 °C. Sanidine mineral, which was observed in the Clay 2 sample, is also the high-temperature form of potassium feldspar. Sanidine is a high-temperature stable form of feldspar and is stable up to 1300 °C [52]. Hence, sanidine peaks are still available in the Clay 2 sample calcined at 700 °C.

Shvarzman et al. investigated the effect of dehydroxylation degree of calcined samples on pozzolanic activity. According to XRD patterns of calcined samples at different temperatures, a kaolinite peak was observed in the calcined sample at 500 °C, and kaolinite peaks were disappeared in a calcined sample at 700 °C. In addition, quartz peaks were observed at all temperatures (500, 570, 700 ºC) [53].

Elimbi et al. studied thermal analyses showing that the dehydroxylation of kaolinite started at 440 °C. According to this result, it is seen that the temperature of 450 °C is not enough to transform kaolin to metakaolin. Kaolinite peaks are still observed in XRD patterns of 450 ºC heat-treated samples. However, kaolinite peaks disappeared in samples calcined at 600 and 800 °C [54].

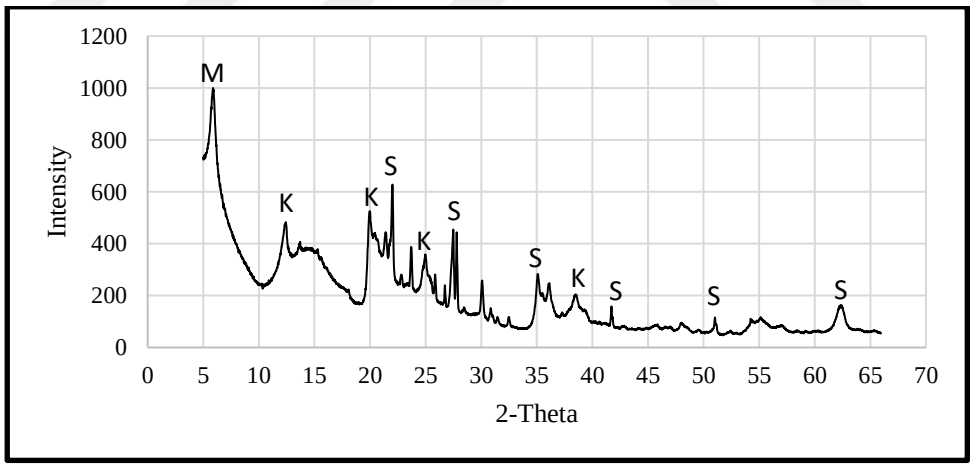

(a)

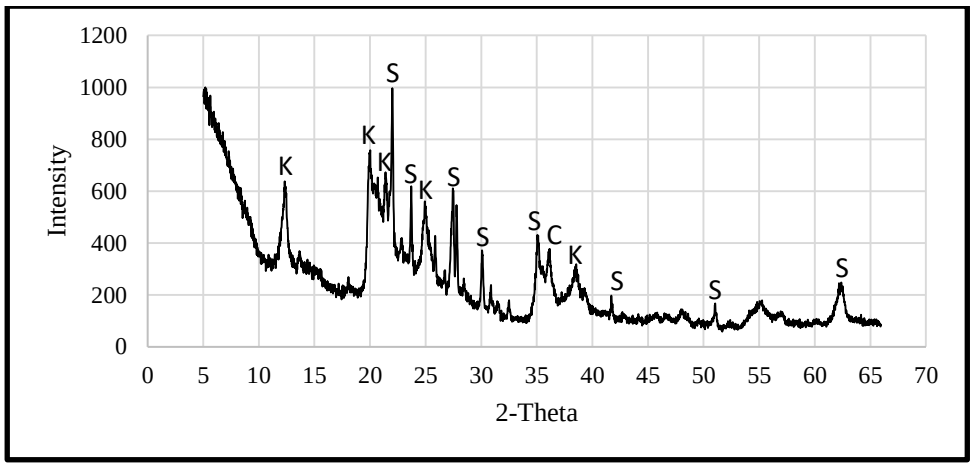

(b)

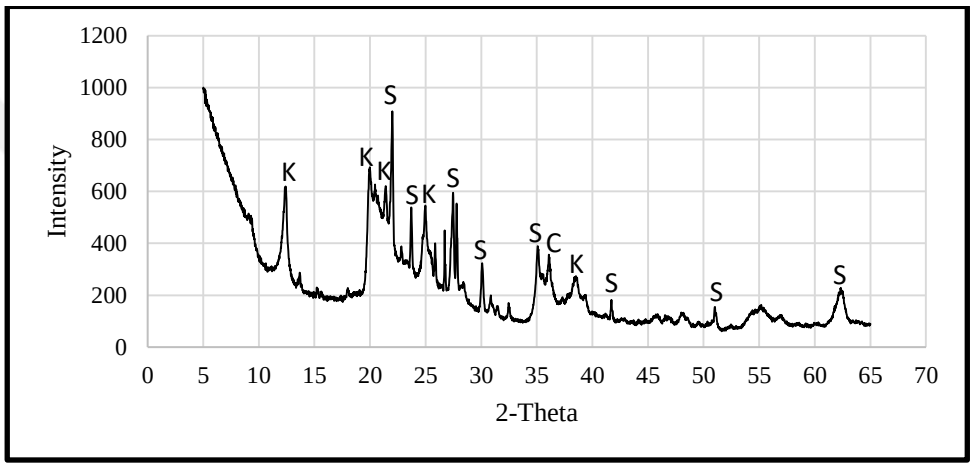

(c)

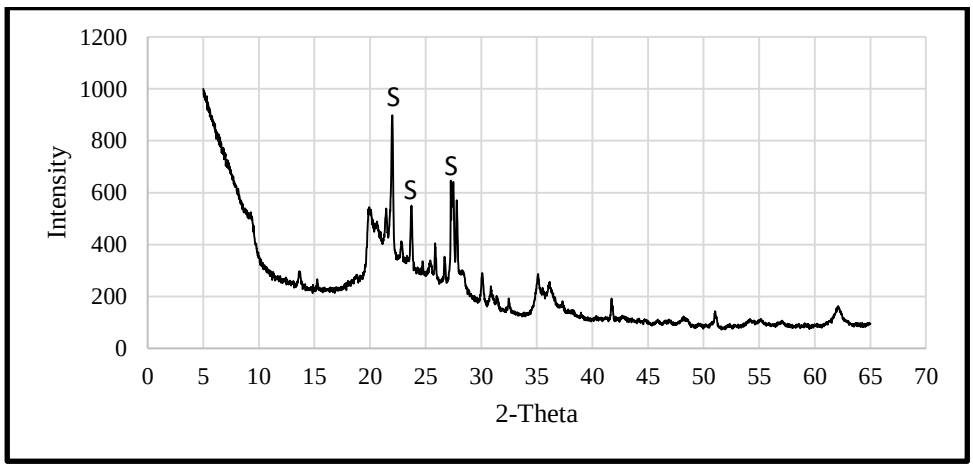

(d)

Figure 4.2.3 XRD pattern of samples (a) C2_raw, (b) C2_400 ºC, (c) C2_520 ºC, and (d) C2_700 ºC (M: Montmorillonite, K: Kaolinite, S: Sanidine)

4.3 Pozzolanic Reactivity of Calcined Clays

Thermal analysis was performed to determine the loss on ignition and kaolinite amounts of the raw and calcined clays. These TGA plots are given in Appendix A. Thermal analysis results were used to determine kaolinite content according to weight loss between 400-700 ºC. As shown in Table 4.3.1, the kaolinite content of Clay1 is more than Clay 2. Kaolinite has the highest potential as pozzolanic activity compared to minerals such as montmorillonite, and illite. Since kaolinite contains more hydroxyl groups and Al^5 groups on the surface during dehydroxylation leads to a more amorphous phase [32]. Therefore, pozzolanic activity is expected to be higher in clay containing more kaolinite minerals.

Kaolinite amounts of calcined clays are presented in Table 4.3.1 as described in experimental study chapter. When both clays were calcined at 400 °C, a small amount of kaolinite minerals were calcined. In the sample calcined at 520 °C, it is seen that Clay 1 contains more calcined kaolinite than Clay 2. Calcination of Clay 2 at 400 or 520 °C did not affect the of calcined kaolinite amount. XRD analyses for 400 and 520 ºC calcined samples of Clay 2 support this result. When the XRD patterns of the two samples were compared, it was observed that the crystal structure was almost unchanged. In calcined samples at 700 ºC, the calcined kaolinite content in Clay 1 is considerably higher than Clay 2. Calcination of Clay 1 at 1150 ºC nearly calcined all kaolinite minerals. However, at high temperatures, calcination has different negative effects such as agglomeration and sintering.

Tironi et al. have studied the pozzolanic activity of clays with kaolinite contents of high (94%, 76%), medium (65%, 48%), and poor (16%). Clays containing high and medium kaolinite minerals have the highest pozzolanic activity after calcination. Clays containing over 45% kaolinite and calcined at 700 °C perform better when substituted with cement [35].

Table 4.3.1 Kaolinite content of samples

Samples	Amount, %
Kaolinite	
Clay 1_raw	69.7
Clay 2_raw	45.2
Calcined kaolinite	
C1_400 ºC	4.2
C1_520 ºC	11.8
C1_700 ºC	55.8
C1_1150 ºC	68.5
C2_400 ºC	2.4
C2_520 ºC	2.8
C2_700 ºC	34.2

Firstly, to determine the pozzolanic activity, $Ca(OH)_2$ consumption of lime-clay pastes was calculated from the TGA plots. TGA plots of lime-clay pastes are given in Appendix B.

As shown in Figure 4.3.1, the Clay 1 700 ºC (C1_700 ºC) sample shows the highest $Ca(OH)_2$ consumption for all test ages (3, 7, 28-days). The high reactivity of the Clay 1 sample is attributed to the high amount of kaolinite. The difference between the consumption of CH between C1_700 ºC and C2_700 ºC at an early age is quite high. However, at the end of 28 days, the gap was closed. At the end of 28 days, the C1_700 ºC sample consumed approximately 60%, and the C2_700 ºC sample 54% of available $Ca(OH)_2$.

In general, consumption of available CH increased for all test ages as Clay 1, and Clay 2 were calcined at higher temperatures. However, the consumption of CH was dramatically reduced compared to the calcination of Clay 1 at 1150 ºC to the calcination at 700 ºC. This is attributed to the changes of the mineralogical structure of calcination at 1150 °C. Compared to Clay 1 and Clay 2 calcined at 400 and 500 ºC for early ages, the Clay 2 sample consumed more CH. Although calcination of clays at 400 and 520 ºC increases CH consumption compared to its raw state, it appears to be unsatisfactory. Calcination at low temperatures, especially for Clay 2, has little effect on CH consumption.

In the study of Uzal et al., the pozzolanic activity of silica fume, zeolite, fly ash and non-zeolitic natural pozzolans were compared. Accordingly, lime-pozzolan pastes were prepared to compare the CH consumption amounts of these materials. In preparing the pastes, the ratio of lime: pozzolan ratio 1:1, water: solid ratio as 0.55 was used. Silica fume, zeolite, fly ash, and non-zeolitic natural pozzolans consumed 83%, 75%, 53%, and 46% CH end of the 28 days, respectively [55]. Compared to this study, C1_700 ºC and C2_700 ºC consumed more CH than fly ash and non-zeolitic natural pozzolan at the end of 28 days.

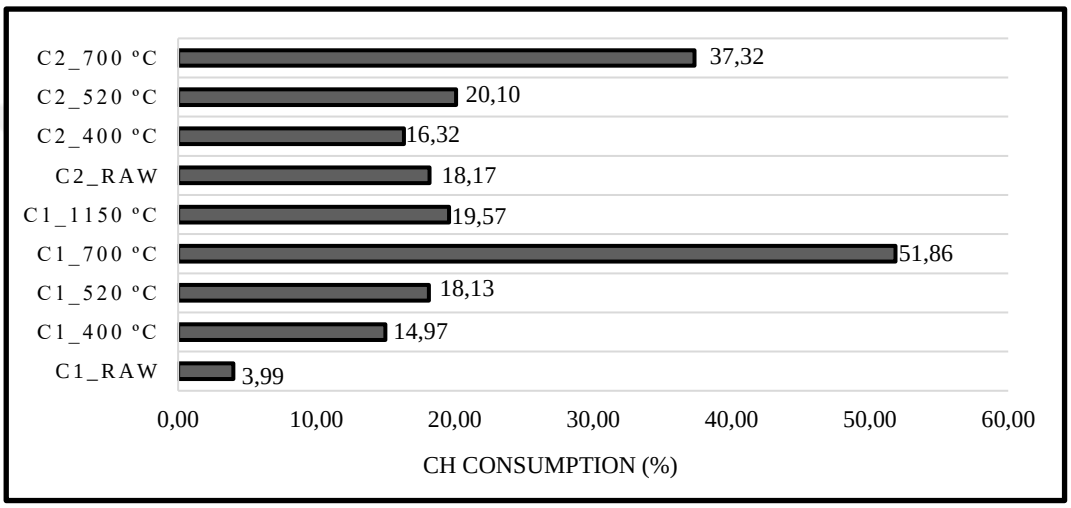

(a)

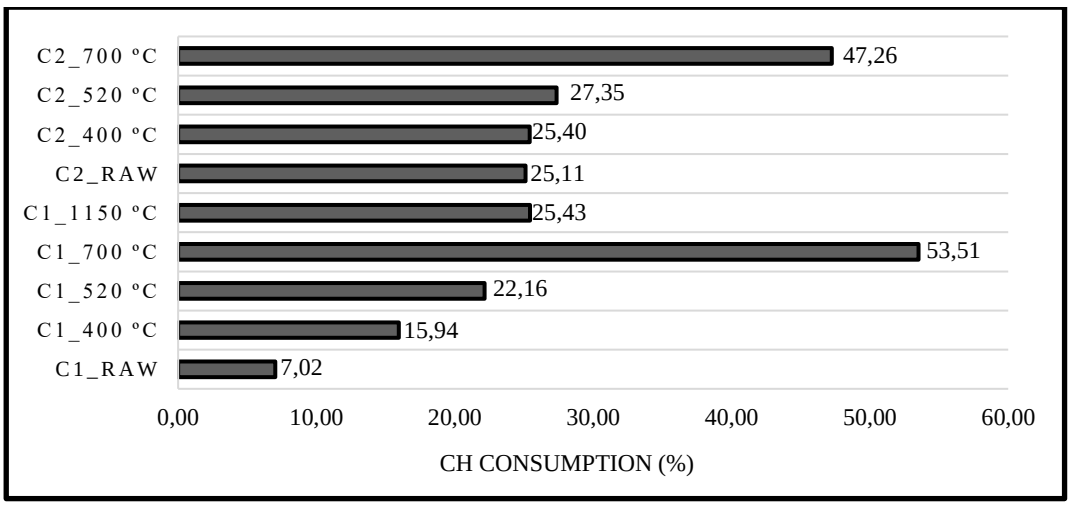

(b)

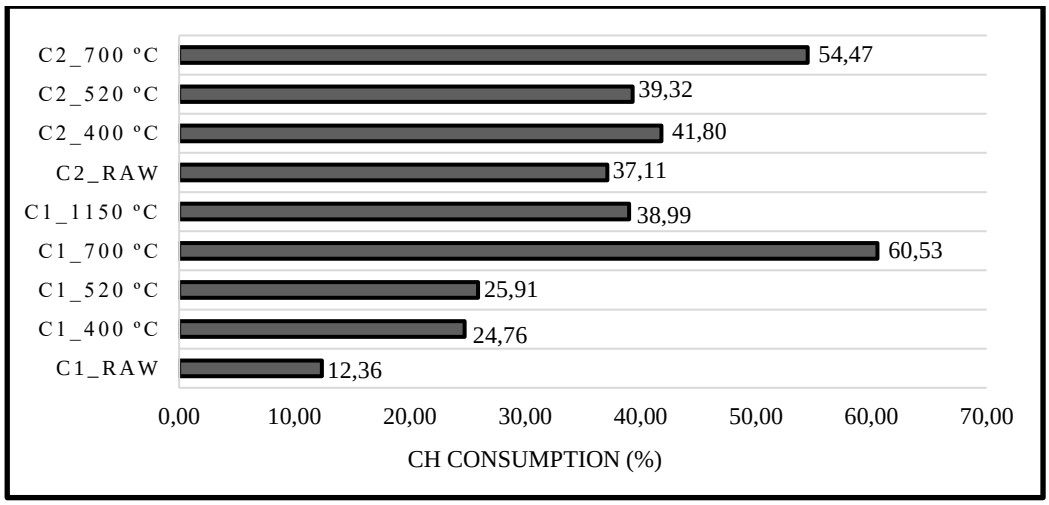

(c)

Figure 4.3.1 CH consumption of lime-clay pastes at (a) 3 days, (b) 7 days, (c) 28 days

Lime-clay-limestone powder pastes were prepared to observe the effect of limestone addition on pozzolanic activity. The consumption of CH from the TGA plots of lime-clay-limestone powder pastes was calculated and compared. TGA plots of lime-clay-limestone powder pastes are given in Appendix B.

In order to determine the amount of limestone powder addition, two different amounts of limestone powder and pastes were prepared. The CH consumptions of two pastes with the addition of 10% and 20% of the total weight of lime, clay, and limestone powder were calculated from the TGA plots. As a result, the paste containing 20% limestone powder consumed 54% CH, while the paste containing 10% limestone powder consumed 56% CH at the end of 3 days. According to these results, pastes containing 10% limestone powder were used in the whole study.

As shown in Figure 4.3.2, C1_700 ºC consumed the most CH at all ages. C1_700 ºC is seen to be dramatically higher in CH consumption compared to other samples, especially for early ages. The C1_700 ºC sample consumed 56%, 59%, 65% CH, at the end of 3, 7, 28 days, respectively. This is the C2_700 ºC sample that provides the values closest to these highest CH consumption values of C1_700 ºC. The C2_700 ºC sample consumed 39%, 49%, 57% CH, at the end of 3, 7, 28 days, respectively. When Clay 1 is calcined at 1150 ºC, CH consumption decreases flashily. The C1_1150 ºC sample consumed 21%, 33%, 43% CH, at the end of 3, 7, 28 days, respectively.

For Clay 2, the highest CH consumption was observed for the sample calcined at 700 ºC. For Clay 2, there is a slight difference for CH consumption between samples

calcined at 400 and 520 °C. In other words, calcination of the samples at 400 and 520 °C did not show a significant change for CH consumption. This can be attributed to the slight difference in the crystal structure between these temperatures.

Although the BET surface area of Clay 2 is higher, it is seen in terms of CH consumption that pozzolanic activity of Clay 1 is higher. This is because the mineralogical structure of Clay 1, and its chemical composition, contains more alumina.

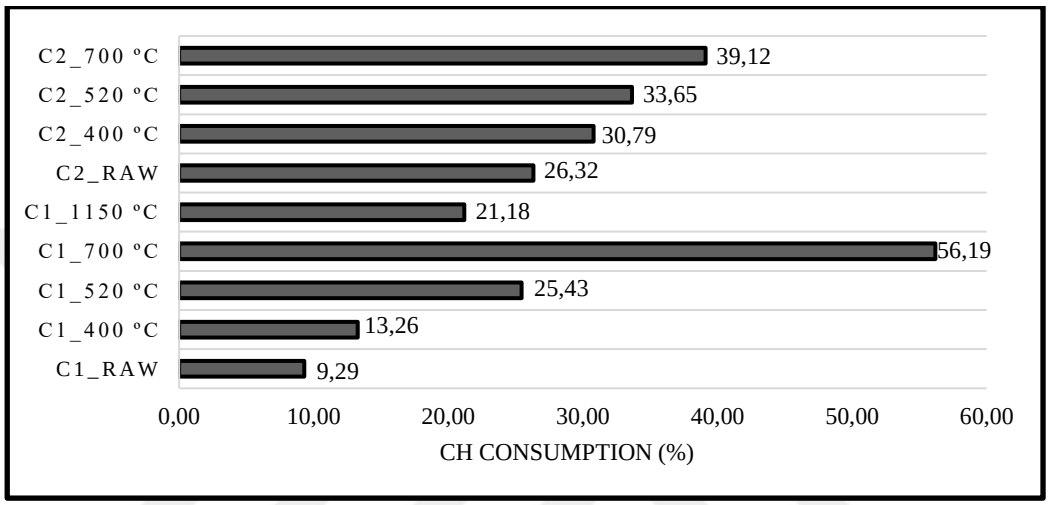

(a)

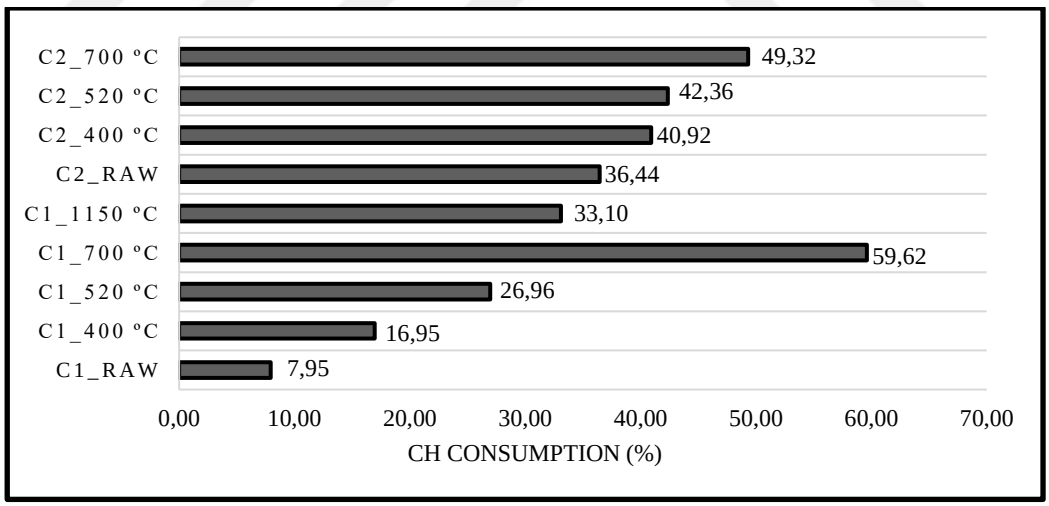

(b)

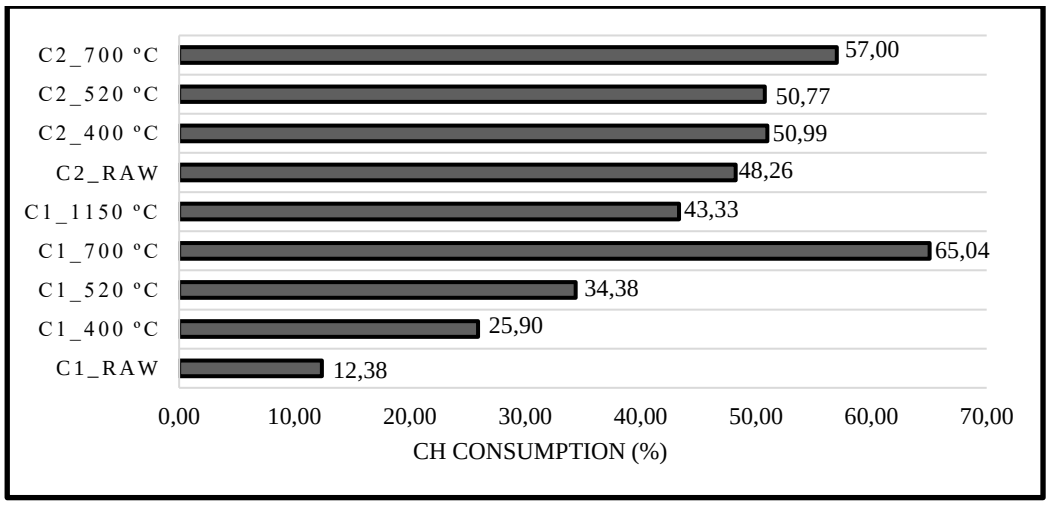

(c)

Figure 4.3.2 CH consumption of lime-clay-limestone powder pastes at (a) 3 days, (b) 7 days, (c) 28 days

As shown in Figures 4.3.3 and 4.3.4, the addition of limestone powder in almost all pastes increased CH consumption. $CaCO_3$ in limestone powder positively affected pozzolanic activity. CH consumption for C1_700 ºC increased from 60% to 65% at the end of 28 days. For C2_700 ºC, consumption of CH increased from 54.5% to 57% at the end of 28 days.

An increase in CH consumption is observed in calcined samples of Clay 1 at temperatures such as 400, 500 and 1150 ºC. CH consumption in the C2_400 ºC and C2_520 ºC increased from 41% to 51%, 39% to 51%, respectively. Limestone powder addition significantly increased the consumption of CH at low temperatures. However, none of the samples reached CH consumption of the samples calcined at 700 °C.

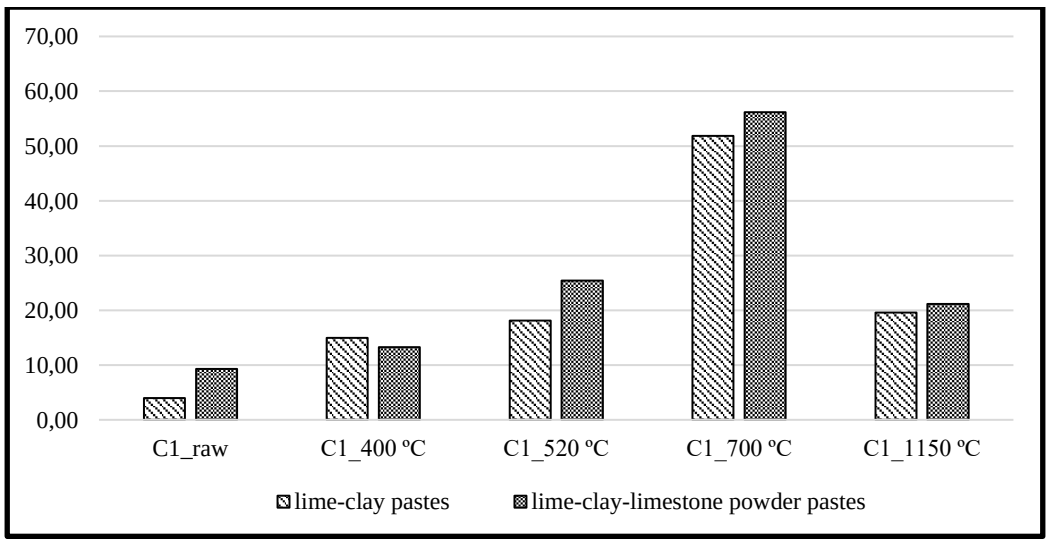

(a)

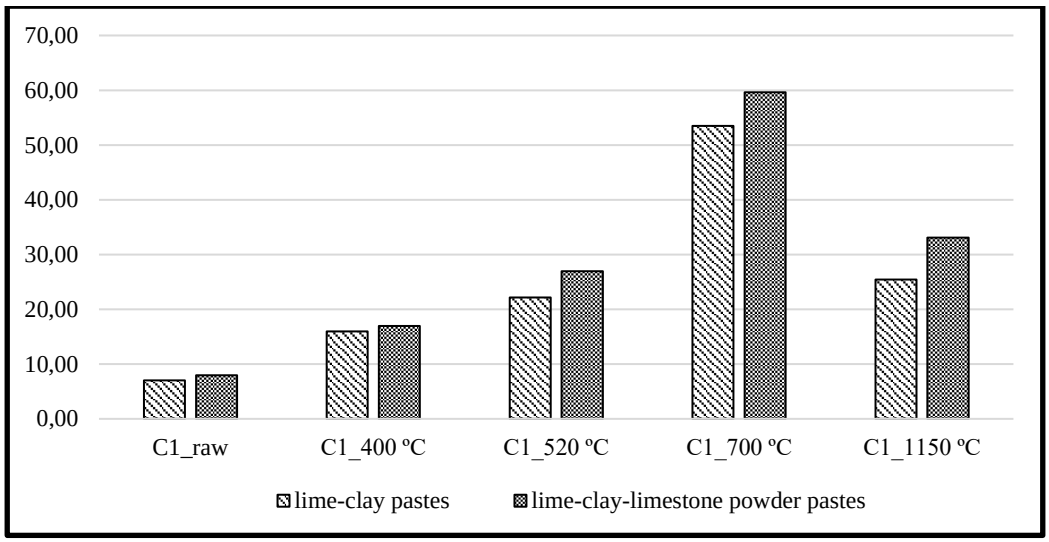

(b)

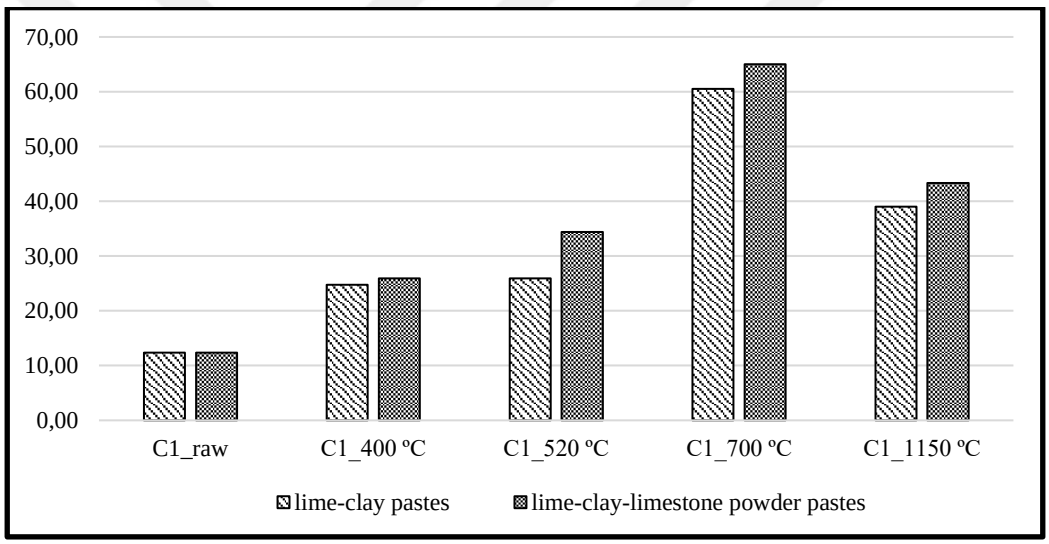

(c)

Figure 4.3.3 CH consumption comparison of lime-Clay 1 pastes with lime-Clay 1-limestone powder pastes at (a) 3 days, (b) 7 days, (c) 28 days

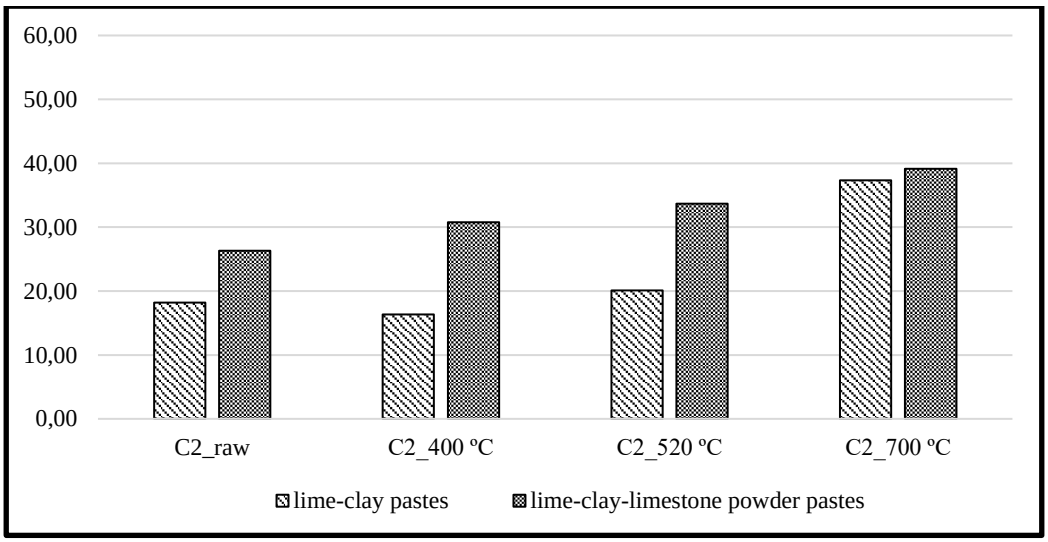
60,00
50,00
40,00
30,00
20,00
10,00
0,00
C2_raw
C2_400 ºC
C2_520 ºC
C2_700 ºC
lime-clay pastes
lime-clay-limestone powder pastes

(a)

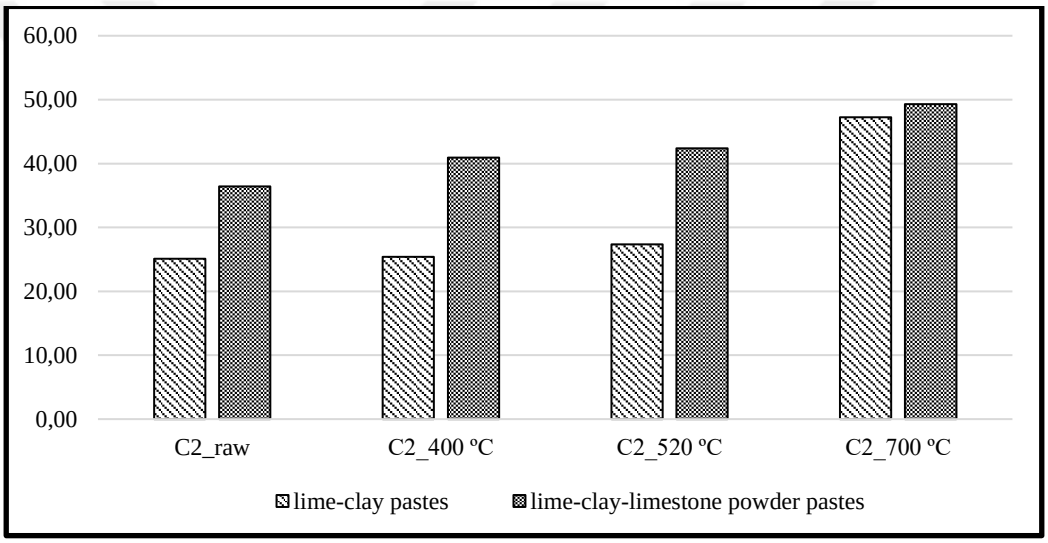
60,00
50,00
40,00
30,00
20,00
10,00
0,00
C2_raw
C2_400 ºC
C2_520 ºC
C2_700 ºC
lime-clay pastes
lime-clay-limestone powder pastes

(b)

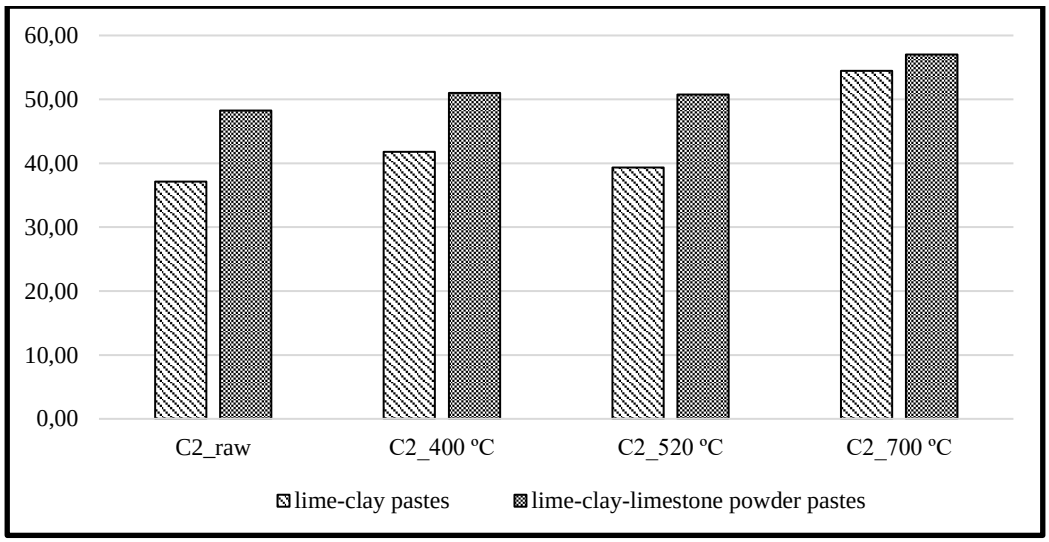

(c)

Figure 4.3.4 CH consumption comparison of lime-Clay 2 pastes with lime-Clay 2-limestone powder pastes at (a) 3 days, (b) 7 days, (c) 28 days

4.4 Isothermal Calorimetry

Paste prepared as a water/binder ratio of 0.4 was analysed in isothermal calorimetry, according to ASTM C 1679 [41]. The rate of heat evolution and cumulative heat determined by isothermal calorimetry method are presented in the bellow figures. The PC-Clay samples include Portland cement and calcined clay; the PC-Clay-Limestone powder samples contain cement, calcined clay, and limestone powder as a solid.

As shown in Figure 4.4.1, in raw samples, the maximum reaction rate has reached at about the same time. However, it was observed that raw clays and limestone powder addition accelerated maximum reaction rate. PC-C1_raw and PC-C1_raw-LS accelerated cement hydration between the hours of 6-21. However, after 21 hours, the rate of hydration heat release decreases. PC-C2_raw and PC-C2_raw-LS sample accelerated cement hydration from the first hour to the end of the 19 hours. However, after 19 hours, the rate of hydration heat release decreases. Both clay samples accelerated cement hydration for a while. When PC-Clay and PC-Clay-LS samples were compared, it was observed that the addition of limestone powder accelerated cement hydration.

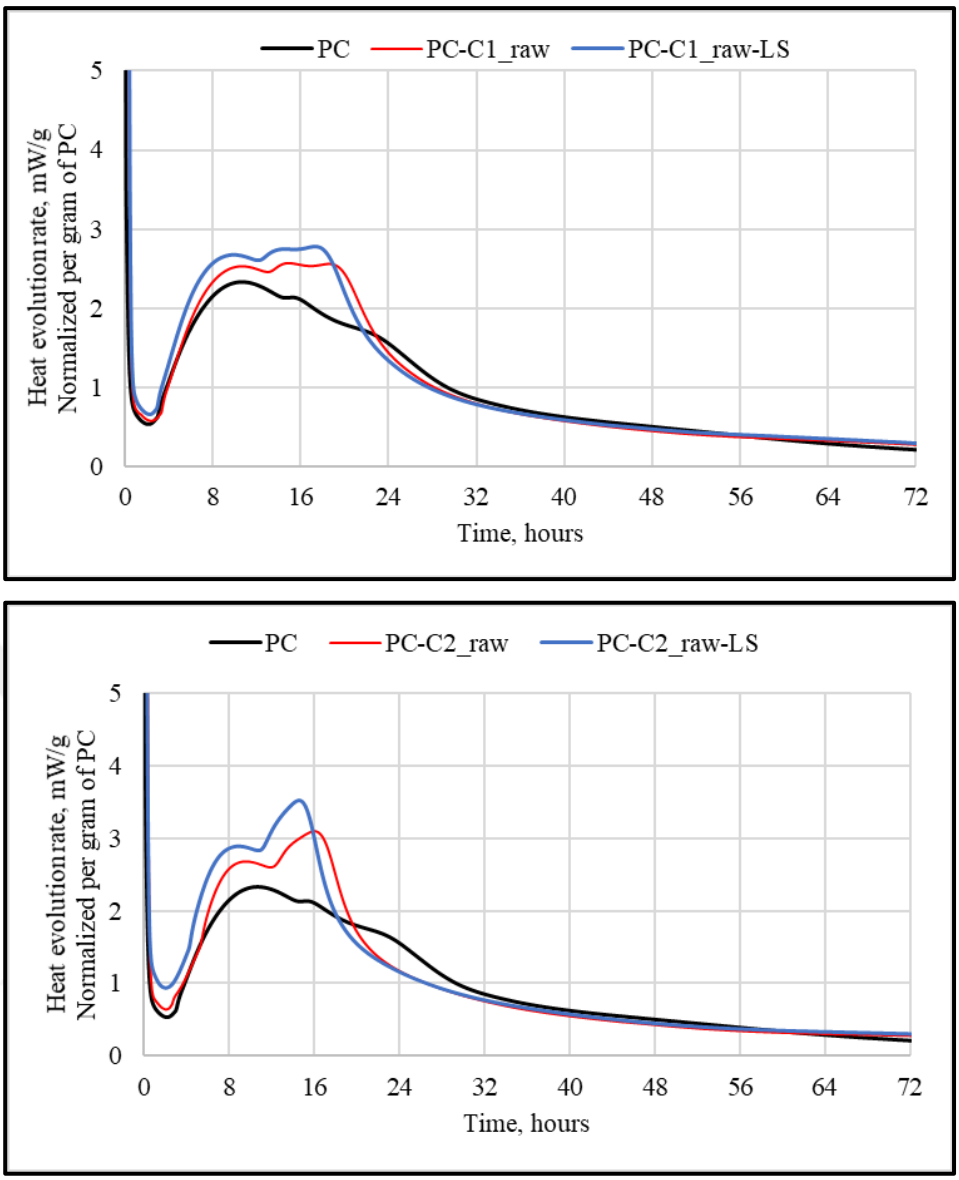

Figure 4.4.1 Heat release per gram of PC for PC and raw clays

The cumulative heat released is shown in Figure 4.4.2 per gram of PC for raw clays. The cumulative heat release by all clay samples as a result of hydration is more than the PC. Moreover, the addition of limestone powder in both clay samples resulted in more cumulative heat release. It has been observed that limestone powder addition is more effective especially in Clay 1 sample. In addition, it was also found that PC-C1_raw-LS had more cumulative heat release than PC-C2_raw-LS.

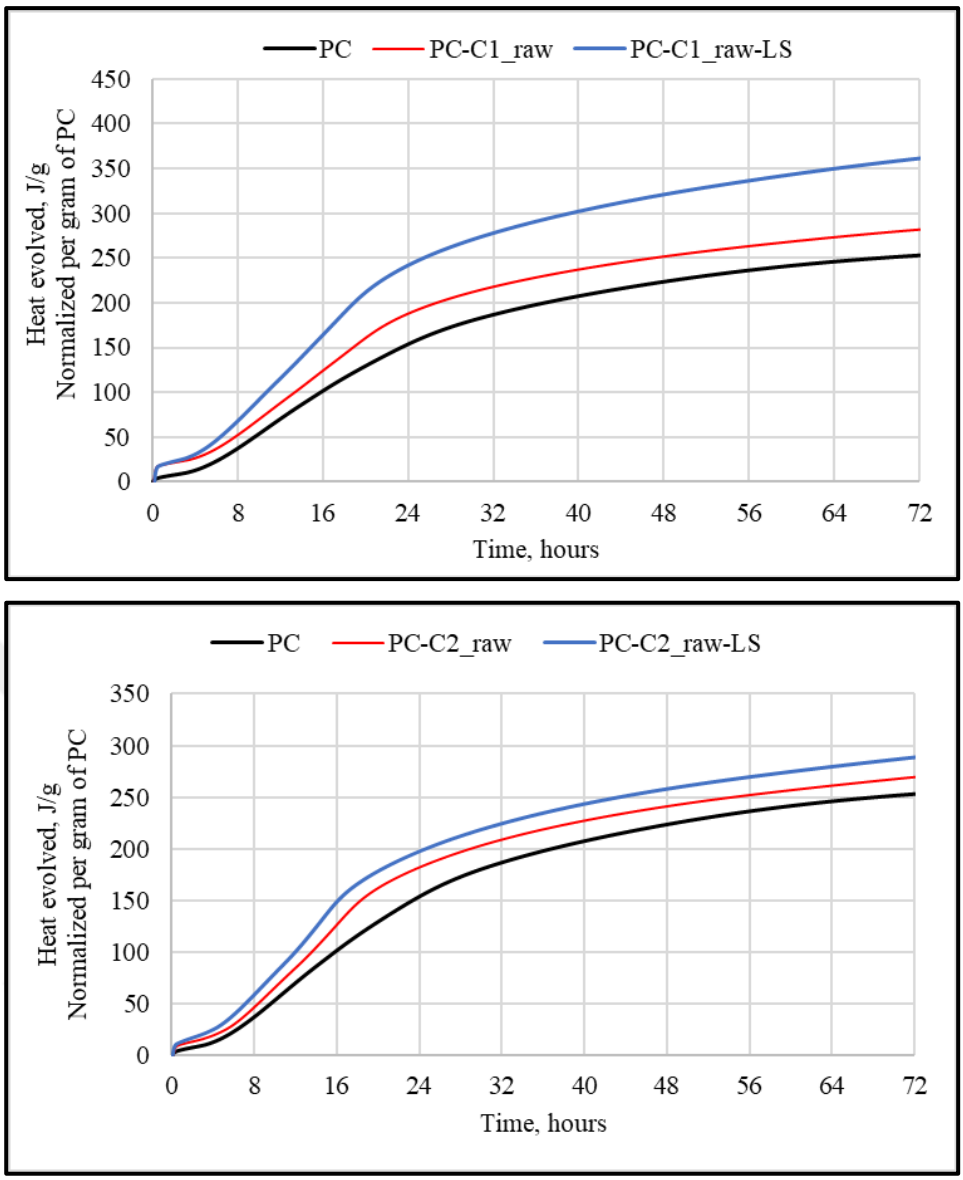

Figure 4.4.2 Cumulative heat release per gram of PC for PC and raw clays

As shown in Figure 4.4.3, in 400 ºC calcined samples the maximum reaction rate has reached at about the same time. However, it was observed that limestone powder addition accelerated maximum reaction rate. PC-C1_400 accelerated cement hydration between the hours of 10-25. However, after 25 hours, the rate of hydration heat release decreases. PC-C1_400-LS sample accelerated cement hydration from the first hour to the end of the 23 hours. However, after 23 hours, the rate of hydration heat release decreases. PC-C2_400 sample had almost no effect on cement hydration. PC-C2_400-LS accelerated cement hydration between the hours of 6-23. However, after 23 hours, the rate of hydration heat release decreases. When PC-Clay and PC-Clay-LS samples

were compared, it was observed that the addition of limestone powder accelerated cement hydration.

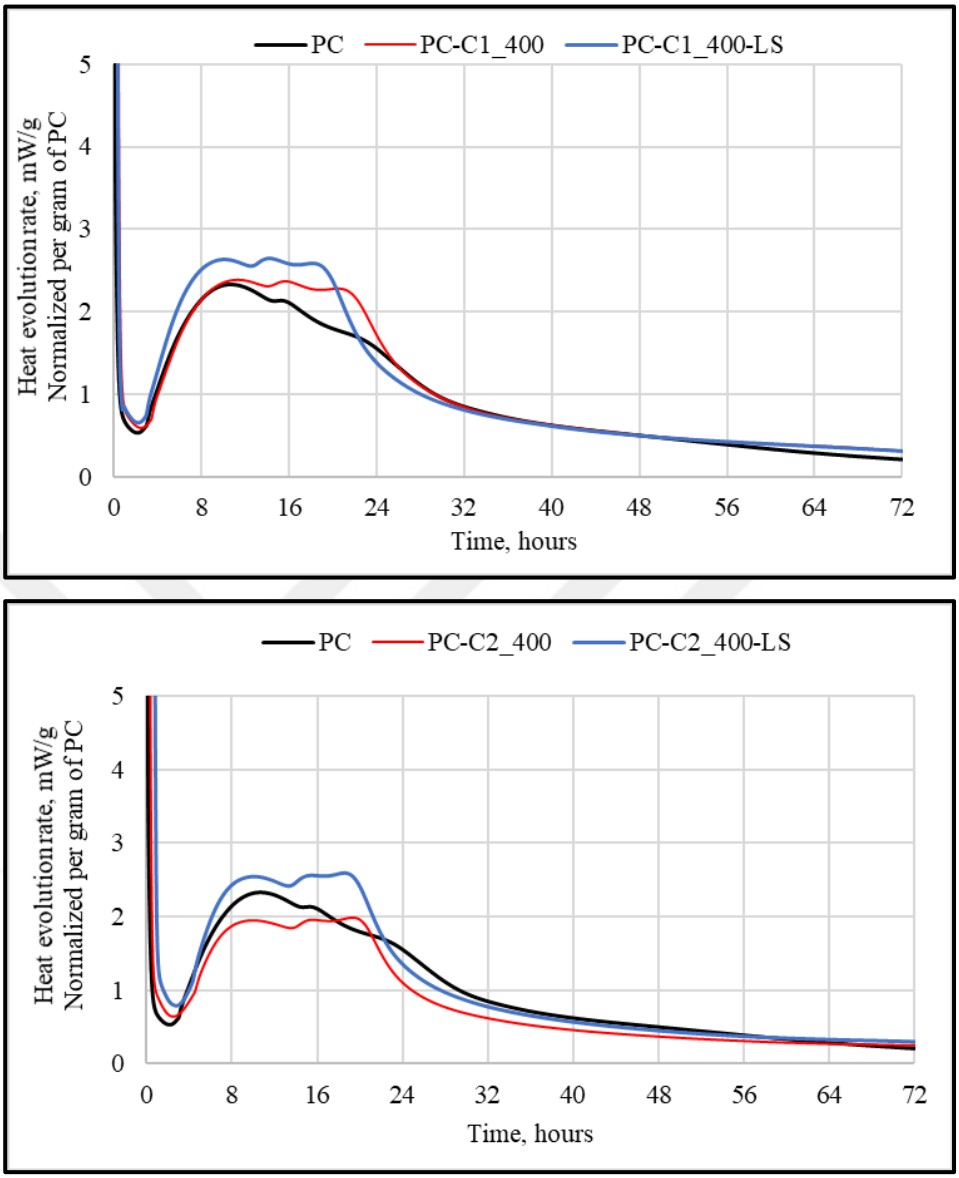

Figure 4.4.3 Heat release per gram of PC for PC and calcined clays at 400 ºC

The cumulative heat released is shown in Figure 4.4.4 per gram of PC for 400 ºC calcined clays. The cumulative heat release by all clay samples as a result of hydration is more than the PC. Moreover, the addition of limestone powder in Clay 1 samples resulted in more cumulative heat release. However, the addition of limestone powder in the Clay 2 sample had almost no effect on the cumulative heat release. It has been observed that limestone addition is more effective especially in Clay 1 sample. In addition, the cumulative heat release in PC_C1_400-LS and PC-C2_400-LS is almost equal.

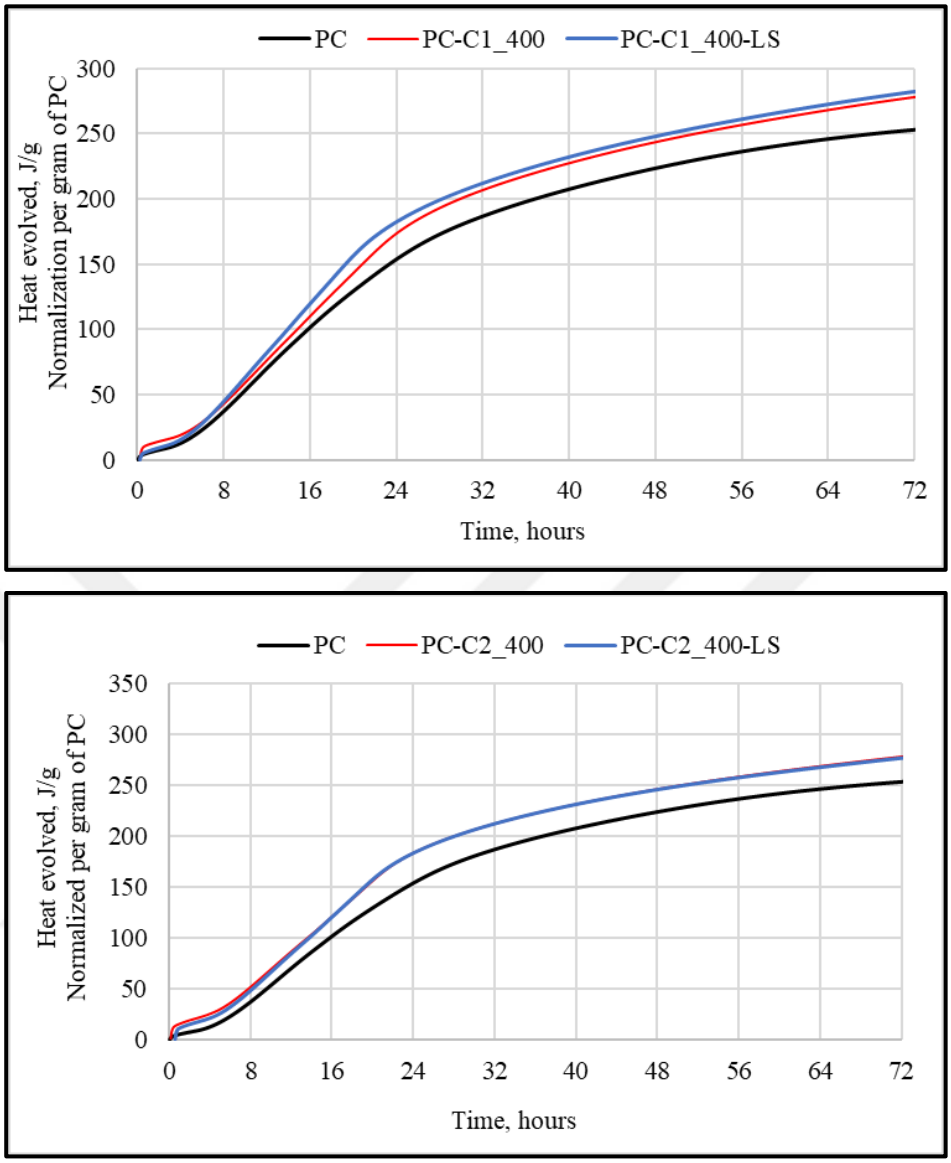

Figure 4.4.4 Cumulative heat release per gram of PC for PC and calcined clays at 400 ºC

As shown in Figure 4.4.5, in 520 ºC calcined samples the maximum reaction rate has reached at about the same time. However, it was observed that limestone powder addition accelerated maximum reaction rate PC-C1_520 accelerated cement hydration between the hours of 14-24. However, after 24 hours, the rate of hydration heat release decreases. PC-C1_520-LS sample accelerated cement hydration from the first hour to the end of the 22 hours. However, after 22 hours, the rate of hydration heat release decreases. PC-C2_520 and PC-C2_520-LS sample accelerated cement hydration from the first hour to the end of the 22 hours. However, after 22 hours, the rate of hydration

heat release decreases. When PC-Clay and PC-Clay-LS samples were compared, it was observed that the addition of limestone powder accelerated cement hydration.

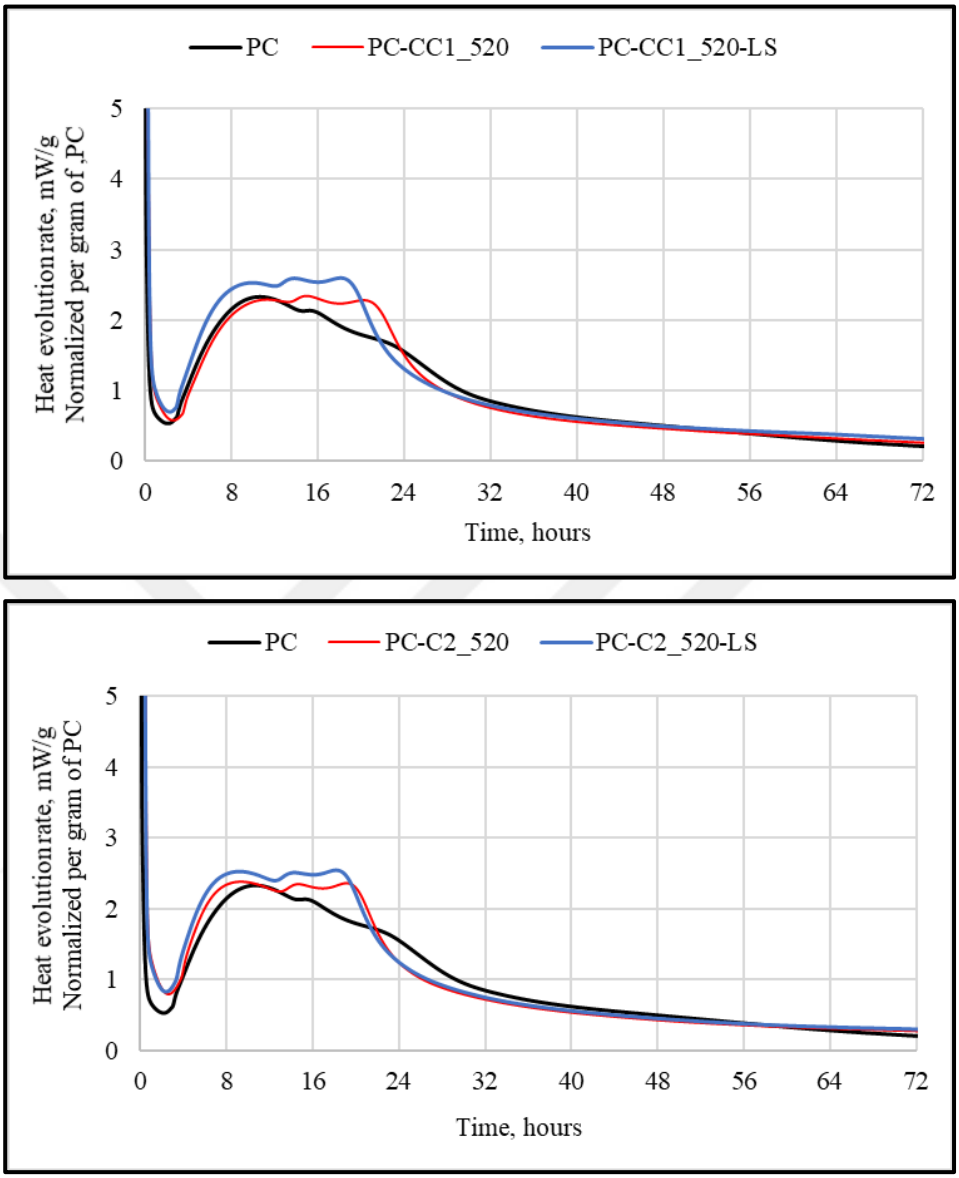

Figure 4.4.5 Heat release per gram of PC for PC and calcined clays at 520 ºC

The cumulative heat released is shown in Figure 4.4.6 per gram of PC for 520 ºC calcined clays. The cumulative heat release by all clay samples as a result of hydration is more than the PC. The addition of limestone powder in Clay 1 samples resulted in more cumulative heat release. However, the addition of limestone powder in the Clay 2 sample had almost no effect on the cumulative heat release. In addition, the cumulative heat release in PC-C1_520-LS and PC-C2_520-LS is almost equal.

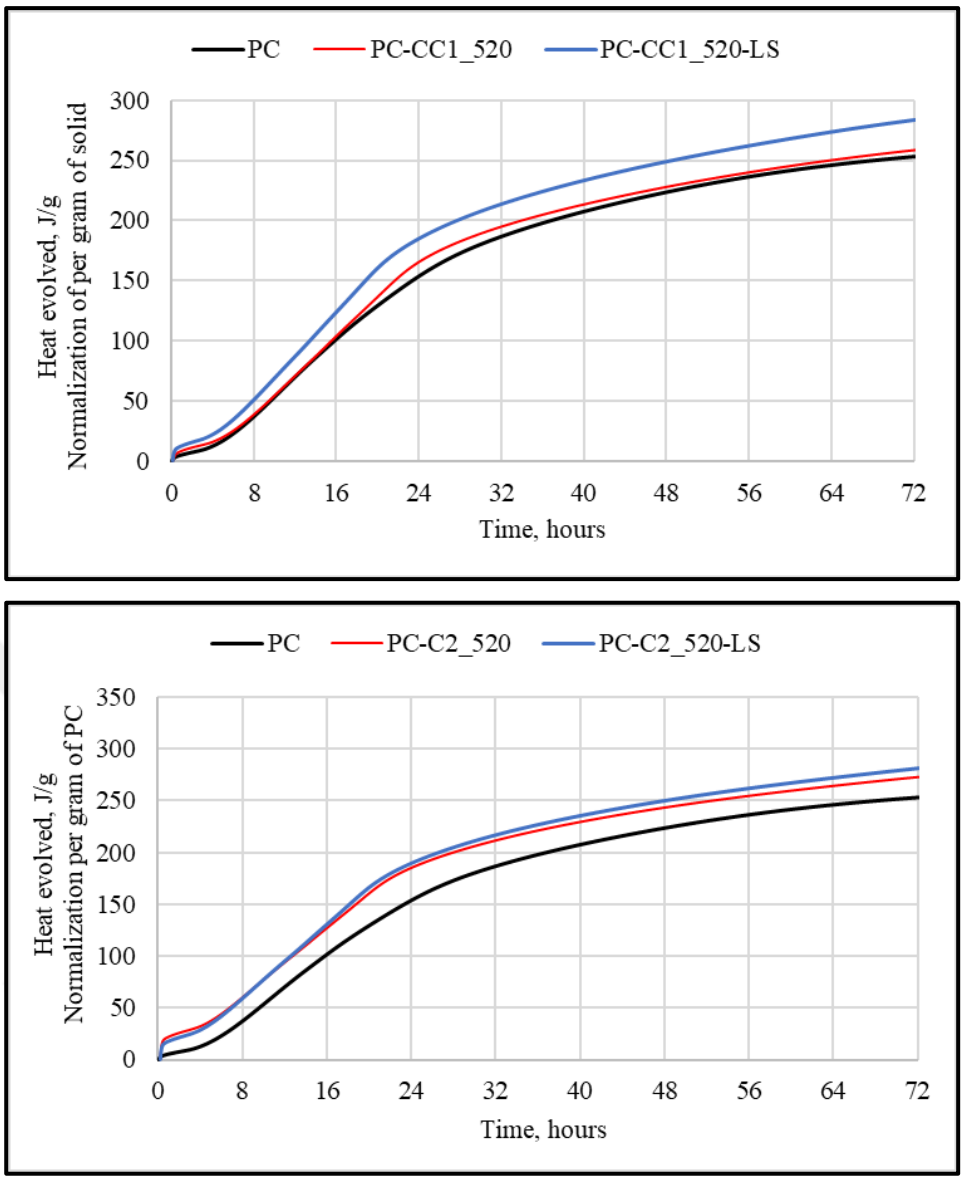

Figure 4.4.6 Cumulative heat release per gram of PC for PC and calcined clays at 520 ºC

As shown in Figure 4.4.7, in 700 ºC calcined samples the maximum reaction rate was reached late. However, it was observed that calcined clays and limestone powder addition accelerated maximum reaction rate. PC-C1_700 accelerated cement hydration between the hours of 10-20. PC-C1_700-LS sample accelerated cement hydration between the hours of 8-20. However, after 20 hours, the rate of hydration heat release decreases for both samples. PC-C2_700 sample accelerated cement hydration from the first hour to the end of the 22 hours. However, after 22 hours, the rate of hydration heat release decreases. PC-C2_700-LS sample accelerated cement hydration between the hours of 8-21. However, after 21 hours, the rate of hydration heat release decreases.

When PC-Clay and PC-Clay-LS samples were compared, it was observed that the addition of limestone powder accelerated cement hydration.

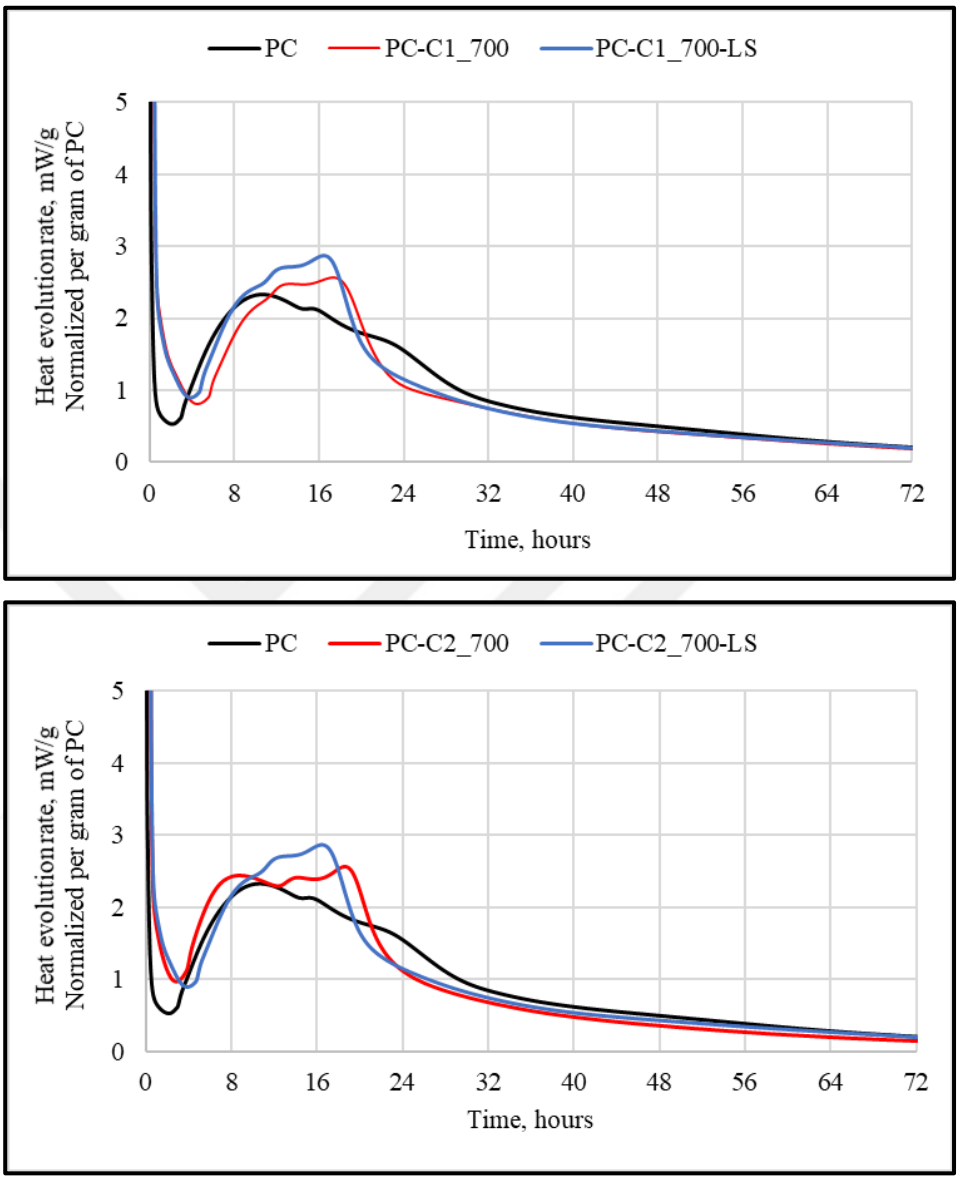

Figure 4.4.7 Heat release per gram of PC for PC and calcined clays at 700 ºC

The cumulative heat released is shown in Figure 4.4.8 per gram of PC for 700 ºC calcined clays. The cumulative heat release by all clay samples as a result of hydration is more than the PC. The addition of limestone powder in Clay 1 samples resulted in more cumulative heat release. However, the addition of limestone powder in the Clay 2 sample had almost no effect on the cumulative heat release. In addition, the cumulative heat release in PC-C1_700-LS and PC-C2_700-LS is almost equal.

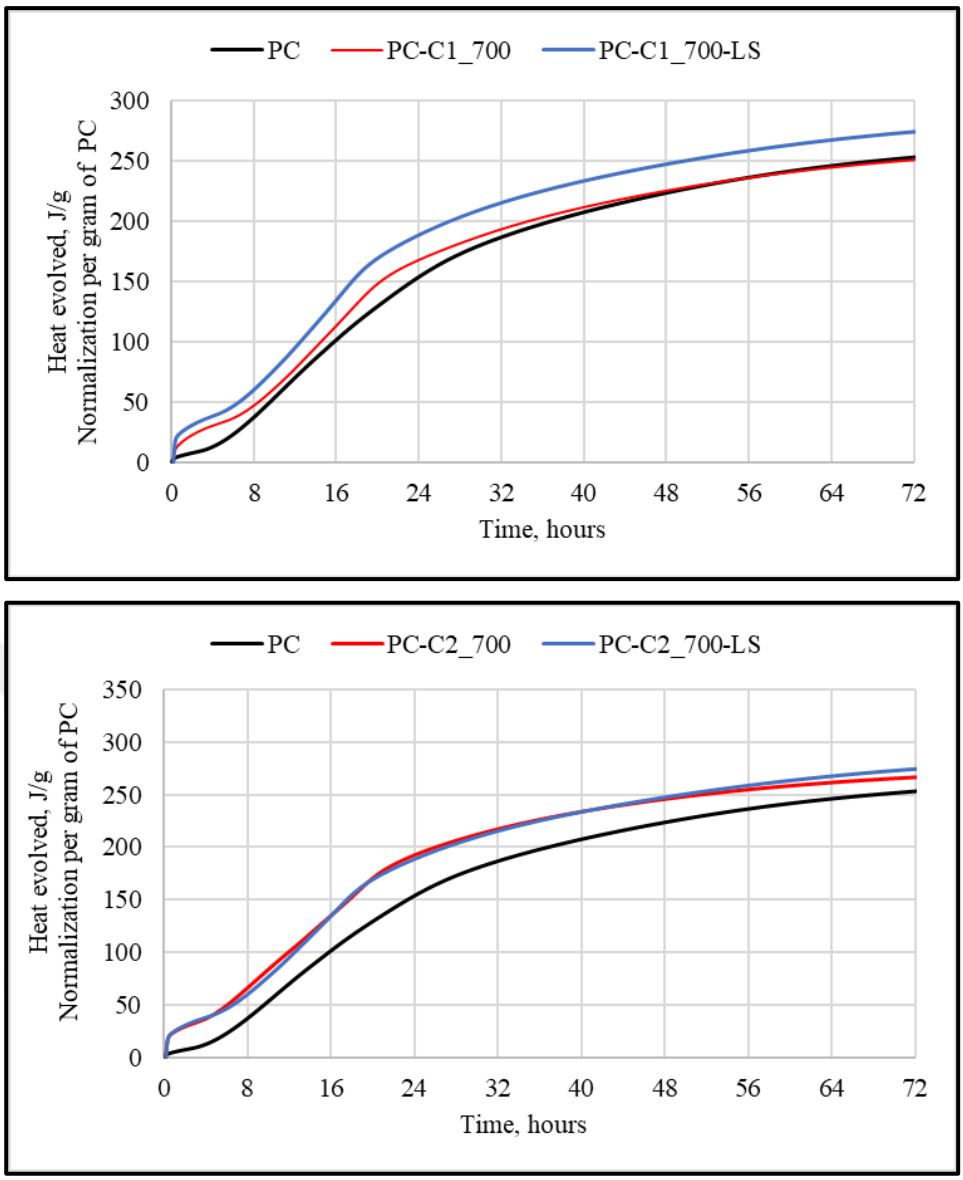

Figure 4.4.8 Cumulative heat release per gram of PC for PC and calcined clays at 700 ºC

As shown in Figure 4.4.9, in 1150 ºC calcined samples the maximum reaction rate has reached at about the same time. However, it was observed that limestone powder addition accelerated maximum reaction rate. PC-C1_1150 accelerated cement hydration between the hours of 13-25. However, after 25 hours, the rate of hydration heat release decreases. PC-C1_1150-LS sample accelerated cement hydration from the first hour to the end of the 23 hours. However, after 23 hours, the rate of hydration heat release decreases. When PC-Clay and PC-Clay-LS samples were compared, it was observed that the addition of limestone powder accelerated cement hydration.

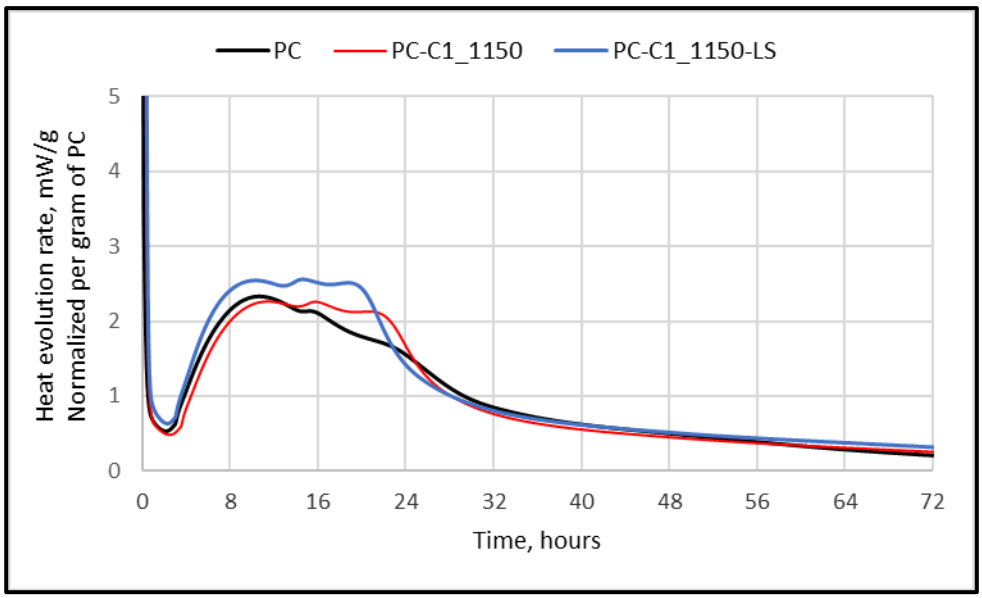

Figure 4.4.9 Heat release per gram of PC for PC and calcined clay 1 at 1150 ºC

The cumulative heat released is shown in Figure 4.4.10 per gram of PC for 1150 ºC calcined clays. The cumulative heat release by PC-C1_1150-LS sample as a result of hydration is more than the PC and PC-C1_1150. The cumulative heat release of the PC-C1_1150 sample is almost identical to that of the PC. The addition of only calcined clay had almost no effect on the cumulative heat release.

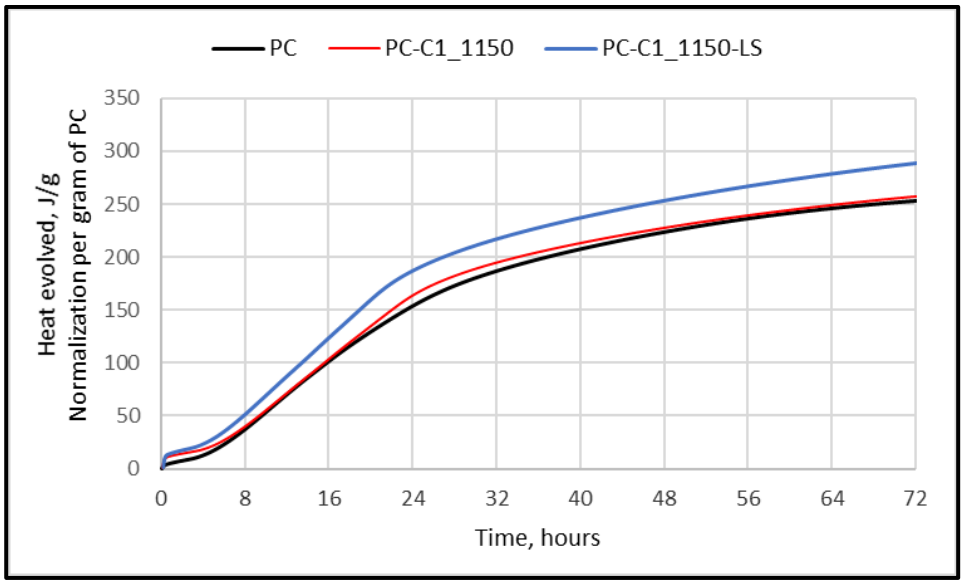

Figure 4.4.10 Cumulative heat release per gram of PC for PC and calcined clay 1 at 1150 ºC

4.5 Strength Activity Index

Water requirements and strength activity indices of the pozzolanic materials were determined following ASTM C 311 [42] and given in Table 4.5.1 (calcined clay at 520 ºC) and Table 4.5.2 (calcined clays at 700 ºC). Strength activity index values were calculated according to the compressive strength of mortar values given in Table 4.5.1. The PC-C samples do not contain limestone powder, and the PC-C-LS contain limestone powder. Thus, the effect of limestone powder addition on SAI value was observed.

Regarding water requirement of the natural pozzolans, it is seen that the water requirement of all samples used is lower than the limit value (115%) recommended by ASTM C618 [19]. In all mortars, Clay 1 sample has a lower water requirement than Clay 2. Kaolinite is very stable and consists of silica alumina layers, which are strongly bonded to each other. Montmorillonite is consisting of two silica, one alumina layer. It is not as stable as kaolinite; the inter-layer bonds are very weak. Therefore, a large amount of water can easily enter the structure [56]. Clay 2 contains montmorillonite mineral; the high-water requirement is attributed to this feature. When the samples calcined at 520 and 700 °C were compared, it was observed that the water requirement increased as the temperature increased. However, water requirement cannot be attributed only to the mineralogical structure. The water requirement varies depending on the type of dominant clay mineral, degree of dehydroxylation, fineness, or BET surface of the calcined clay [57]. Since the BET surface area of Clay 2 is higher than Clay 1, it is seen that Clay 2 water requirement is also higher. When the PC-Clay and PC-Clay-LS were compared, it was observed that the addition of limestone powder reduced the water requirement. This is due to the decrease in the amount of calcined clay. Since the higher the amount of calcined clay, the higher the need for water.

Kucukyıldırım and Uzal, have determined the water requirements for the raw and calcined states of two different zeolites. The highest water requirement for the first zeolite was determined as 120% and the lowest as 110%. The highest water requirement for the second zeolite was determined as 110% and the lowest as 105% [58]. Clay 1 has lower water requirements than zeolites. On the other hand, the water requirements of Clay 2 are very close to zeolites. Hence, the water requirement of Clay 2 did not exceed the limit value (115%) like zeolite.

According to ASTM C618, any of the 7- or 28-day strength activity index values should meet 75%. Experimental results showed that only PC-CC1_700 ºC and PC-CC1_700 ºC-LS sample is more than 75% of the 7-day SAI values. However, the 28-day SAI values for all samples meet the limit value of ASTM C618. When 7- or 28-day values were evaluated, it was seen that the addition of limestone powder increased SAI value in all samples. The samples with the lowest strength activity index value for 7 days are PC-C1_520 ºC and PC-C2_700 ºC samples. The highest SAI values for 7 days are PC-C1_700 ºC-LS sample. The 7-day SAI value of PC-C2_700 ºC was lower than PC-C1_520 ºC-LS and 28-day values were equal. From this point of view, instead of calcining and using Clay 2 at 700 °C, Clay 1 can be used by calcining at a much lower temperature, such as 520 °C, and adding limestone powder. Furthermore, the calcined form of PC-CC2_520 °C-LS meets the limit value (75%) given in accordance with ASTM C618. The samples PC-CC1_520 °C and PC-CC2_520 °C do not meet the ASTM C618 limit value without the addition of limestone powder. Since Clay 1 is finer than Clay 2, Clay 1 also shows filler effect. Filler effect is more dominant especially in 7 days due to low pozzolanic activity at early ages.

Tangpagasit et al. studied effect of particle size of fly ash on pozzolanic reaction. Fly ash used in the study was examined in four different sizes as original (OF), small (SF), medium (MF) and large (LF). These fly ashes were then subjected to SAI testing according to ASTM C311. The 7-day SAI values for OF, SF, MF and LF are 77, 94, 82 and 66%, respectively. The 28-day SAI values for OF, SF, MF and LF are 81, 108, 93 and 66%, respectively. Only the large size fly ash does not meet the limit value of ASTM C618 [59].

Rose-Lam et al. conducted a study on the pozzolanic activities of natural Cuban zeolite rocks. These zeolites were crushed using a ball mill for 20 (Z1), 40 (Z2), 60 (Z3) and 90 (Z4) minutes. These zeolites were then subjected to SAI testing according to ASTM C311. The 7-day SAI values for Z1, Z2, Z3 and Z4 are 29.7, 46.6, 76.3 and 109.2%, respectively. The 28-day SAI values for Z1, Z2, Z3 and Z4 are 53.1, 71.7, 94.5 and 127.2%, respectively. Due to the increased surface area depending on the crushed time, only Z3 and Z4 meet ASTM C618 values [60].

Mardani-Aghabaglou et al. compared the mortars containing fly ash, silica fume and metakaolin in terms of mechanical properties and durability performances. Strength activity indices of the SCMs were determined according to ASTM C311. The 7-day SAI values for fly ash, silica fume and metakaolin are 69, 101 and 102%, respectively.

The 28-day SAI values for fly ash, silica fume and metakaolin are 79, 132 and 110%, respectively [61].

SAI values of the C1_700 ºC sample are very promising compared to the different SCMs in the literature. Especially as a result of the addition of limestone powder, the 28-day SAI value is 112%. This value is higher than the SAI values of many SCMs such as fly ash and zeolite in the literature.

Table 4.5.1 Compressive strength of mortar

Sample No	Compressive strength, MPa	
	7-d	28-d
Control mixture	36.8	45.5
PC-C1_520 ºC	24.1	33.6
PC-C1_520 ºC-LS	27.1	38.3
PC-C2_520 ºC	24.9	32.5
PC-C2_520 ºC-LS	27.1	35.5
PC-C1_700 ºC	28.7	46.5
PC-C1_700 ºC-LS	30.9	51
PC-C2_700 ºC	24.1	38.4
PC-C2_700 ºC-LS	26.8	43.2

Table 4.5.2 Water requirements and SAI of calcined clays at 520 ºC

	PC-C1 520 ºC	PC-C1 520 ºC-LS	PC-C2 520 ºC	PC-C2 520 ºC-LS
Water/binder	0.508	0.498	0.540	0.528
Water Requirement, %	105	103	111	109
Strength activity index, %				
7-days	65.5	73.6	67.7	73.6
28-days	73.7	84.2	71.3	78.0

Table 4.5.3 Water requirements and SAI of calcined clays at 700 ºC

	PC-C1 700 ºC	PC-C1 700 ºC-LS	PC-C2 700 ºC	PC-C2 700 ºC-LS
Water/binder	0.520	0.506	0.548	0.534
Water Requirement, %	107	104	113	110
Strength activity index, %				
7-days	77.9	83.9	65.4	72.8
28-days	102.1	112.1	84.3	94.8

4.6 CO_2 emissions of Calcined Clay

The contribution of the cement industry to CO_2 emissions worldwide is indisputable. In recent years, efforts have been accelerated to increase energy efficiency in the cement production process and to reduce CO_2 emissions. Low-energy clinker production and alternative materials to replace cement are researched to reduce CO_2 emissions [62].

If slag and pulverized fuel ash are used as a substitute in cement clinker at a ratio of 1:1, CO_2 emissions are reduced by 17%. The future of slag and pulverized fuel ash is at risk due to the decline in worldwide interest in steel production and fossil fuels. Therefore, the search for alternative SCM is very significant. Clays are a good alternative because they are easily accessible and calcined at low temperatures. The reason that calcined clays have been used less so far is that they are not commercially available, and their chemical composition varies. However, this is changing due to increased controls on CO_2 emissions [63].

The following interpretation of CO_2 emissions was made with the help of a preliminary assessment method proposed by Zhou et. al. Accordingly, the energy used to calcine a ton of clay from 25 ºC to a certain temperature is calculated as follows [63]:

$$E = m \times c \times \Delta T$$

in this equation E is the energy, m is the mass, c is the specific heat capacity and ΔT is the change in temperature. In experimental studies, it is seen that 700 ºC calcination

temperature is suitable for both clay samples. The specific heat capacity of the clays was selected as 900 J/kgK according to the different specific heat capacity values obtained from the literature in Table 4.6.1. The E value calculated based on all data is as follows:

$$E= 1000 \times 900 \times (700-25) = 608 \text{ MJ} = 170 \text{ kWh}$$

Table 4.6.1 Specific heat capacity of different clays

Sample No	Specific heat capacity (J/kgK)	Reference
1	851-889	[64]
2	930	[65]
3	900	[63]
4	930-974	[66]

The CO_2 emissions of natural gas combustion is 0.21 $kgCO_2$/kWh [67]. CO_2 emissions associated with the production of one tonne of calcined clay is:

$$170 \text{ kWh} \times 0.21 \text{ kgCO}_2/\text{kWh} = 36 \text{ kgCO}_2$$

Production of one tonne of Portland cement clinker emits ~ 800 $kgCO_2$ [63]. Thus, the CO_2 emission of the calcined clay is approximately 95% lower than that of CEM I. A 20 wt% replacement of cement in concrete by calcined clay therefore reduces carbon emissions from 800 $kgCO_2$/tonne for 100% CEM I, to 645 $kgCO_2$/tonne for an 80:20 CEM I:calcined clay binder, equivalent to an 19% reduction overall. At 30 wt% replacement CO_2 are reduced by 28%.

Gettu et al. studied on life cycle assessment for ordinary Portland cement (OPC), Portland pozzolan cement (PPC), Portland slag cement (PSC) and limestone calcined clay (LC_3) systems. The composition ratios of the cements used in this study are as follows: PPC: 65% clinker and 30% fly ash, PSC: 45% clinker and 50% slag, and LC_3: 50% clinker. In case studies used different system boundaries such as ground-to-gate, gate-to-gate and cement sustainability initiative protocol. For ground-to-gate system OPC, PPC, PSC and LC_3 systems, CO_2 emissions are 820, 625, 490 and 550 $kgCO_2$,

respectively. When OPC and LC_3 systems are compared for three different system boundaries, it is seen that LC_3 systems cause approximately 30% less CO_2 emission [68].

Andres et al. and Berriel et al. conducted an LCA study in the Cuban cement industry using the cradle-to-gate approach method. The unit CO_2 emissions for OPC, PPC and LC_3 systems were 890, 765 and 562 $kgCO_2$/tonne, respectively. In this study, LC_3 technology was found to be a good option for reducing CO_2 emissions [69, 70].

Chapter 5

5 Conclusions and Future Prospects

5.1 Conclusions

In this dissertation study, potential use of the clay samples obtained from two different regions of Turkey (Balıkesir and Niğde) as SCM was examined. The aim of the study is to contribute to sustainable concrete production by calcining low-quality clays at lower temperatures than Portland cement. The following conclusions can be drawn based on the experimental studies;

1. According to the XRF analyses of the raw and calcined clay samples used, as the calcination temperature increases, the materials are enriched in silica and alumina content. Furthermore, after high temperatures, the amount of sulphate is decreased. However, even at 1100 ºC, the sulphate did not completely disappear.
2. XRD patterns of raw and calcined clay samples were examined and their mineralogical compositions were compared. Clay 1 contained kaolinite and quartz minerals, and when calcined at 400 and 520 ºC, the mineralogical structure was almost unchanged. However, it was observed that the kaolinite peaks disappeared when calcined at 700 °C. At 1150 °C, mullite peaks were observed as a result of the sintering of the sample. The sample began to transition from the amorphous phase to the crystal phase. Therefore, the pozzolanic activities of the samples calcined at 1150 °C are lower than those calcined at 700 °C. The mineralogical structure of the Clay 2 sample is quite different from that of Clay 1. Montmorillonite, kaolinite, and sanidine peaks were observed in Clay 2, as well as glassy phases. Sanidine peaks are still observed even in samples calcined at 700 °C, because the decomposition of the sanidine occurs at around 1300 °C. Clay 2 sample was not a completely amorphous phase at 700 °C.

3. Kaolinite and calcined kaolinite amounts were calculated from the weight loss between 400-700 ºC from TGA curves. The amount of kaolinite of Clay 1 was found to be higher than Clay 2. Accordingly, the amount of calcined kaolinite is higher in Clay 1.
4. Considering CH consumption in lime pastes, it was determined that 700 ºC is the most efficient temperature for both clay samples at all ages. It was also found that the samples calcined at relatively low temperatures (400 ºC and 520 ºC) did not increase the consumption of CH much more than the raw samples. Calcination of the Clay 1 sample at 1100 °C decreased the consumption of CH compared to the consumption at 700 °C. When the CH consumption of lime-clay and lime-clay-limestone powder pastes was compared at the end of 28 days, it was determined that CH consumption for C1_700 ºC increased from 60.5 to 65.04 and 54.4 to 57 for C2_700 ºC. It was observed that consumption of CH increased at almost all temperature values as a result of the addition of limestone powder. In other words, the addition of limestone powder positively affected pozzolanic activity. Although the BET surface area of Clay 2 is higher, it is seen in terms of CH consumption that pozzolanic activity of Clay 1 is higher. Due to the chemical and mineralogical composition of Clay 1, it contains more alumina.
5. As a result of the isothermal calorimeter experiments, it was observed that calcined clays and limestone powder generally accelerated maximum reaction rate when the heat release rates were compared. However, as a result of the addition of clay samples, the maximum reaction rate was reached later. Also, when PC-Clay and PC-Clay-LS samples were compared, it was observed that the addition of limestone powder accelerated Portland cement hydration. The cumulative heat release by all clay samples as a result of hydration is more than the PC. The addition of limestone powder in clay samples resulted in more cumulative heat release.
6. The BET surface area of Clay 2 is higher than Clay 1, and the water requirement is also higher. The positive effect of limestone powder addition is evident on the compressive strength of mortar samples. The positive effect of the addition of limestone powder is because of filler effect and reducing the water requirement. In addition, as seen in the results of CH consumption, pozzolanic activity increases. Furthermore, it was found that the PC-C1_520 ºC-LS sample calcined at was comparable to the PC-CC2_700 ºC sample . This shows that the addition

of limestone powder makes the clays calcined at lower temperatures more efficient. The addition of limestone powder allowed the samples to meet the ASTM C618 limit value (75%) at low temperatures, such as 520 ° C. In addition, PC-CC1_700 ºC-LS sample has a 28-day SAI value (112%) which is superior to many SCMs such as fly ash and zeolite in the literature. Since Clay 1 is finer than Clay 2, Clay 1 also shows filler effect. Filler effect is more dominant especially in 7 days due to low pozzolanic activity at early ages.

7. As a result of the calculations made with the preliminary assessment method for CO_2 emissions, 20% substitution of Portland cement with calcined clay reduced carbon dioxide emissions by 19%. At 30 wt% replacement level CO_2 reduction could be increased to 28%.
8. As a result of all experimental studies, it is understood that the potential of using clays of lower quality as SCM is quite high. In addition, for the use of calcined clays as SCM, variables such as pozzolanic activity, water requirement, surface area and filling effect should be evaluated together.

5.2 Future Prospects

More clay samples obtained from different regions of Turkey can be studied. Thus, the potential use of the calcined clay as a supplementary cementing material in Turkey more clearly understandable. Besides, it can be compared with other supplementary cementing materials used in terms of pozzolanic activity, water requirement, workability, setting time, strength, and durability.

Experiments can be repeated with clays containing SiO_2, Al_2O_3, and alkali in suitable amounts to produce metakaolin. Therefore, the performances of low-quality calcined clays and metakaolin can be evaluated comparatively for the cementitious system. With the obtained calcined clays, strength and durability tests can be performed, and the performance of the materials in concrete can be examined in more detail.

Studies have shown that the addition of limestone powder positively affects pozzolanic activity. For better observation of the limestone calcined clay cement system, concrete strength and durability tests should be performed in addition to paste and mortar tests.

In the study, it was found that calcined clays increased the water requirement. Hence, the use of calcined clays with other additives such as superplasticizer is also an interesting research topic.

For a clear assessment of environmental impacts, life cycle assessment can be employed for cementitious systems substituted with calcined clays.

BIBLIOGRAPHY

[1] R. M. Andrew, "Global CO_2 emissions from cement production, 1928-2017," *Earth System Science Data*, vol. 10, pp. 2213-2239, Dec 10 2018.

[2] H. G. v. Oss, *Cement. USGS 2014 Minerals Yearbook*: United States Geological Survey, 2014.

[3] H. G. v. Oss, *USGS Mineral commodity summaries*: United States Geological Survey, 2018.

[4] S. C. Taylor-Lange, E. L. Lamon, K. A. Riding, and M. C. G. Juenger, "Calcined kaolinite-bentonite clay blends as supplementary cementitious materials," *Applied Clay Science*, vol. 108, pp. 84-93, May 2015.

[5] A. A. Ramezanianpour, *Cement Replacement Materials: Properties, Durability, Sustainability*: Springer Berlin Heidelberg, 2013.

[6] S. Mindess, *Developments in the Formulation and Reinforcement of Concrete*: Woodhead Publishing, 2008.

[7] K. Scrivener, F. Martirena, S. Bishnoi, and S. Maity, "Calcined clay limestone cements (LC_3)," *Cement and Concrete Research*, vol. 114, pp. 49-56, Dec 2018.

[8] S. Hollanders, R. Adriaens, J. Skibsted, O. Cizer, and J. Elsen, "Pozzolanic reactivity of pure calcined clays," *Applied Clay Science*, vol. 132, pp. 552-560, Nov 2016.

[9] Z. Li, *Advanced Concrete Technology*: Wiley, 2011.

[10] J. Newman and B. S. Choo, *Advanced Concrete Technology 1: Constituent Materials*: Elsevier Science, 2003.

[11] P. Mehta and P. J. M. Monteiro, *Concrete: Microstructure, Properties, and Materials*: McGraw-Hill Education, 2006.

[12] ASTM, "ASTM C150 " in *Standard Specification for Portland Cement*, ed. West Conshohocken: ASTM International, 2019.

[13] D. J. M. Flower and J. G. Sanjayan, "Green house gas emissions due to concrete manufacture," *The International Journal of Life Cycle Assessment*, vol. 12, p. 282, May 02 2007.

[14] C. Y. Zhang, R. Han, B. Y. Yu, and Y. M. Wei, "Accounting process-related CO2 emissions from global cement production under Shared Socioeconomic Pathways," *Journal of Cleaner Production*, vol. 184, pp. 451-465, May 20 2018.

[15] A. Bosoaga, O. Masek, and J. E. Oakey, "CO2 Capture Technologies for Cement Industry," *Greenhouse Gas Control Technologies 9*, vol. 1, pp. 133-140, 2009.

[16] M. Thomas, *Supplementary Cementing Materials in Concrete*: CRC Press, 2013.

[17] *Pumice and Roman Concrete*. Available: http://pumiceconcrete.com/pumice-roman-concrete.html (02 Oct 2019)

[18] F. M. Lea and P. C. Hewlett, *Lea's Chemistry of Cement and Concrete*: Arnold, 1998.

[19] ASTM, "ASTM C618 " in *Standard Specification for Coal Fly Ash and Raw or Calcined Natural Pozzolan for Use in Concrete*, ed. West Conshohocken: ASTM International, 2019.

[20] A. Askarinejad, A. R. Pourkhorshidi, and T. Parhizkar, "Evaluation the pozzolanic reactivity of sonochemically fabricated nano natural pozzolan," *Ultrasonics Sonochemistry*, vol. 19, pp. 119-124, Jan 2012.

[21] B. B. Sabir, S. Wild, and J. Bai, "Metakaolin and calcined clays as pozzolans for concrete: a review," *Cement & Concrete Composites*, vol. 23, pp. 441-454, Dec 2001.
[22] G. Kakali, T. Perraki, S. Tsivilis, and E. Badogiannis, "Thermal treatment of kaolin: the effect of mineralogy on the pozzolanic activity," *Applied Clay Science*, vol. 20, pp. 73-80, Sep 2001.
[23] E. Amankwah, M. Bediako, and C. Kankam, "Influence of calcined clay pozzolana on strength characteristics of Portland cement concrete," *International Journal of Material Science and Application*, vol. 3(3), 01/01 2014.
[24] N. Garg and J. Skibsted, "Pozzolanic reactivity of a calcined interstratified illite/smectite (70/30) clay," *Cement and Concrete Research*, vol. 79, pp. 101-111, Jan 2016.
[25] S. Ng, B. P. Jelle, and T. Staehli, "Calcined clays as binder for thermal insulating and structural aerogel incorporated mortar," *Cement & Concrete Composites*, vol. 72, pp. 213-221, Sep 2016.
[26] P. Suraneni and J. Weiss, "Examining the pozzolanicity of supplementary cementitious materials using isothermal calorimetry and thermogravimetric analysis," *Cement & Concrete Composites*, vol. 83, pp. 273-278, Oct 2017.
[27] N. S. Msinjili, G. J. G. Gluth, P. Sturm, N. Vogler, and H. C. Kuhne, "Comparison of calcined illitic clays (brick clays) and low-grade kaolinitic clays as supplementary cementitious materials," *Materials and Structures*, vol. 52, Oct 2019.
[28] S. Maisanaba, S. Pichardo, M. Puerto, D. Gutierrez-Praena, A. M. Camean, and A. Jos, "Toxicological evaluation of clay minerals and derived nanocomposites: A review," *Environmental Research*, vol. 138, pp. 233-254, Apr 2015.
[29] A. Tironi, C. C. Castellano, V. L. Bonavetti, M. A. Trezza, A. N. Scian, and E. F. Irassar, "Kaolinitic calcined clays - Portland cement system: Hydration and properties," *Construction and Building Materials*, vol. 64, pp. 215-221, Aug 14 2014.
[30] R. Siddique and J. Klaus, "Influence of metakaolin on the properties of mortar and concrete: A review," *Applied Clay Science*, vol. 43, pp. 392-400, Mar 2009.
[31] A. Teklay, C. G. Yin, L. Rosendahl, and M. Bojer, "Calcination of kaolinite clay particles for cement production: A modeling study," *Cement and Concrete Research*, vol. 61-62, pp. 11-19, Jul-Aug 2014.
[32] R. Fernandez, F. Martirena, and K. L. Scrivener, "The origin of the pozzolanic activity of calcined clay minerals: A comparison between kaolinite, illite and montmorillonite," *Cement and Concrete Research*, vol. 41, pp. 113-122, Jan 2011.
[33] K. Scrivener, F. Avet, H. Maraghechi, F. Zunino, J. Ston, W. Hanpongpun, *et al.*, "Impacting factors and properties of limestone calcined clay cements (LC3)," *Green Materials*, vol. 7, pp. 3-14, Mar 2019.
[34] M. Frias and J. Cabrera, "Pore size distribution and degree of hydration of metakaolin-cement pastes," *Cement and Concrete Research*, vol. 30, pp. 561-569, Apr 2000.
[35] A. Tironi, M. A. Trezza, A. N. Scian, and E. F. Irassar, "Kaolinitic calcined clays: Factors affecting its performance as pozzolans," *Construction and Building Materials*, vol. 28, pp. 276-281, Mar 2012.

[36] T. Danner, G. Norden, and H. Justnes, "Characterisation of calcined raw clays suitable as supplementary cementitious materials," *Applied Clay Science*, vol. 162, pp. 391-402, Sep 15 2018.
[37] M. Antoni, J. Rossen, F. Martirena, and K. Scrivener, "Cement substitution by a combination of metakaolin and limestone," *Cement and Concrete Research*, vol. 42, pp. 1579-1589, Dec 2012.
[38] F. Avet and K. Scrivener, "Investigation of the calcined kaolinite content on the hydration of Limestone Calcined Clay Cement (LC3)," *Cement and Concrete Research*, vol. 107, pp. 124-135, May 2018.
[39] T. S. Institution, "Methods of testing cement-Part 1: Determination of strength," ed. Ankara, 2016.
[40] X. Zhou, D. Liu, H. L. Bu, L. L. Deng, H. M. Liu, P. Yuan, *et al.*, "XRD-based quantitative analysis of clay minerals using reference intensity ratios, mineral intensity factors, Rietveld, and full pattern summation methods: A critical review," *Solid Earth Sciences*, vol. 3, pp. 16-29, Mar 2018.
[41] ASTM, "ASTM C1679," in *Standard Practice for Measuring Hydration Kinetics of Hydraulic Cementitious Mixtures Using Isothermal Calorimetry*, ed. West Conshohocken: ASTM International, 2017.
[42] ASTM, "ASTM C311," in *Standard Test Methods for Sampling and Testing Fly Ash or Natural Pozzolans for Use in Portland-Cement Concrete*, ed. West Conshohocken: ASTM International, 2018.
[43] ASTM, "ASTM C305," in *Standard Practice for Mechanical Mixing of Hydraulic Cement Pastes and Mortars of Plastic Consistency*, ed. West Conshohocken: ASTM International, 2014.
[44] ASTM, "ASTM C230," in *Standard Specification for Flow Table for Use in Tests of Hydraulic Cement*, ed. West Conshohocken: ASTM International, 2014.
[45] ASTM, "ASTM C1437," in *Standard Test Method for Flow of Hydraulic Cement Mortar*, ed. West Conshohocken: ASTM International, 2015.
[46] ASTM, "ASTM C109," in *Standard Test Method for Compressive Strength of Hydraulic Cement Mortars (Using 2-in. or [50-mm] Cube Specimens)*, ed. West Conshohocken: ASTM International, 2016.
[47] L. Piga, "Thermogravimetry of a Kaolinite-Alunite Ore," *Thermochimica Acta*, vol. 265, pp. 177-187, Nov 1 1995.
[48] H. Chamley, *Clay Sedimentology*: Springer Berlin Heidelberg, 2013.
[49] D. M. Moore, R. C. Reynolds, and P. D. E. S. R. C. Reynolds, *X-ray Diffraction and the Identification and Analysis of Clay Minerals*: Oxford University Press, 1997.
[50] M. A. Sainz, F. J. Serrano, J. M. Amigo, J. Bastida, and A. Caballero, "XRD microstructural analysis of mullites obtained from kaolinite-alumina mixtures," *Journal of the European Ceramic Society*, vol. 20, pp. 403-412, Apr 2000.
[51] H. M. Zhou, X. C. Qiao, and J. G. Yu, "Influences of quartz and muscovite on the formation of mullite from kaolinite," *Applied Clay Science*, vol. 80-81, pp. 176-181, Aug 2013.
[52] J. R. Mackert, S. W. Twiggs, and A. L. Williams, "High-temperature x-ray diffraction measurement of sanidine thermal expansion," *Journal of Dental Research*, vol. 79, pp. 1590-1595, Aug 2000.
[53] A. Shvarzman, K. Kovler, G. S. Grader, and G. E. Shter, "The effect of dehydroxylation/amorphization degree on pozzolanic activity of kaolinite," *Cement and Concrete Research*, vol. 33, pp. 405-416, Mar 2003.

[54] A. Elimbi, H. K. Tchakoute, and D. Njopwouo, "Effects of calcination temperature of kaolinite clays on the properties of geopolymer cements," *Construction and Building Materials,* vol. 25, pp. 2805-2812, Jun 2011.
[55] B. Uzal, L. Turanli, H. Yucel, M. C. Goncuoglu, and A. Culfaz, "Pozzolanic activity of clinoptilolite: A comparative study with silica fume, fly ash and a non-zeolitic natural pozzolan," *Cement and Concrete Research,* vol. 40, pp. 398-404, Mar 2010.
[56] N. Ural, "The Importance of Clay in Geotechnical Engineering," *Current Topics in the Utilization of Clay in Industrial and Medical Applications,* 2018.
[57] S. E. Schulze and J. Rickert, "Suitability of natural calcined clays as supplementary cementitious material," *Cement & Concrete Composites,* vol. 95, pp. 92-97, Jan 2019.
[58] E. Kucukyildirim and B. Uzal, "Characteristics of calcined natural zeolites for use in high-performance pozzolan blended cements," *Construction and Building Materials,* vol. 73, pp. 229-234, Dec 30 2014.
[59] J. Tangpagasit, R. Cheerarot, C. Jaturapitakkul, and K. Kiattikomol, "Packing effect and pozzolanic reaction of fly ash in mortar," *Cement and Concrete Research,* vol. 35, pp. 1145-1151, Jun 2005.
[60] M. Rose-Lam, E. Villar-Cocina, and M. Frias, "Study on the pozzolanic properties of a natural Cuban zeolitic rock by conductometric method: Kinetic parameters," *Construction and Building Materials,* vol. 25, pp. 644-650, Feb 2011.
[61] A. Mardani-Aghabaglou, G. I. Sezer, and K. Ramyar, "Comparison of fly ash, silica fume and metakaolin from mechanical properties and durability performance of mortar mixtures view point," *Construction and Building Materials,* vol. 70, pp. 17-25, Nov 15 2014.
[62] J. S. Damtoft, J. Lukasik, D. Herfort, D. Sorrentino, and E. M. Gartner, "Sustainable development and climate change initiatives," *Cement and Concrete Research,* vol. 38, pp. 115-127, Feb 2008.
[63] D. Zhou, R. Wang, M. Tyrer, H. Wong, and A. C. Cheeseman, "Sustainable infrastructure development through use of calcined excavated waste clay as a supplementary cementitious material," *Journal of Cleaner Production,* vol. 168, pp. 1180-1192, Dec 1 2017.
[64] L. M. Casas, M. Pozo, C. P. Gomez, E. Pozo, L. D. Bessieres, F. Plantier, *et al.*, "Thermal behavior of mixtures of bentonitic clay and saline solutions," *Applied Clay Science,* vol. 72, pp. 18-25, Feb 2013.
[65] R. Hamzaoui, F. Muslim, S. Guessasma, A. Bennabi, and J. Guillin, "Structural and thermal behavior of proclay kaolinite using high energy ball milling process," *Powder Technology,* vol. 271, pp. 228-237, Feb 2015.
[66] D. W. Waples and J. S. Waples, "A Review and Evaluation of Specific Heat Capacities of Rocks, Minerals, and Subsurface Fluids. Part 1: Minerals and Nonporous Rocks," *Natural Resources Research,* vol. 13, pp. 97-122, June 01 2004.
[67] D. Defra, "2012 Guidelines to Defra/DECC's GHG Conversion Factors for Company Reporting," 2012.
[68] R. Gettu, A. Patel, V. Rathi, S. Prakasan, A. S. Basavaraj, S. Palaniappan, *et al.*, "Influence of supplementary cementitious materials on the sustainability parameters of cements and concretes in the Indian context," *Materials and Structures,* vol. 52, p. 10, January 24 2019.

[69] S. S. Berriel, A. Favier, E. R. Dominguez, I. R. S. Machado, U. Heierli, K. Scrivener, *et al.*, "Assessing the environmental and economic potential of Limestone Calcined Clay Cement in Cuba," *Journal of Cleaner Production*, vol. 124, pp. 361-369, Jun 15 2016.

[70] L. M. Vizcaino-Andres, S. Sanchez-Berriel, S. Damas-Carrera, A. Perez-Hernandez, K. L. Scrivener, and J. F. Martirena-Hernandez, "Industrial trial to produce a low clinker, low carbon cement," *Materiales De Construccion*, vol. 65, 2015.

APPENDIX A

TGA PLOTS FOR RAW AND CALCINED CLAY

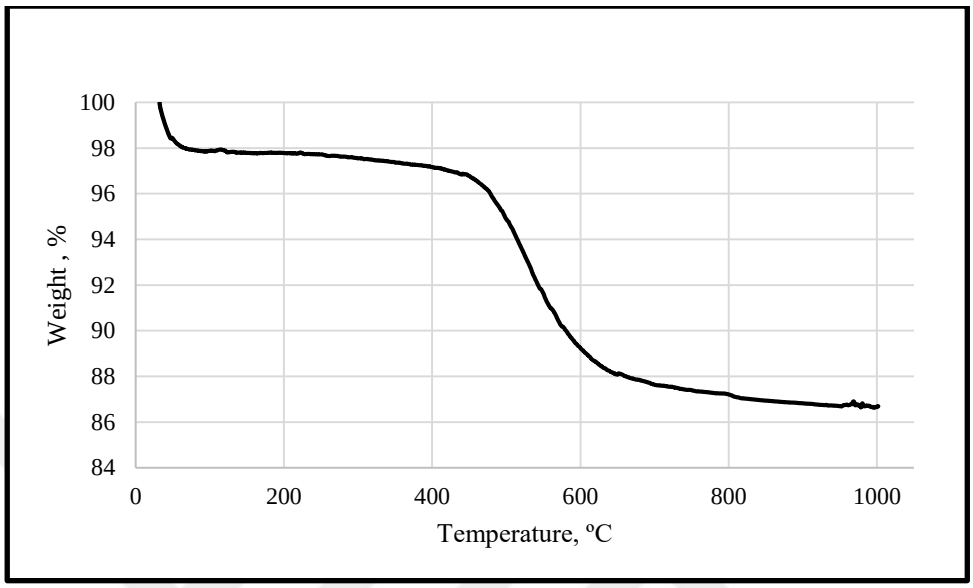

Figure A.1 TGA plot of the raw Clay 1

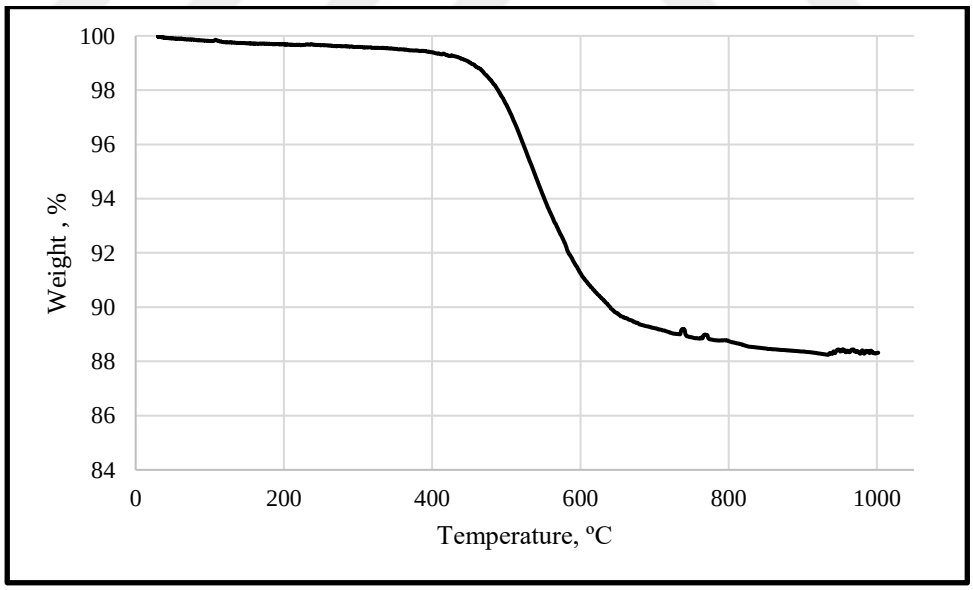

Figure A.2 TGA plot of the raw Clay 1 400 ºC

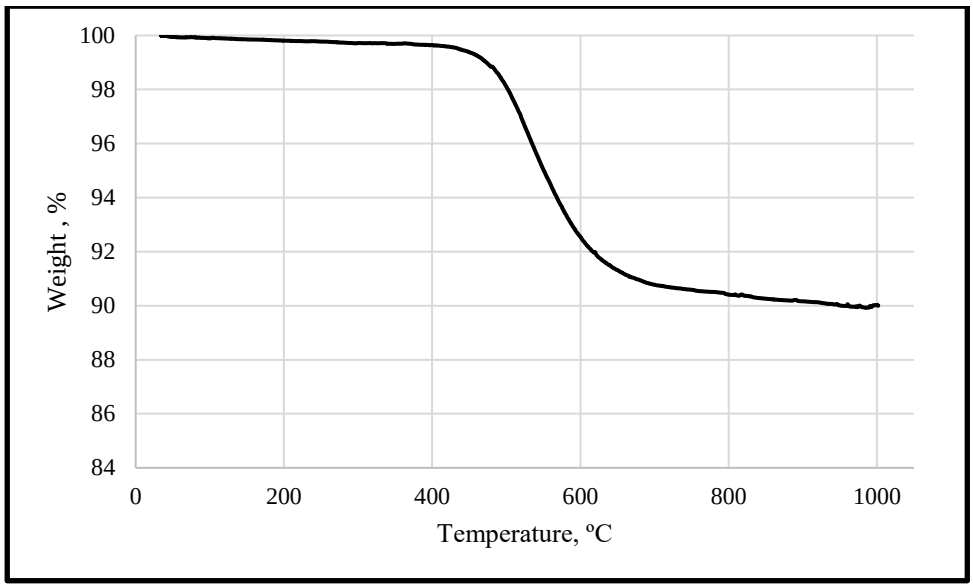

Figure A.3 TGA plot of the raw Clay 1 520 ºC

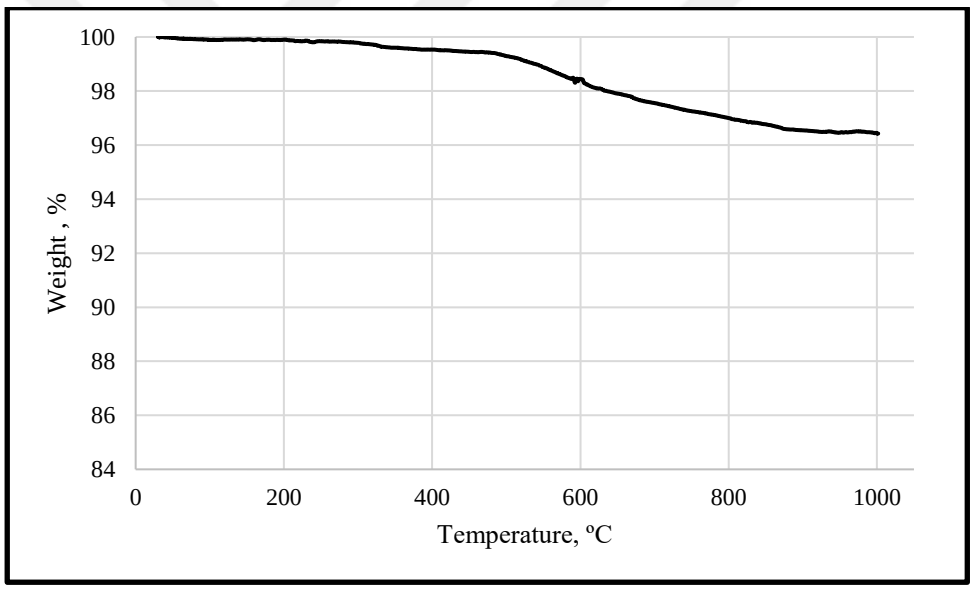

Figure A.4 TGA plot of the raw Clay 1 700 ºC

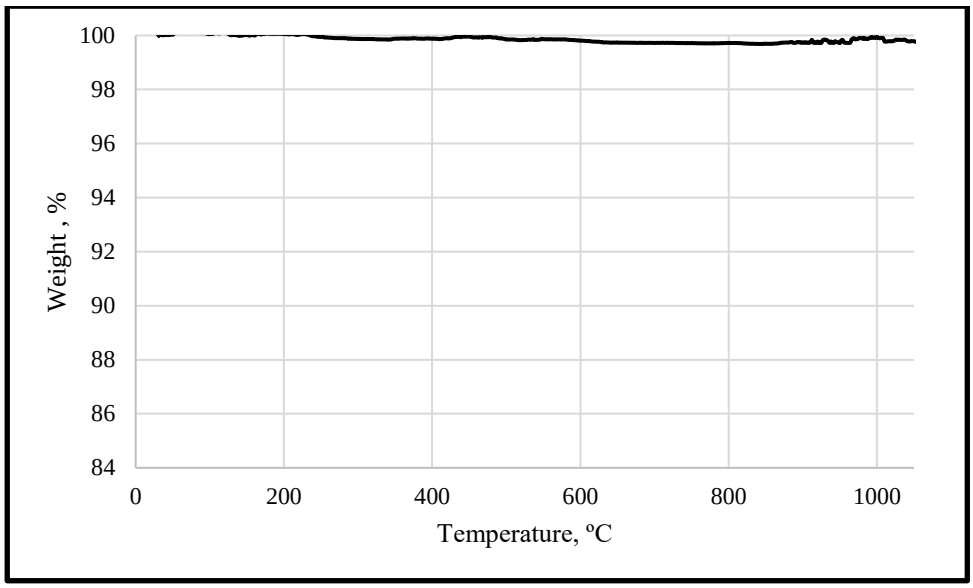

Figure A.5 TGA plot of the Clay 1 1150 ºC

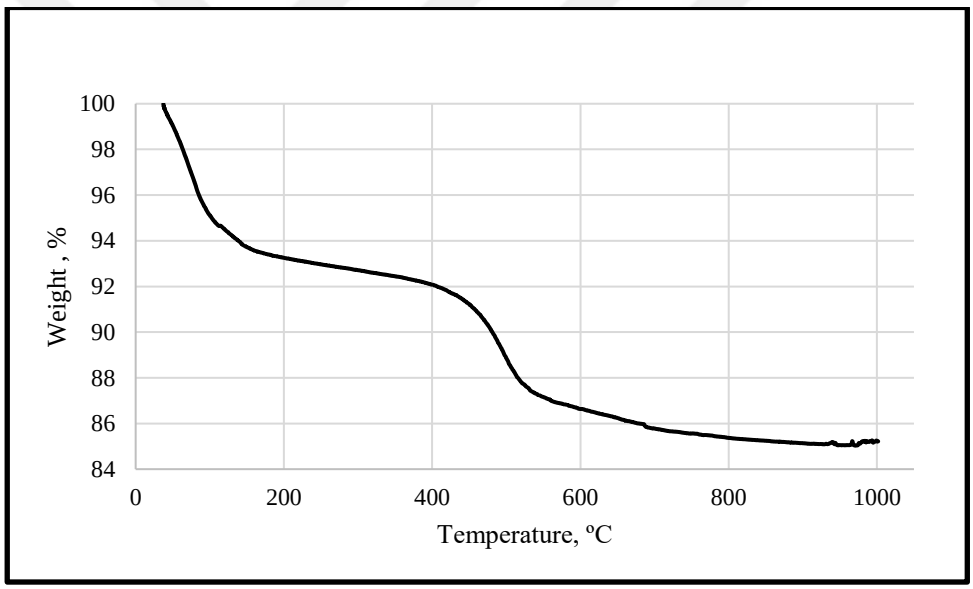

Figure A.6 TGA plot of the raw Clay 2

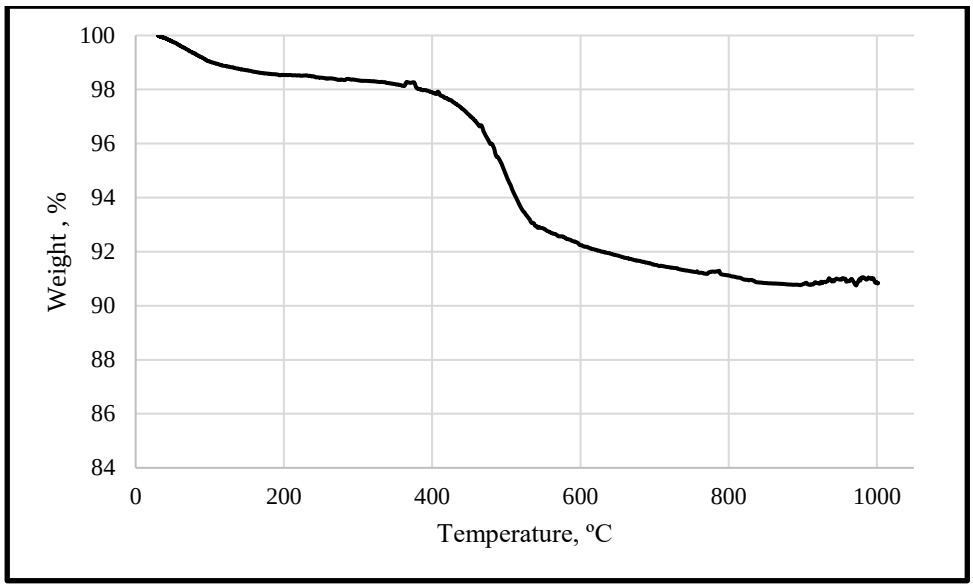

Figure A.7 TGA plot of the Clay 2 400 ºC

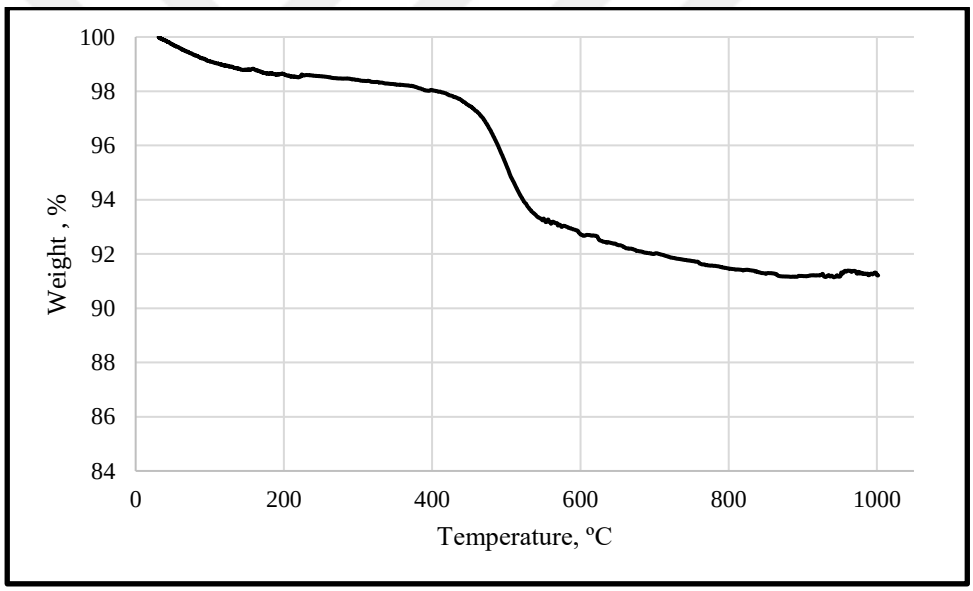

Figure A.8 TGA plot of the Clay 2 520 ºC

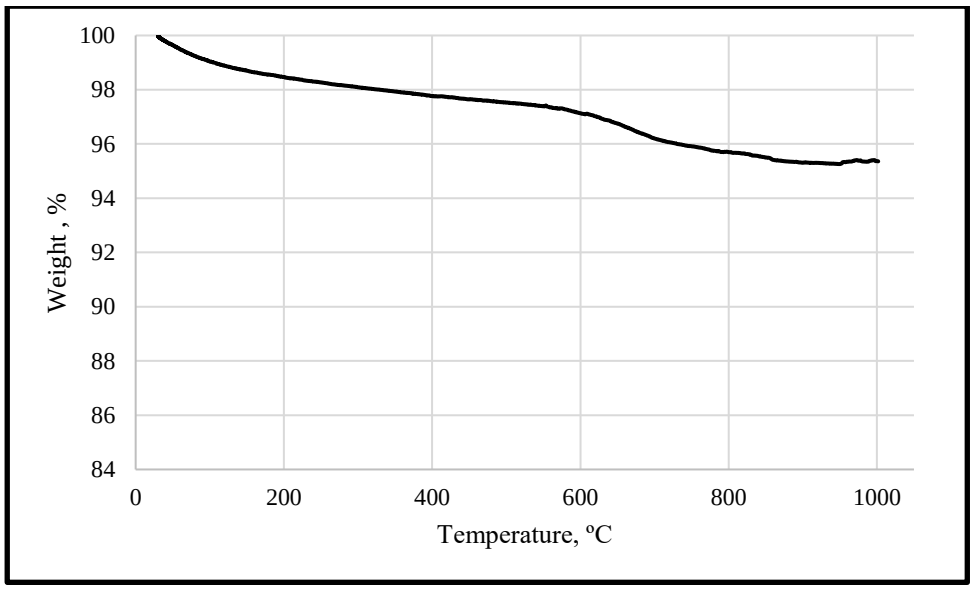

Figure A.9 TGA plot of the Clay 2 700 ºC

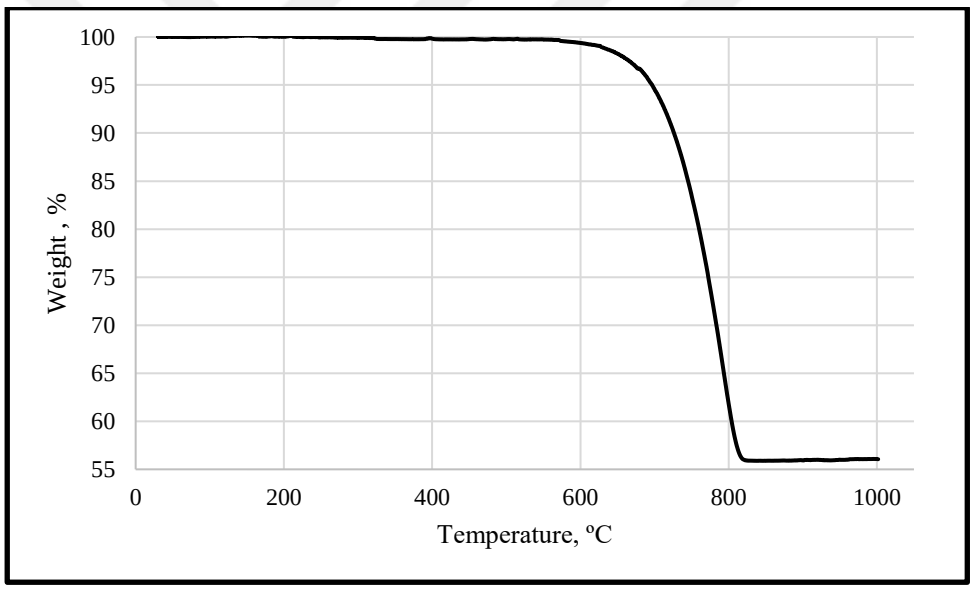

Figure A.10 TGA plot of the limestone powder

APPENDIX B

TGA PLOTS FOR LIME-CLAY PASTES

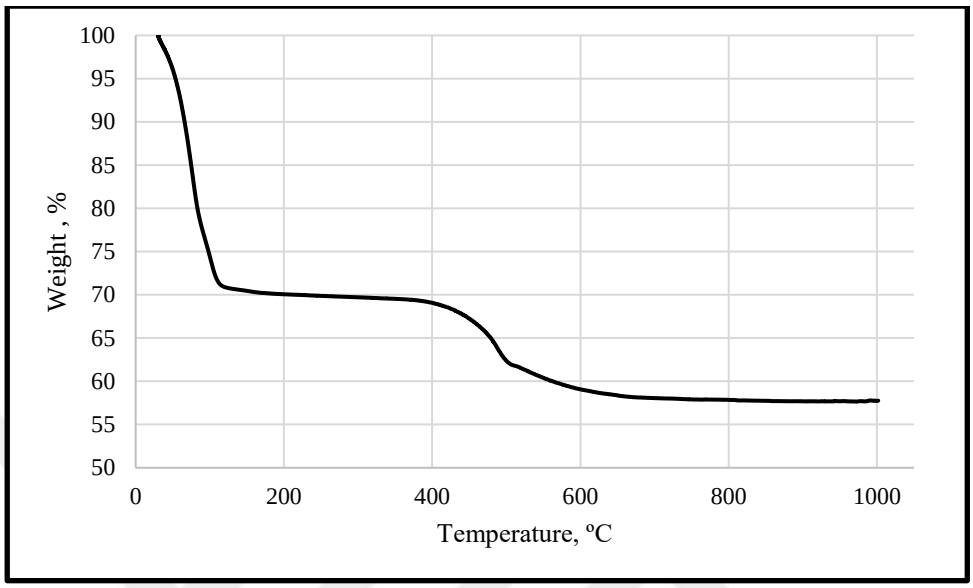

Figure B.1 TGA plot of lime-CC1 raw paste at 3 days

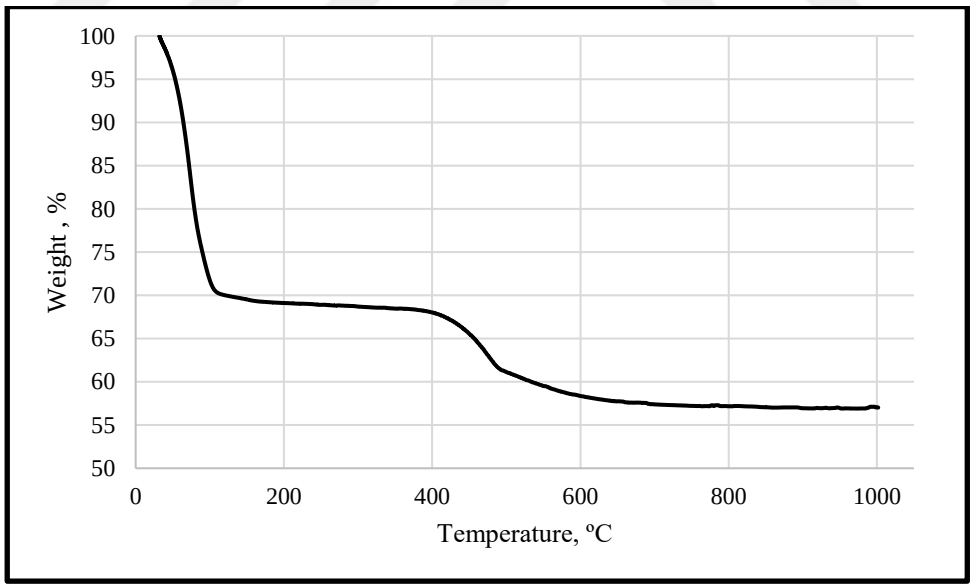

Figure B.2 TGA plot of lime-CC1 raw paste at 7 days

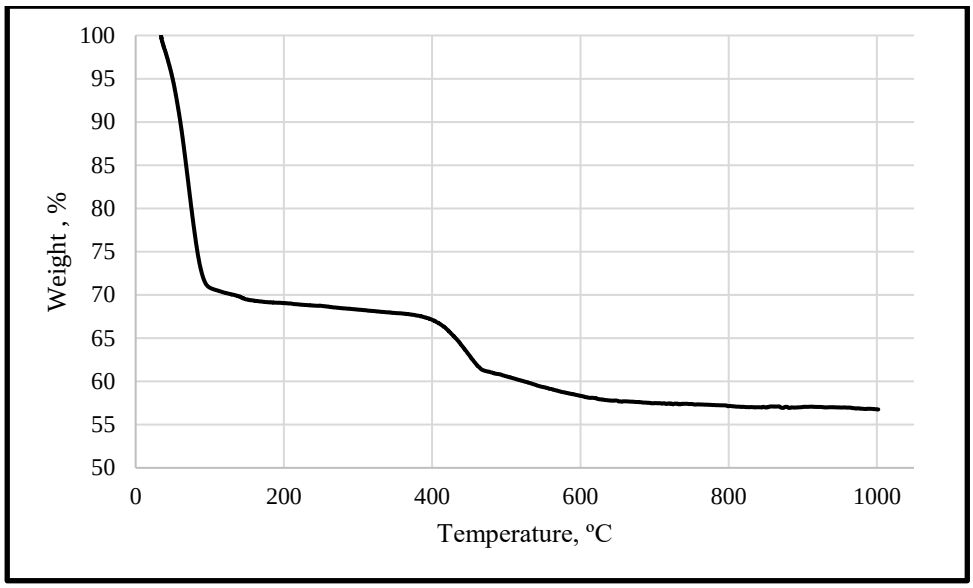

Figure B.3 TGA plot of lime-CC1 raw paste at 28 days

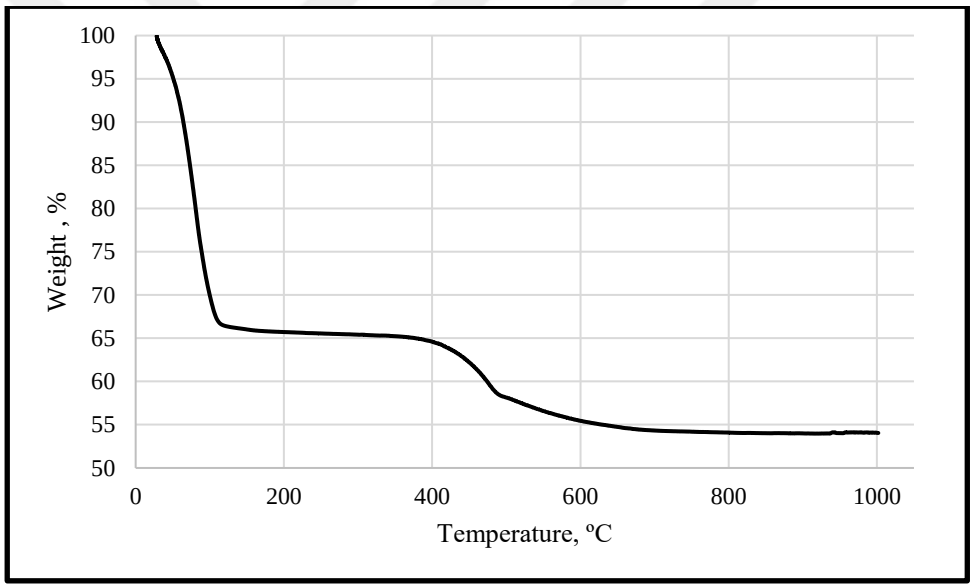

Figure B.4 TGA plot of lime-CC1 400 ºC paste at 3 days

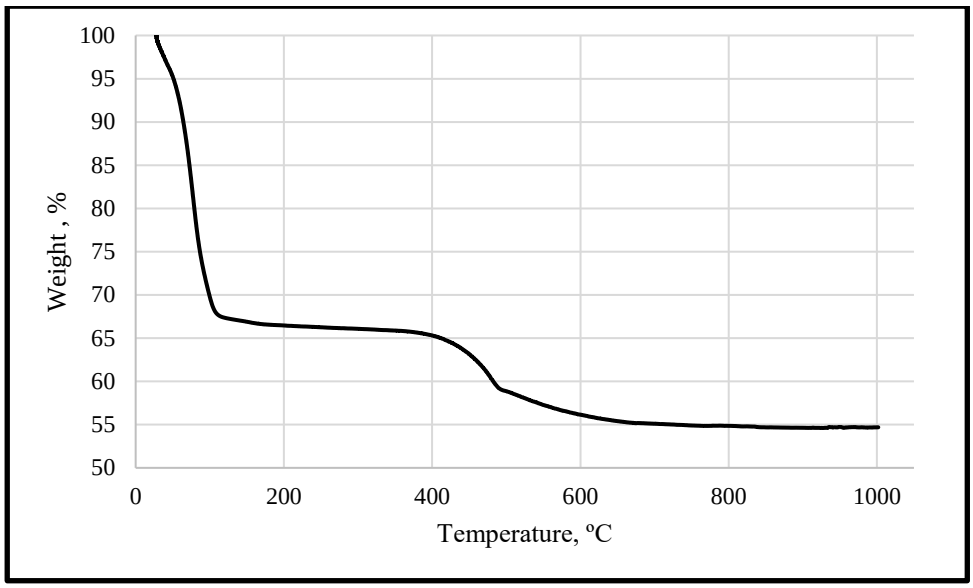

Figure B.5 TGA plot of lime-CC1 400 ºC paste at 7 days

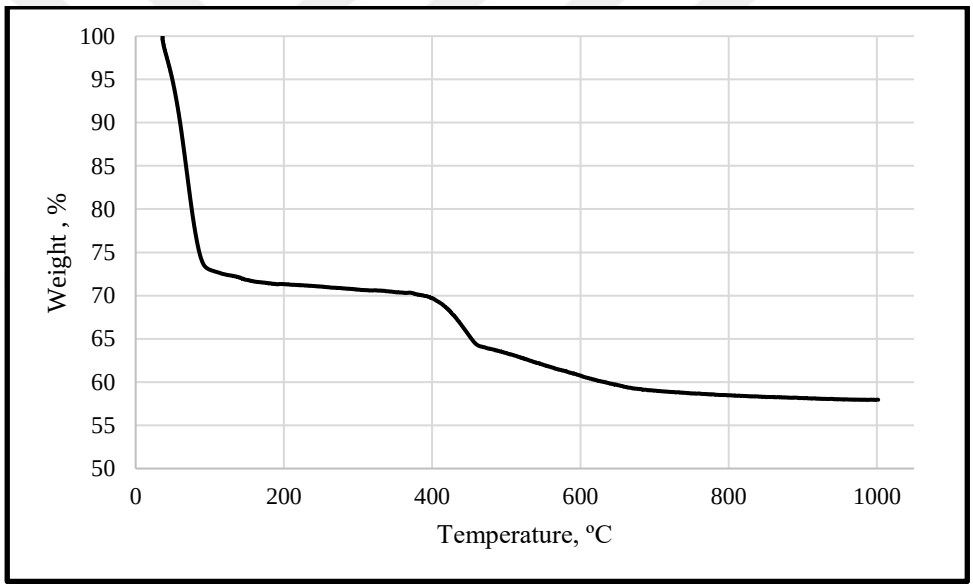

Figure B.6 TGA plot of lime-CC1 400 ºC paste at 28 days

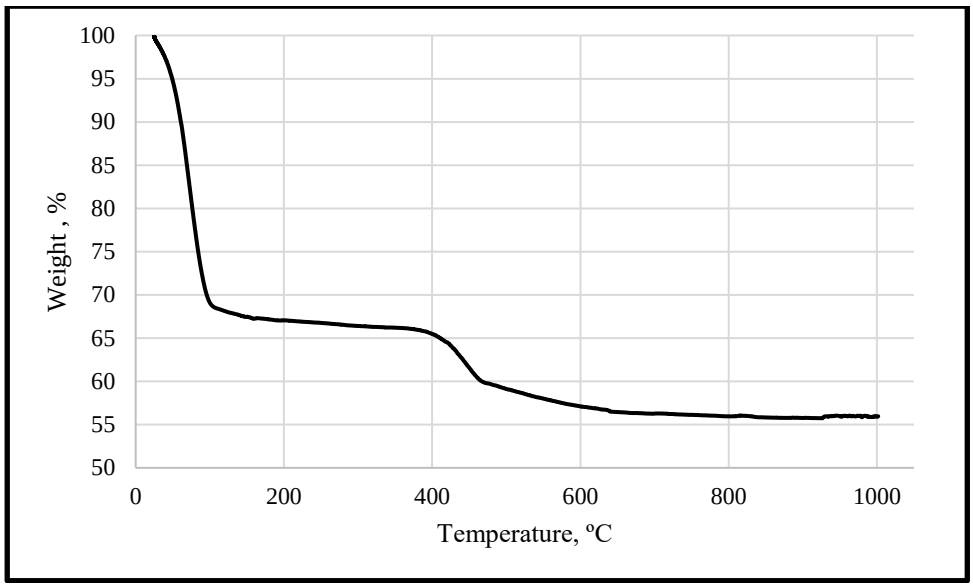

Figure B.7 TGA plot of lime-CC1 520 ºC paste at 3 days

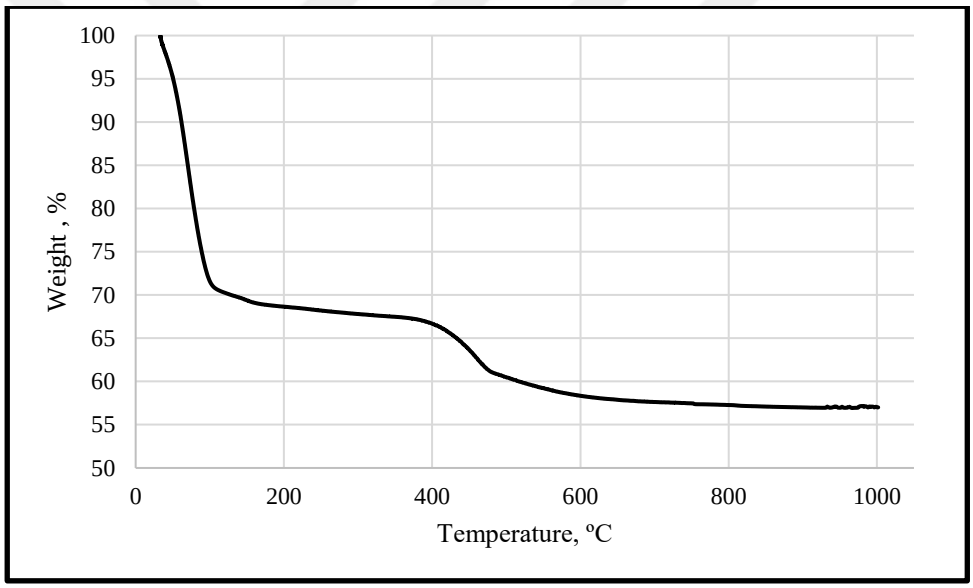

Figure B.8 TGA plot of lime-CC1 520 ºC paste at 7 days

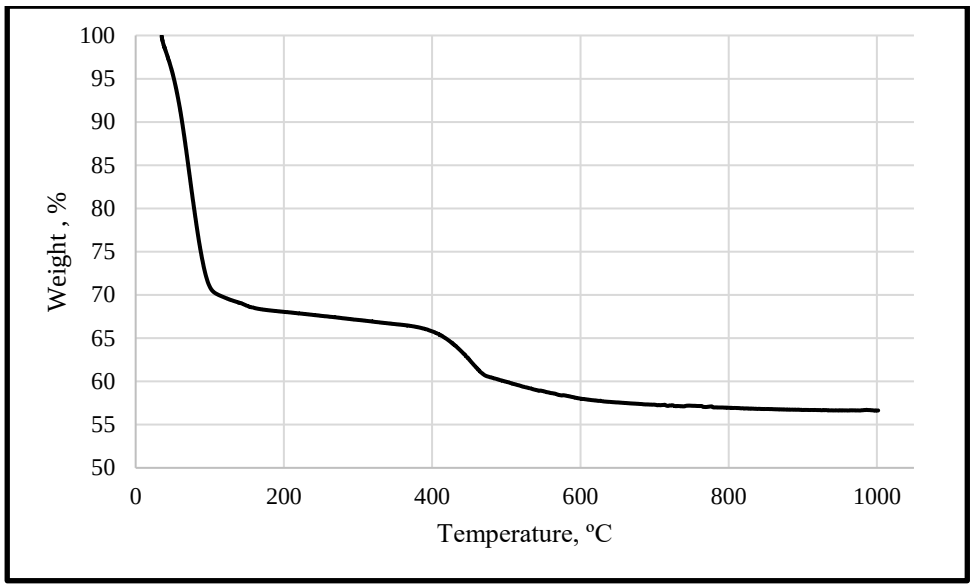

Figure B.9 TGA plot of lime-CC1 520 ºC paste at 28 days

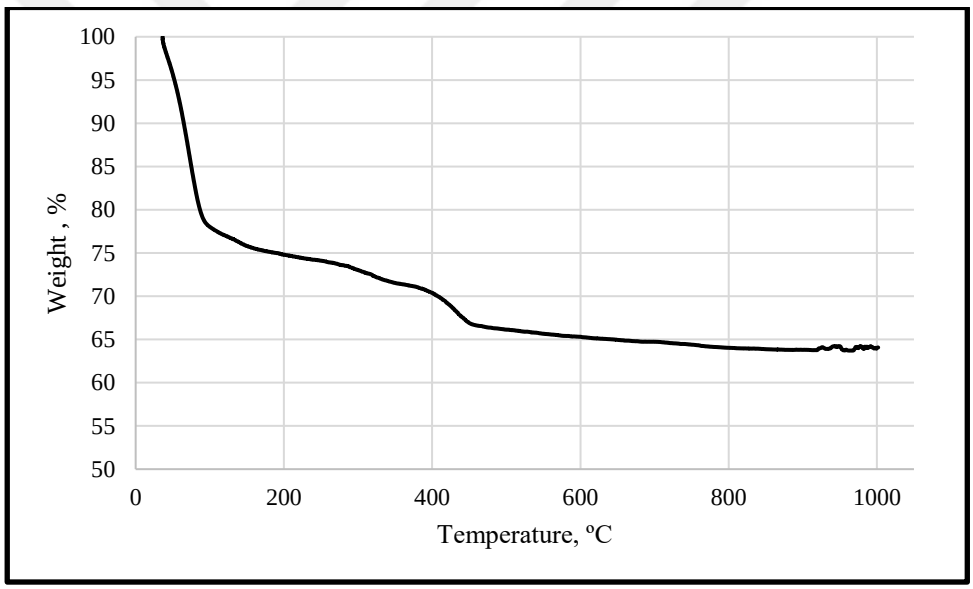

Figure B.10 TGA plot of lime-CC1 700 ºC paste at 3 days

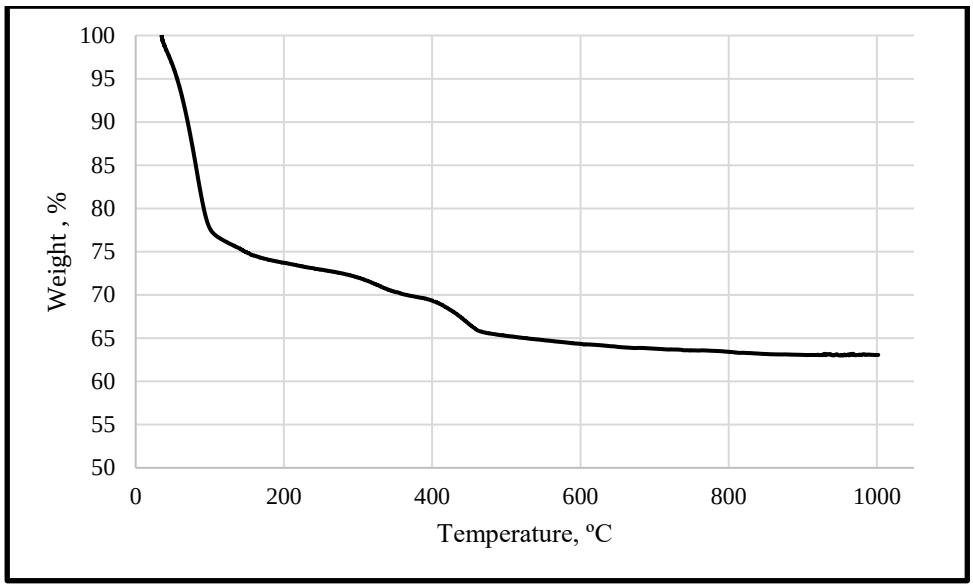

Figure B.11 TGA plot of lime-CC1 700 ºC paste at 7 days

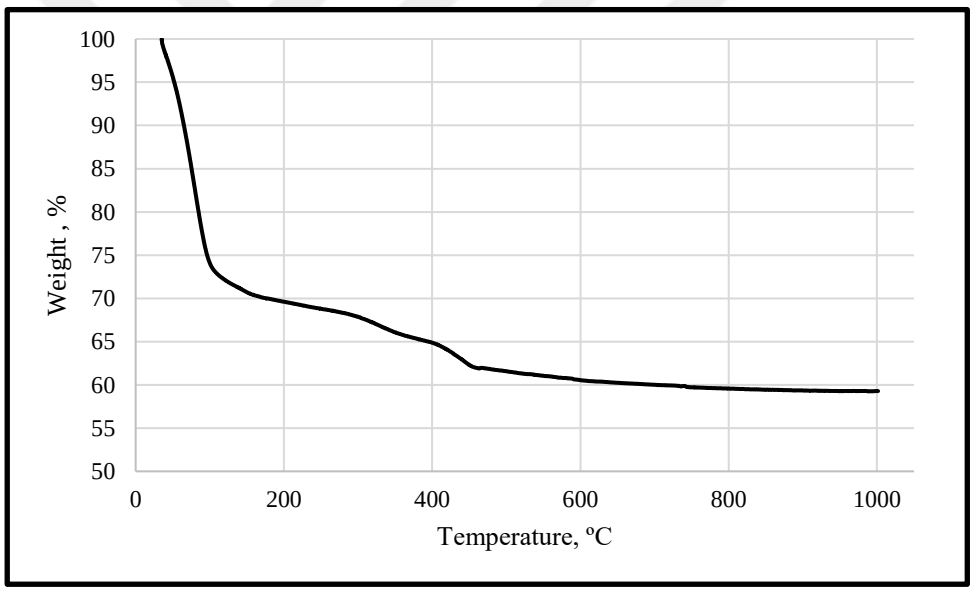

Figure B.12 TGA plot of lime-CC1 700 ºC paste at 28 days

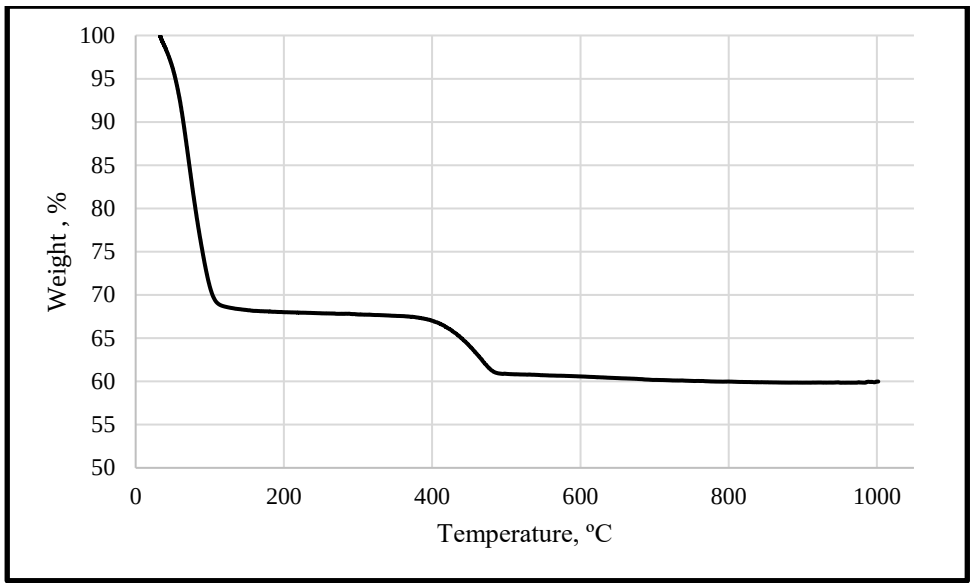

Figure B.13 TGA plot of lime-CC1 1150 ºC paste at 3 days

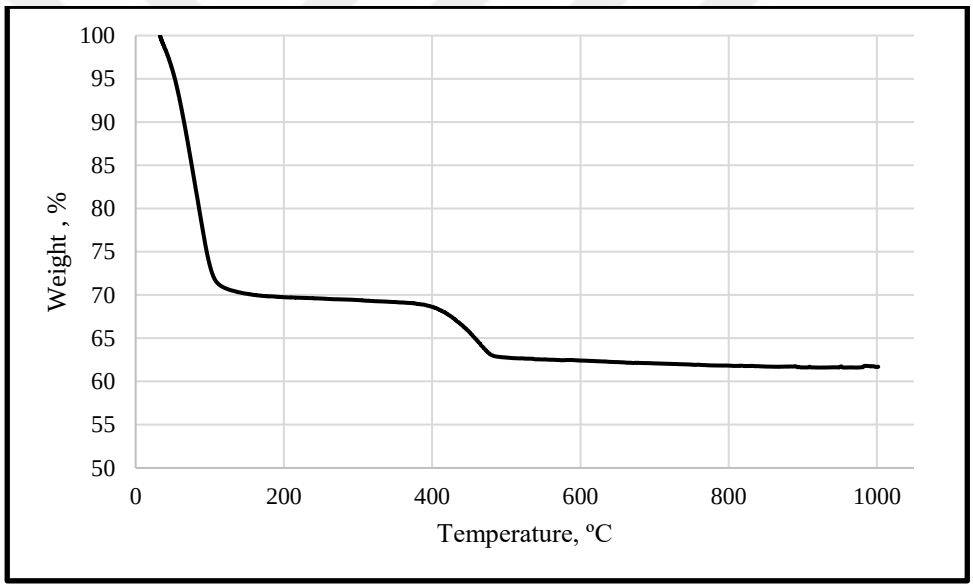

Figure B.14 TGA plot of lime-CC1 1150 ºC paste at 7 days

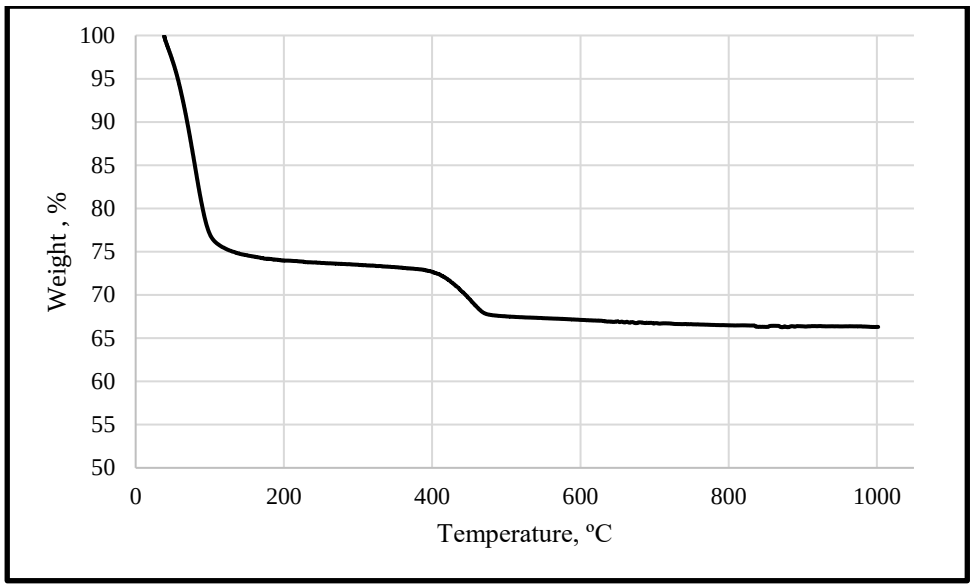

Figure B.15 TGA plot of lime-CC1 1150 ºC paste at 28 days

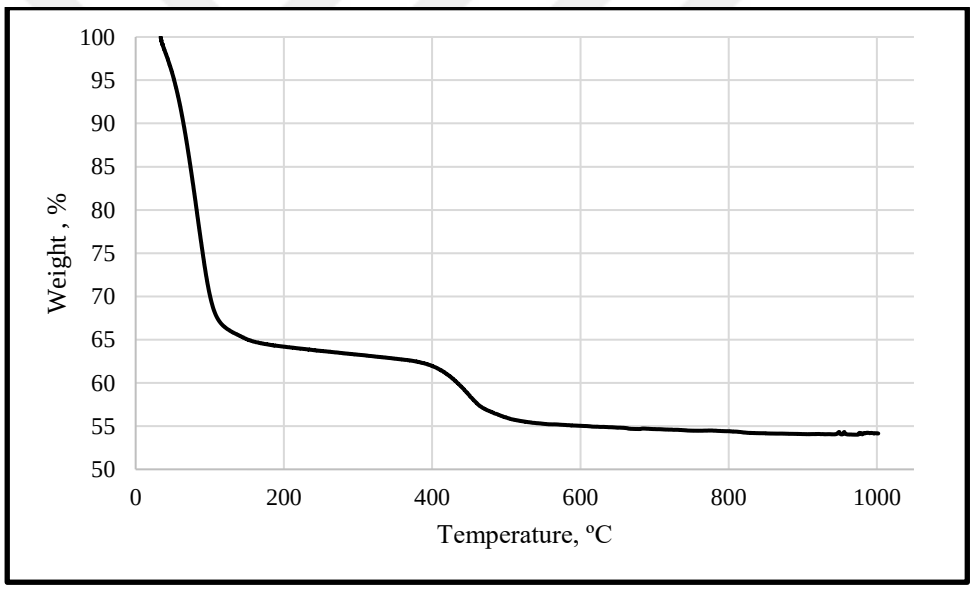

Figure B.16 TGA plot of lime-CC2 raw paste at 3 days

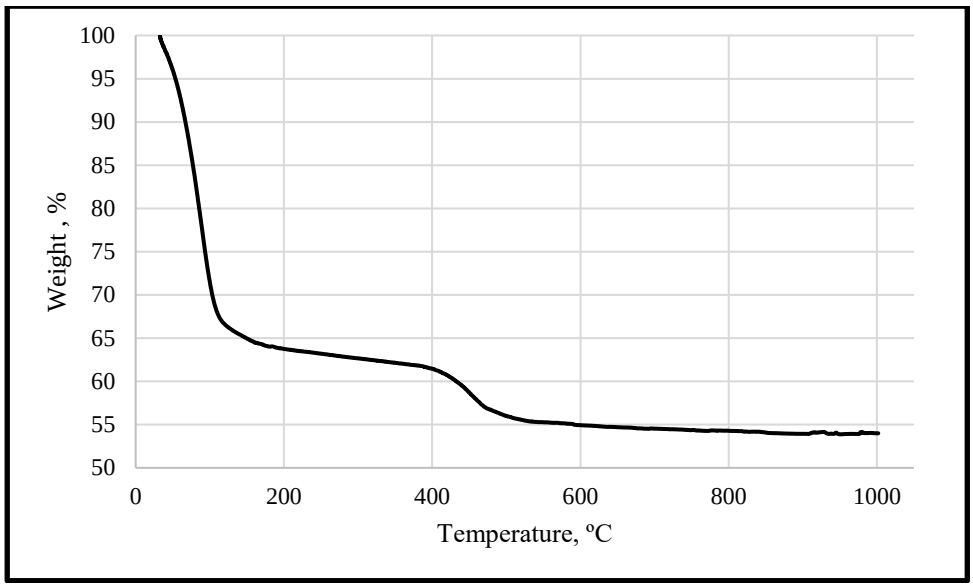

Figure B.17 TGA plot of lime-CC2 raw paste at 7 days

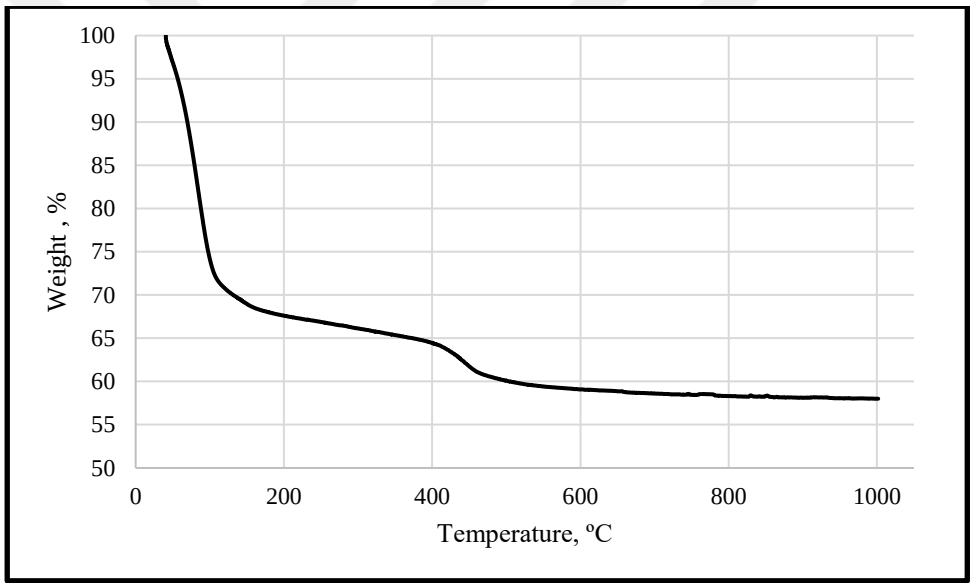

Figure B.18 TGA plot of lime-CC2 raw paste at 28 days

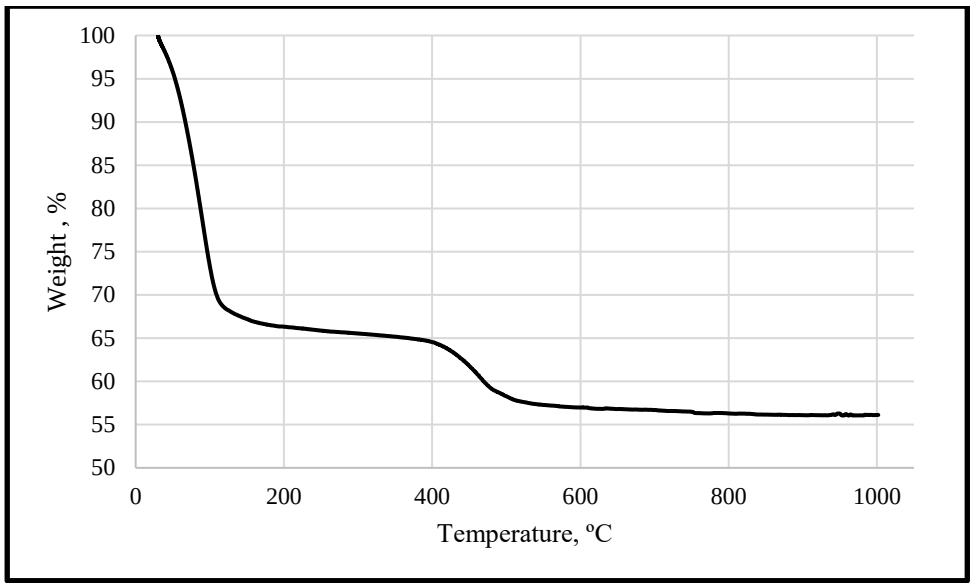

Figure B.19 TGA plot of lime-CC2 400 ºC paste at 3 days

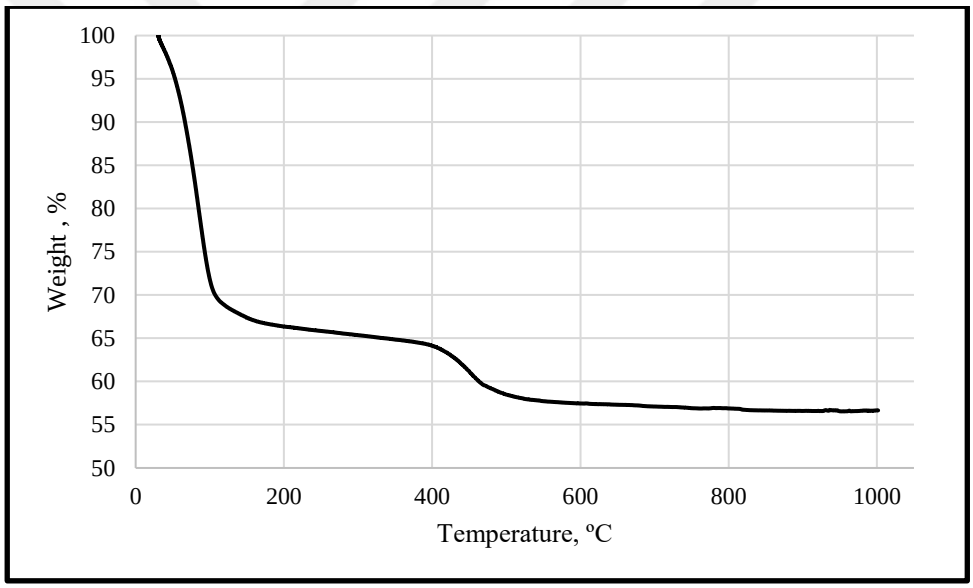

Figure B.20 TGA plot of lime-CC2 400 ºC paste at 7 days

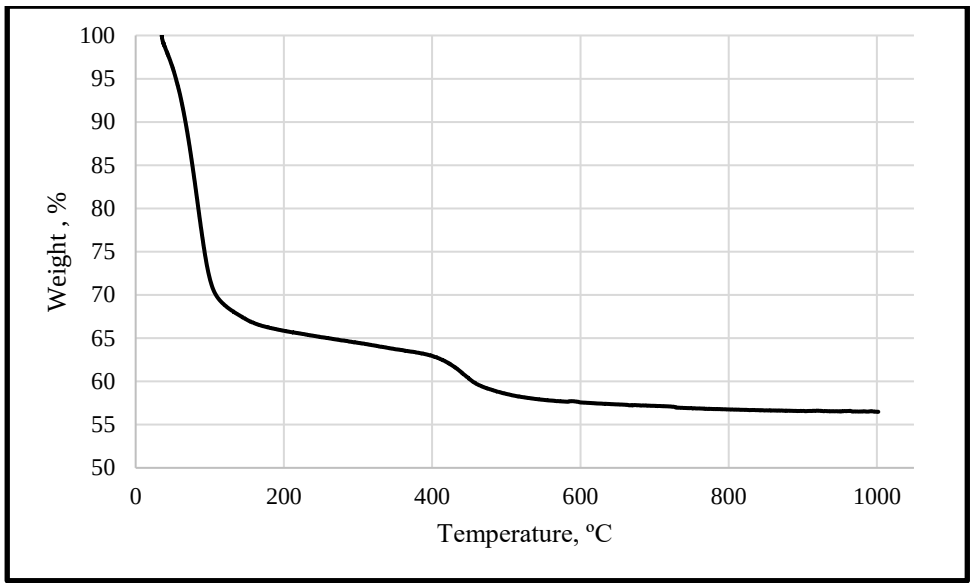

Figure B.21 TGA plot of lime-CC2 400 ºC paste at 28 days

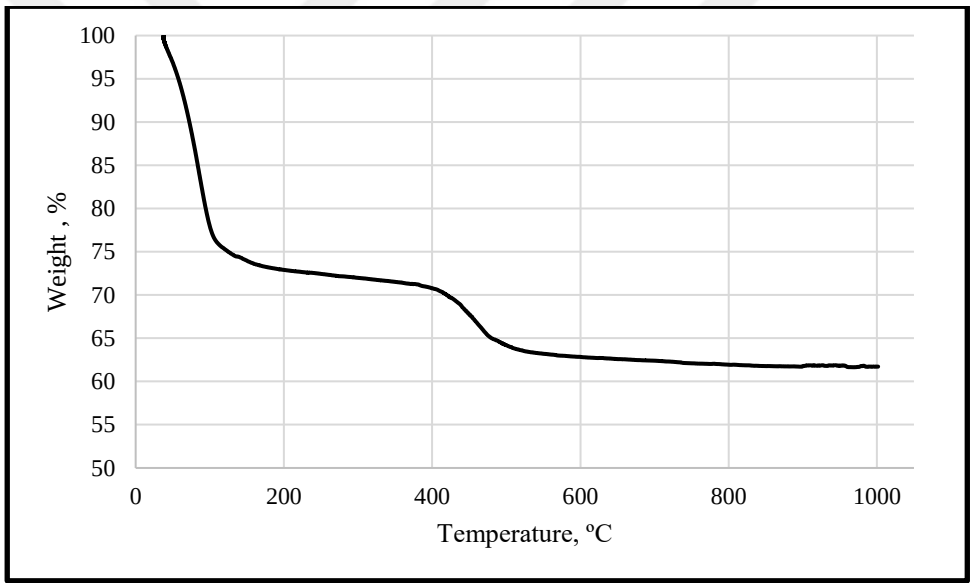

Figure B.22 TGA plot of lime-CC2 520 ºC paste at 3 days

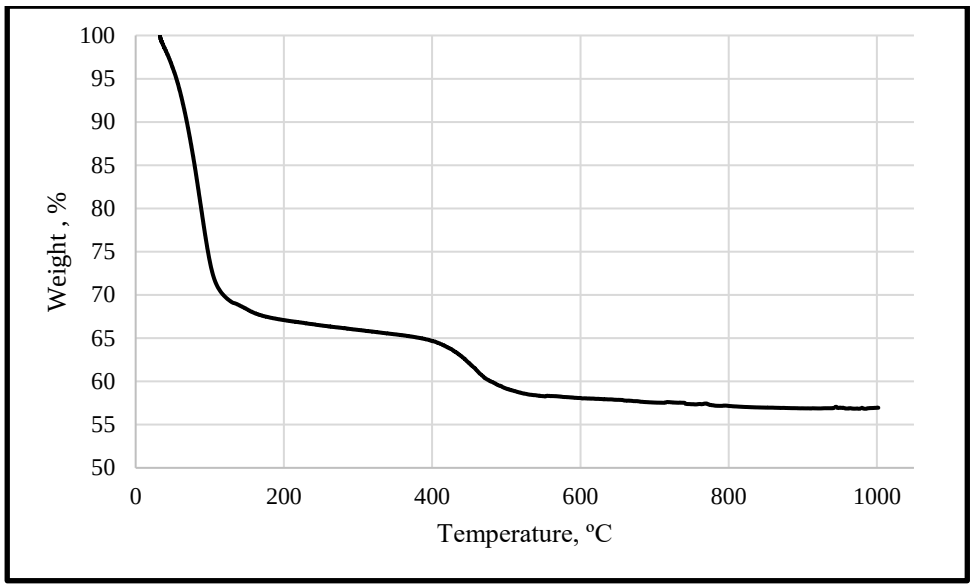

Figure B.23 TGA plot of lime-CC2 520 ºC paste at 7 days

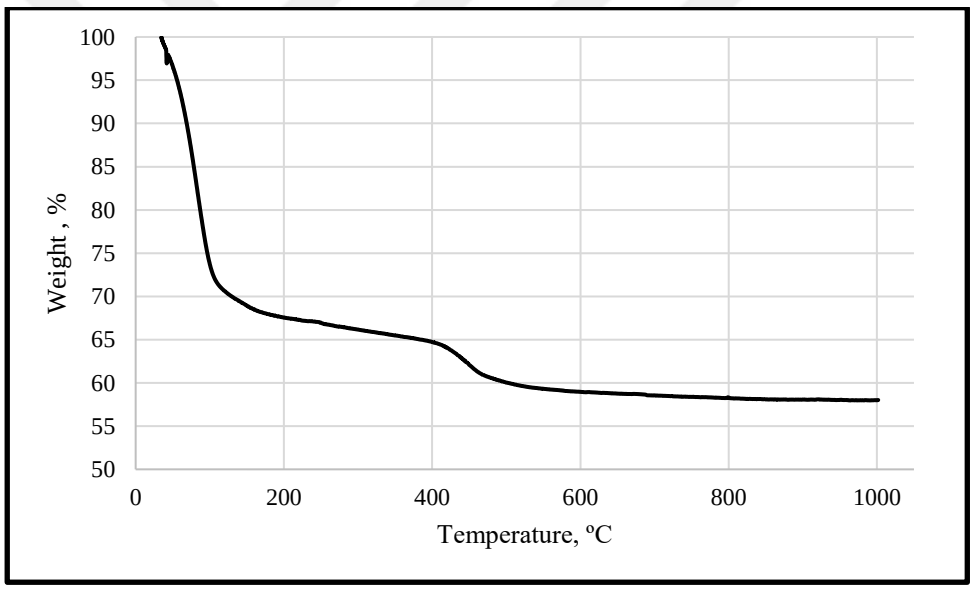

Figure B.24 TGA plot of lime-CC2 520 ºC paste at 28 days

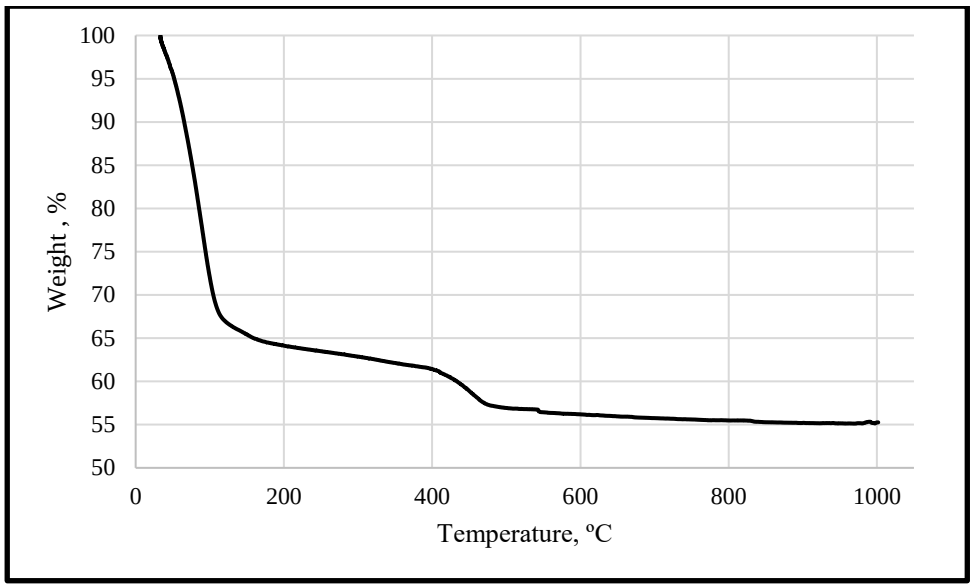

Figure B.25 TGA plot of lime-CC2 700 ºC paste at 3 days

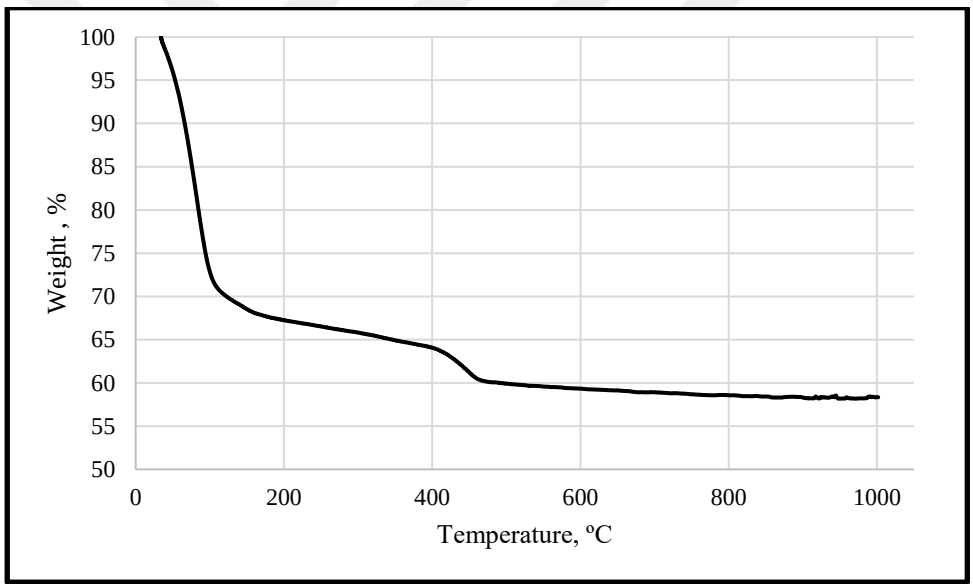

Figure B.26 TGA plot of lime-CC2 700 ºC paste at 7 days

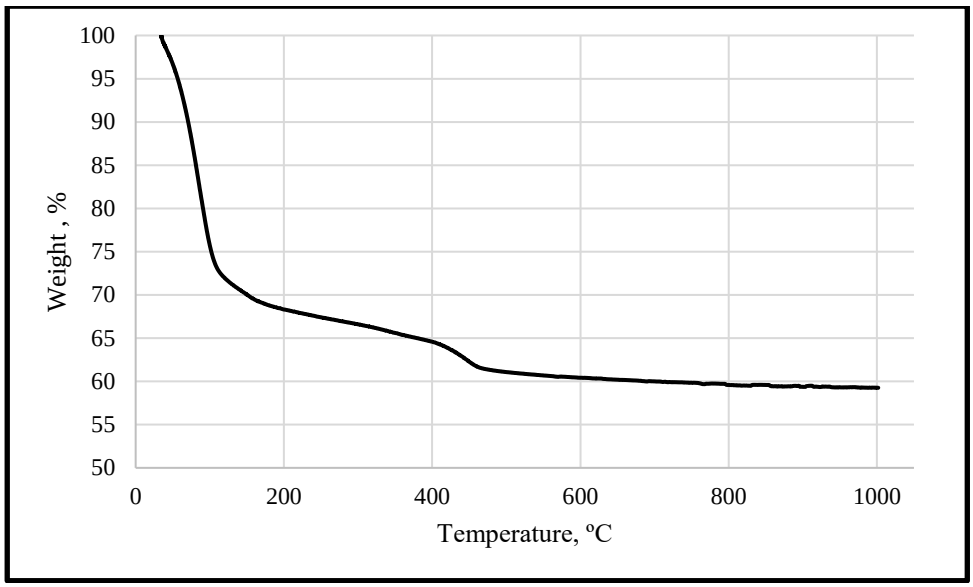

Figure B.27 TGA plot of lime-CC2 700 ºC paste at 28 days

TGA PLOTS FOR LIME-CLAY-LIMESTONE POWDER PASTES

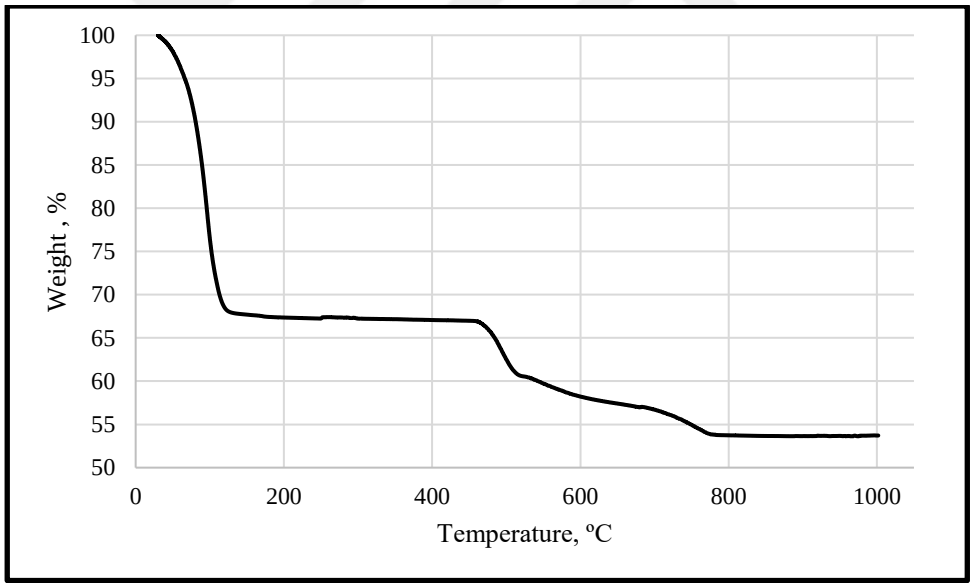

Figure B.28 TGA plot of lime-CC1 raw-limestone powder paste at 3 days

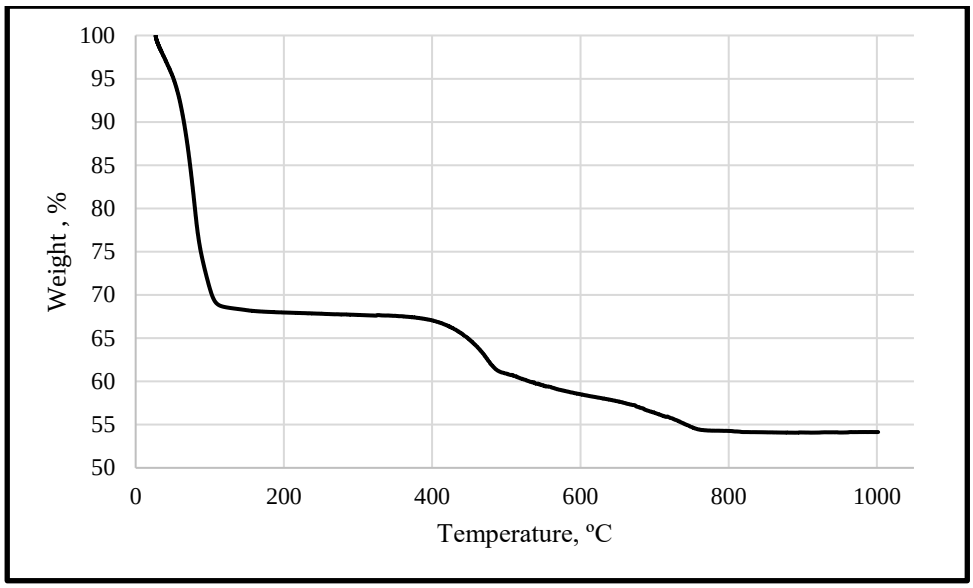

Figure B.29 TGA plot of lime-CC1 raw-limestone powder paste at 7 days

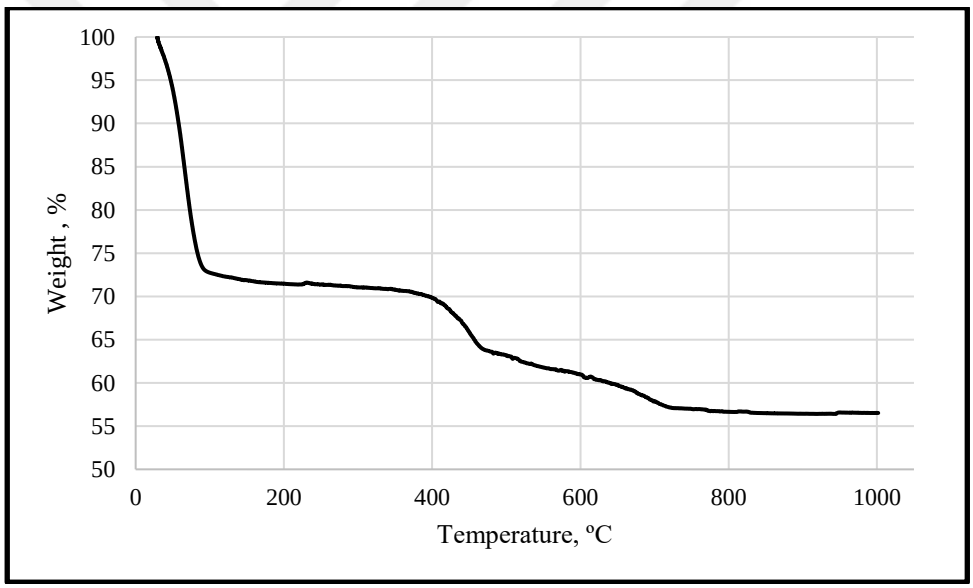

Figure B.30 TGA plot of lime-CC1 raw-limestone powder paste at 28 days

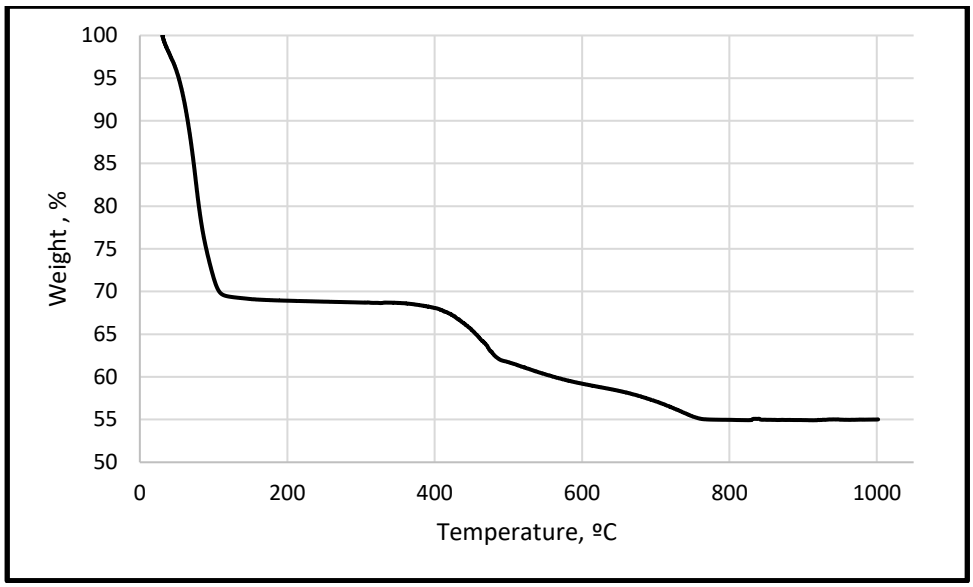

Figure B.31 TGA plot of lime-CC1 400 ºC-limestone powder paste at 3 days

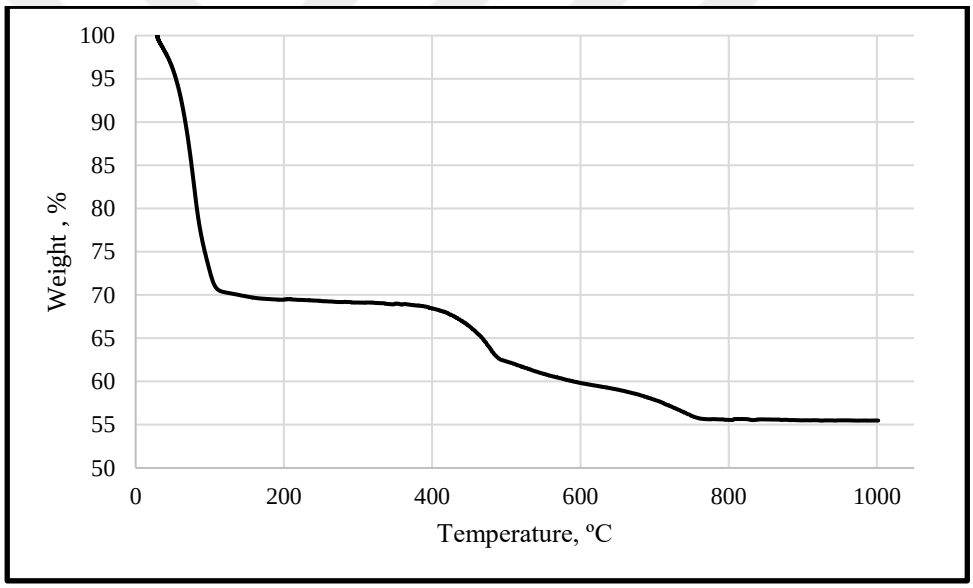

Figure B.32 TGA plot of lime-CC1 400 ºC-limestone powder paste at 7 days

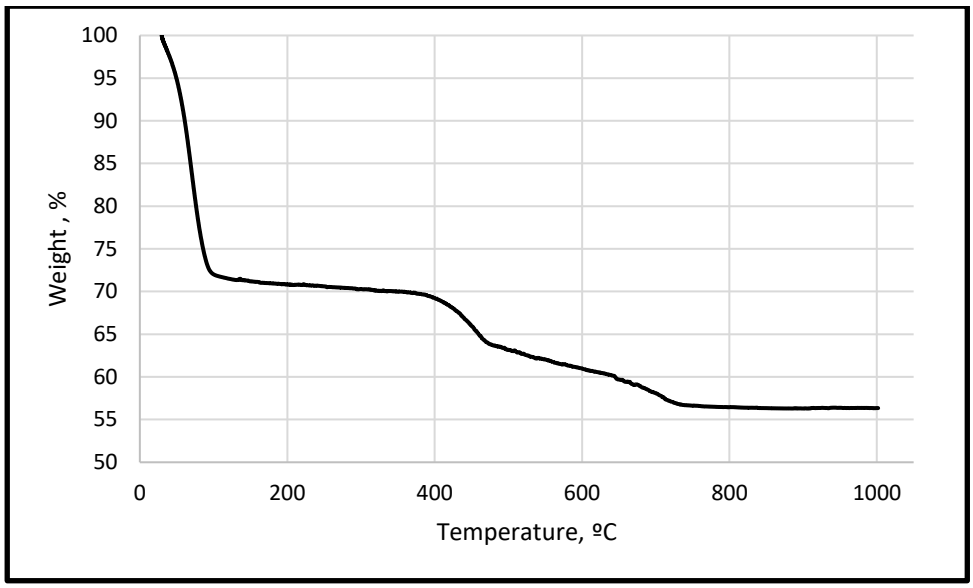

Figure B.33 TGA plot of lime-CC1 400 ºC-limestone powder paste at 28 days

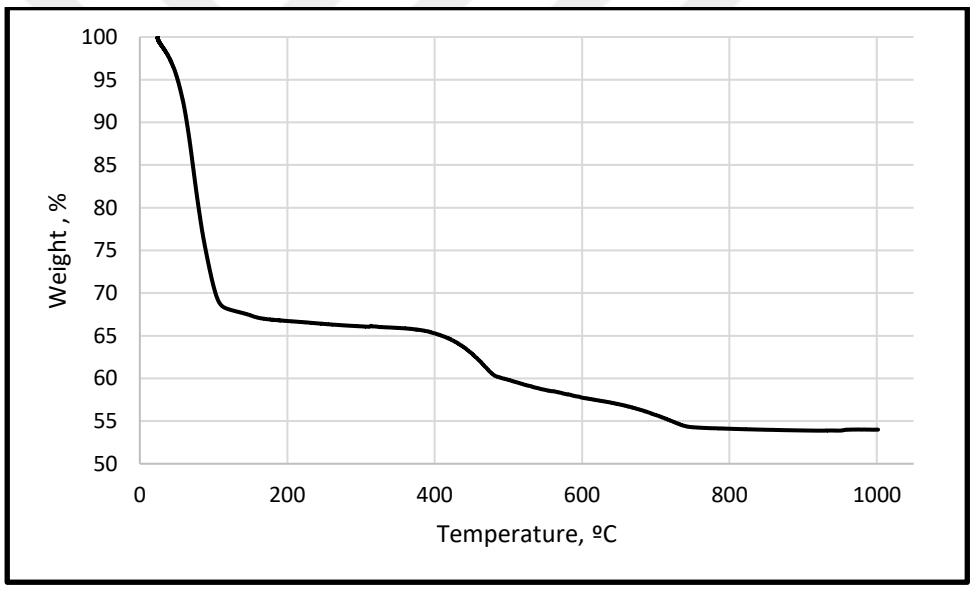

Figure B.34 TGA plot of lime-CC1 520 ºC-limestone powder paste at 3 days

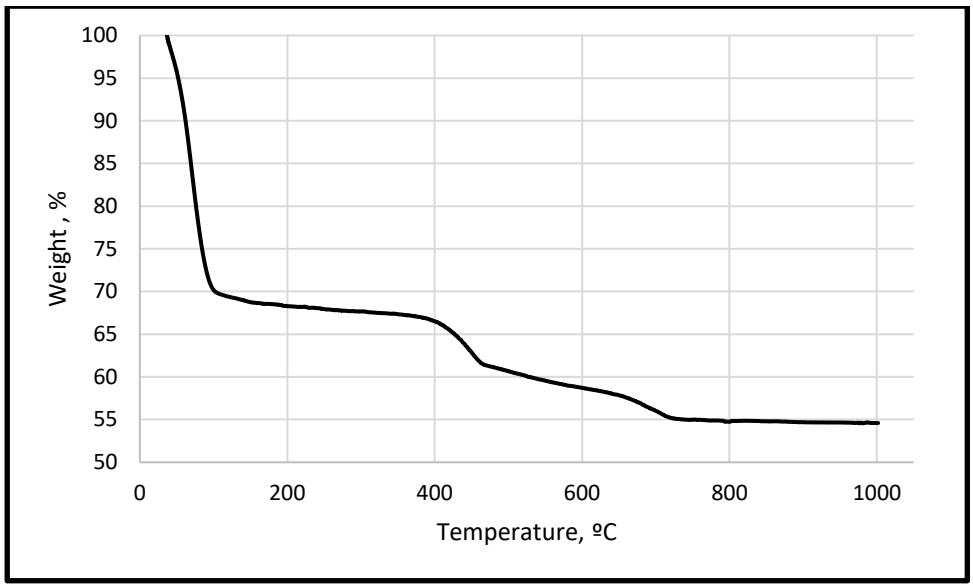

Figure B.35 TGA plot of lime-CC1 520 ºC-limestone powder paste at 7 days

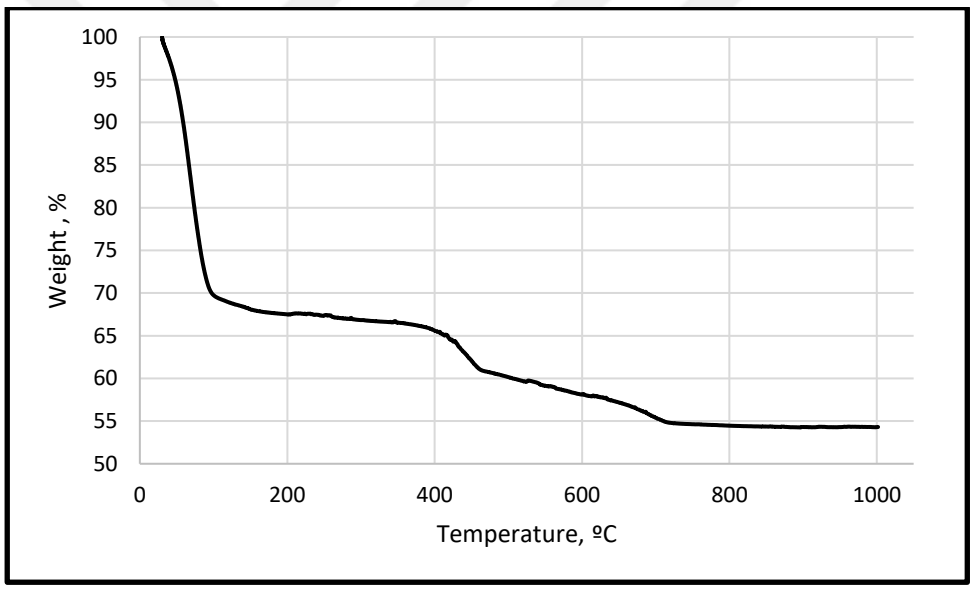

Figure B.36 TGA plot of lime-CC1 520 ºC-limestone powder paste at 28 days

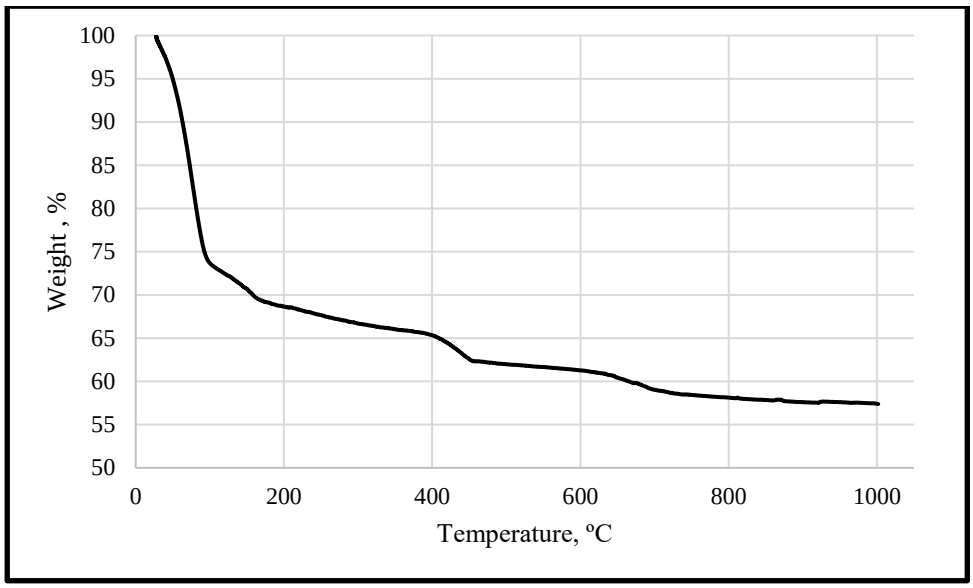

Figure B.37 TGA plot of lime-CC1 700 ºC-limestone powder paste at 3 days

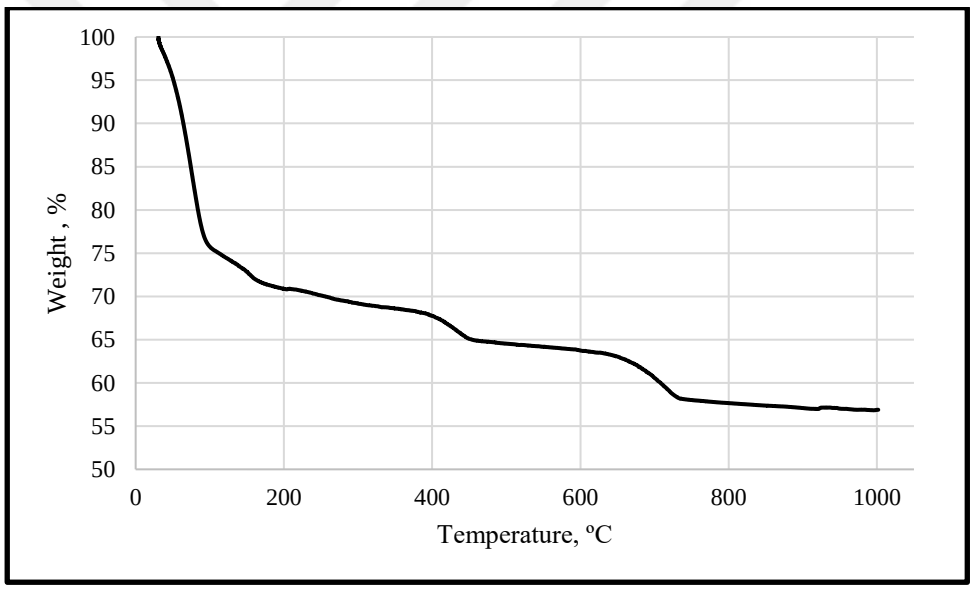

Figure B.38 TGA plot of lime-CC1 700 ºC-limestone powder (20%) paste at 3 days

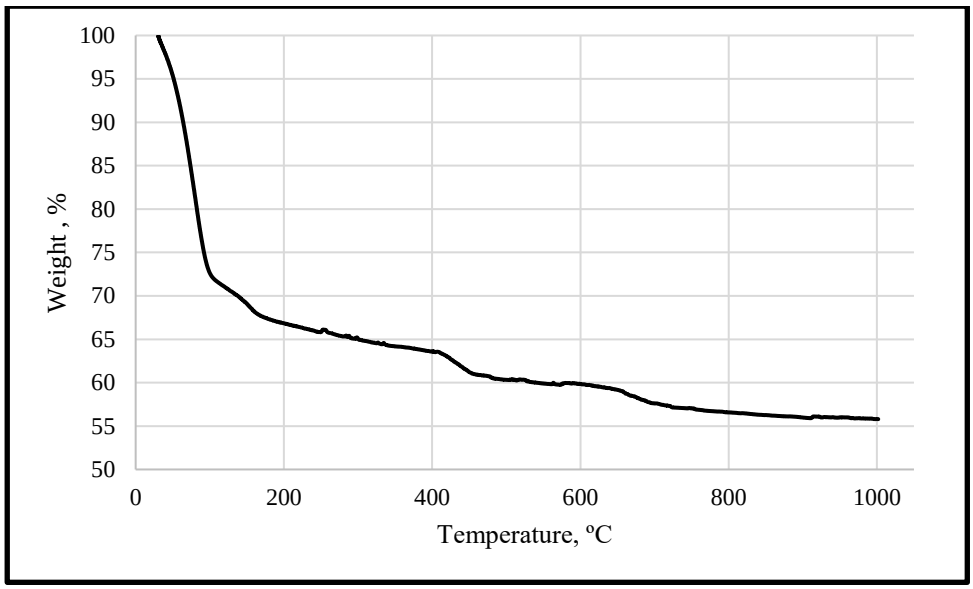

Figure B.39 TGA plot of lime-CC1 700 ºC-limestone powder paste at 7 days

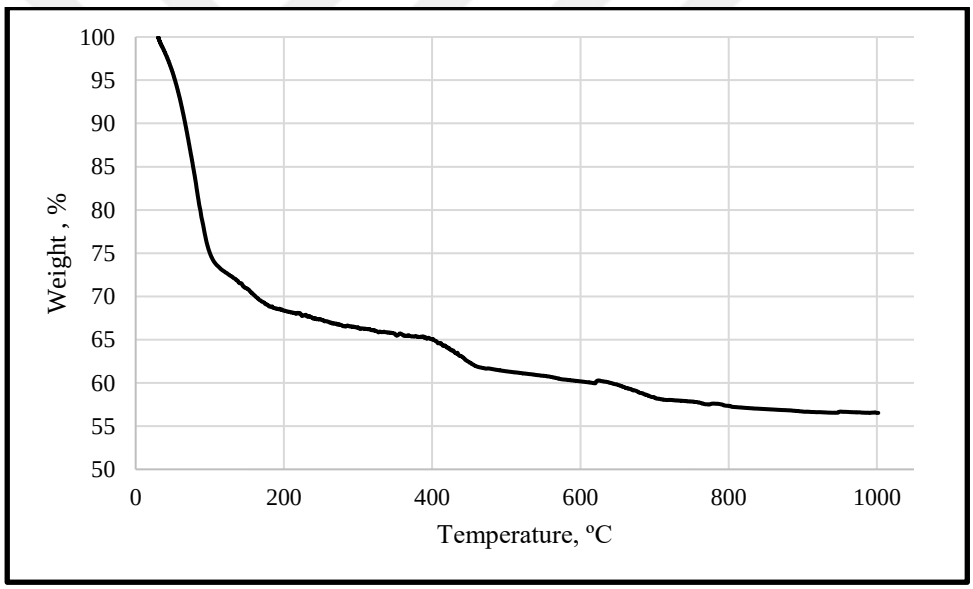

Figure B.40 TGA plot of lime-CC1 700 ºC-limestone powder paste at 28 days

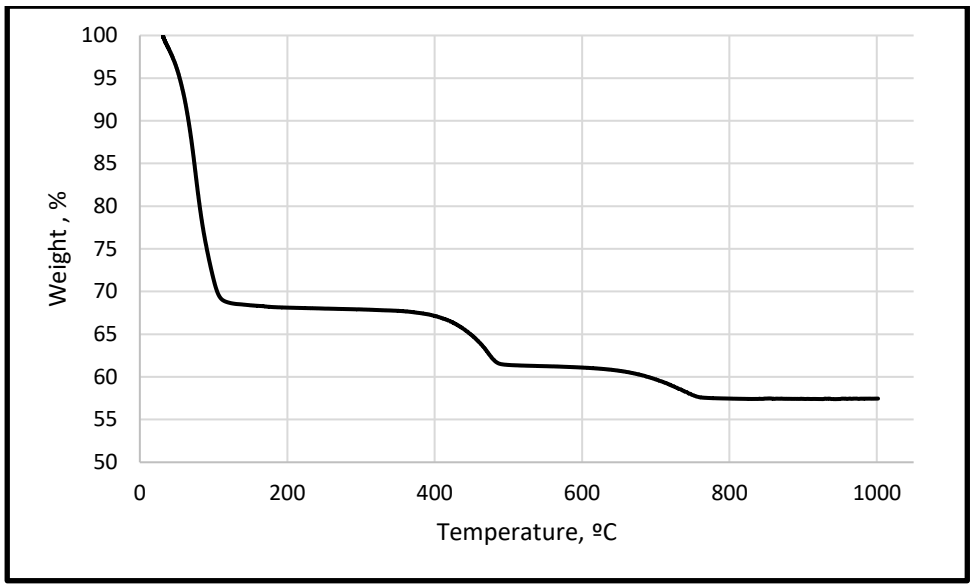

Figure B.41 TGA plot of lime-CC1 1150 ºC-limestone powder paste at 3 days

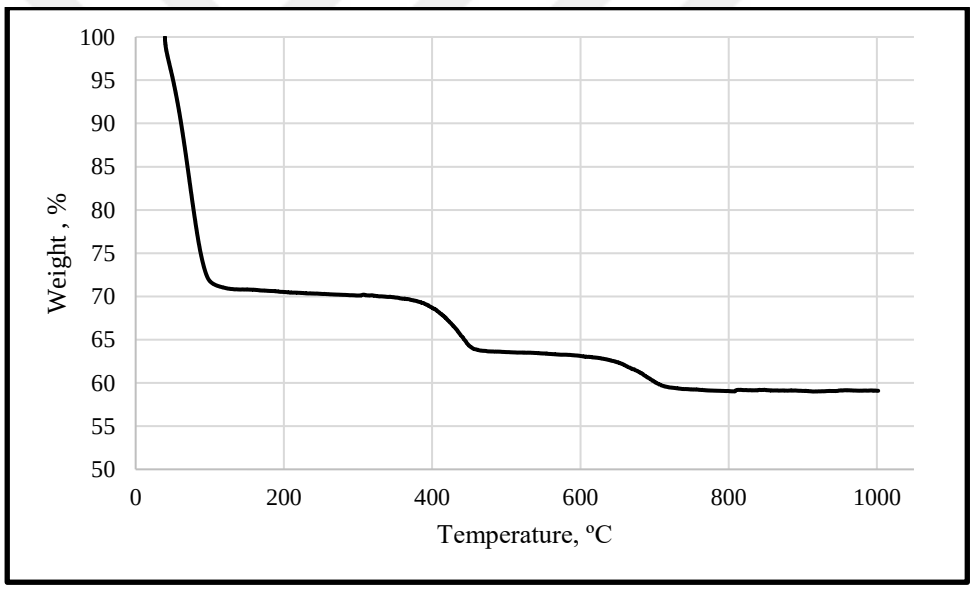

Figure B.42 TGA plot of lime-CC1 1150 ºC-limestone powder paste at 7 days

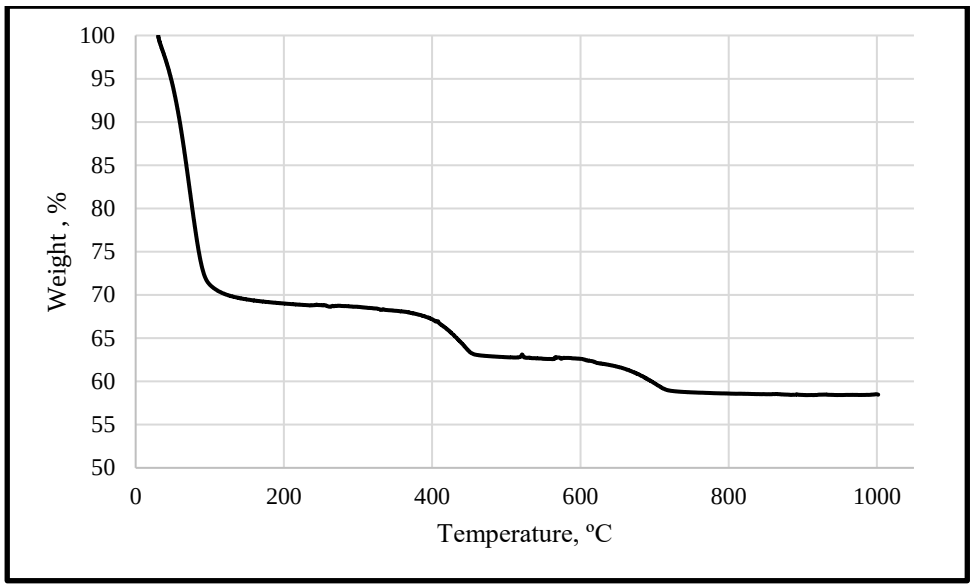

Figure B.43 TGA plot of lime-CC1 1150 ºC-limestone powder paste at 28 days

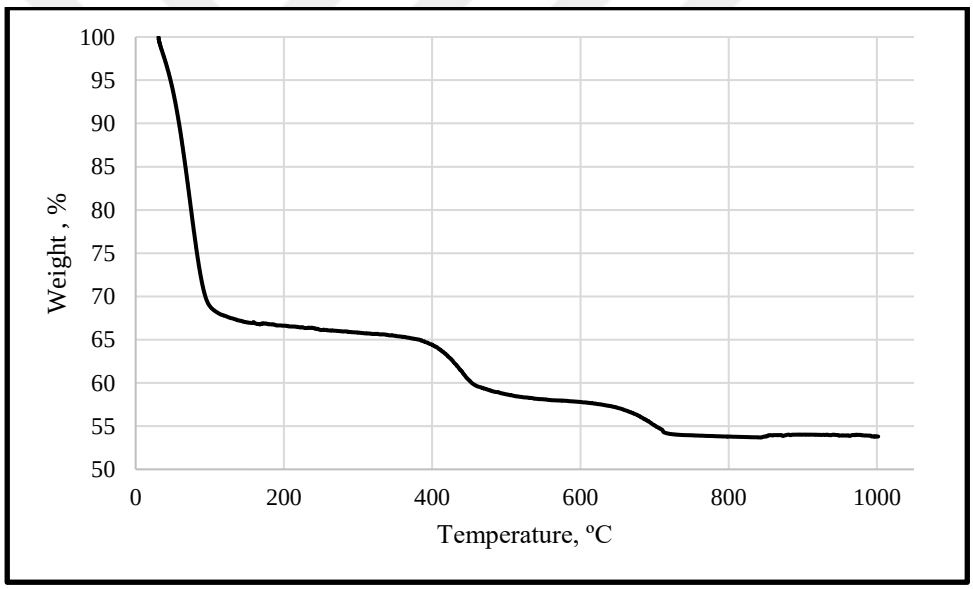

Figure B.44 TGA plot of lime-CC2 raw-limestone powder paste at 3 days

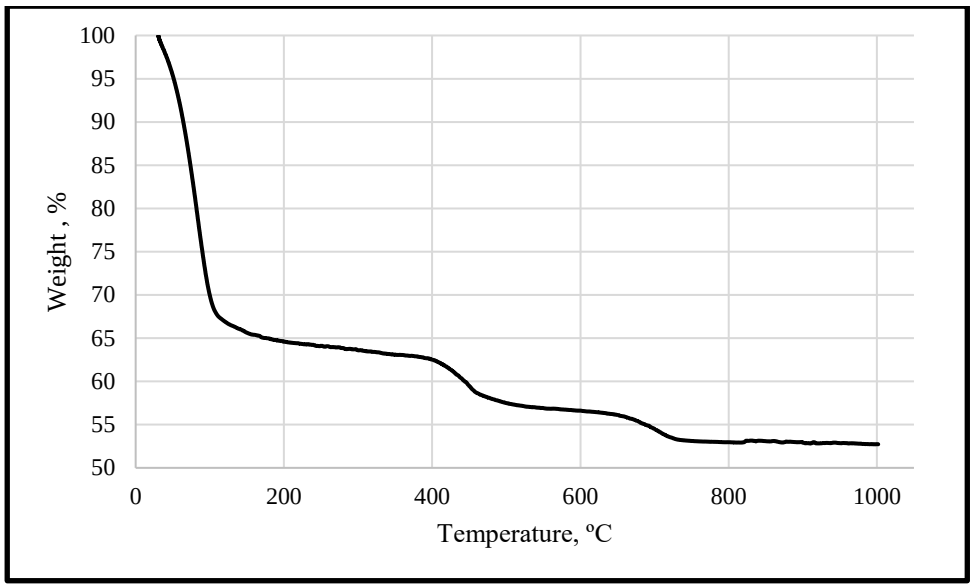

Figure B.45 TGA plot of lime-CC2 raw-limestone powder paste at 7 days

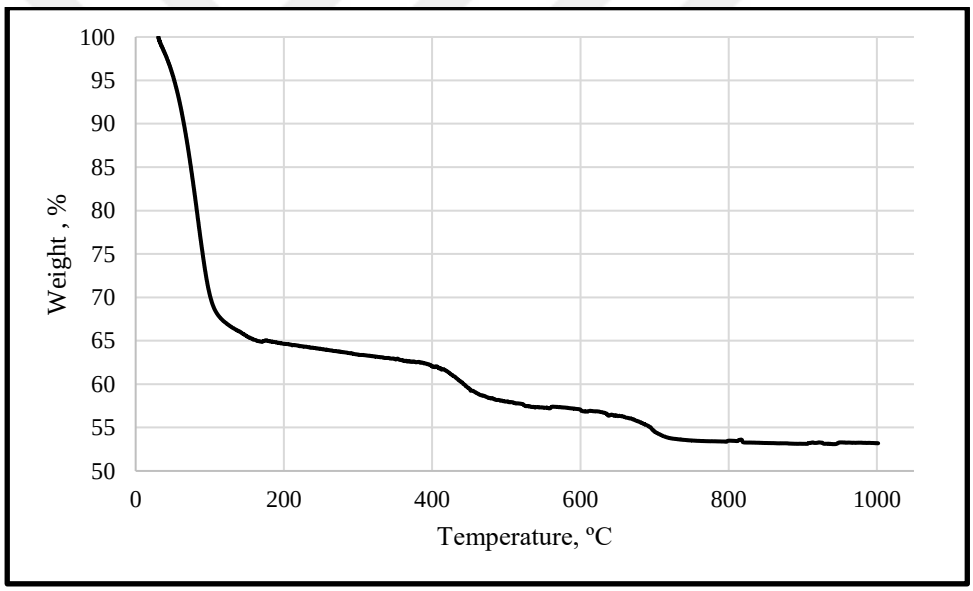

Figure B.46 TGA plot of lime-CC2 raw-limestone powder paste at 28 days

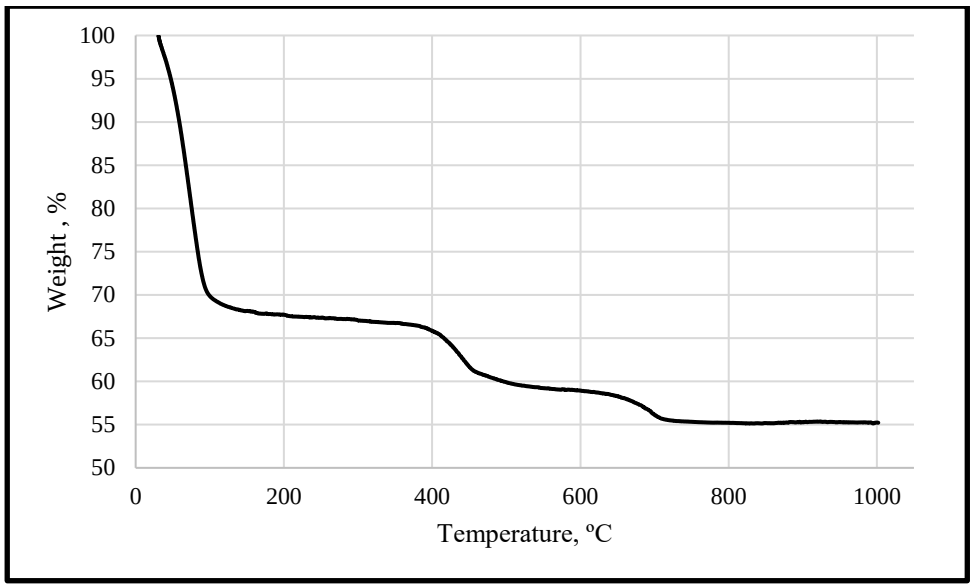

Figure B.47 TGA plot of lime-CC2 400 ºC-limestone powder paste at 3 days

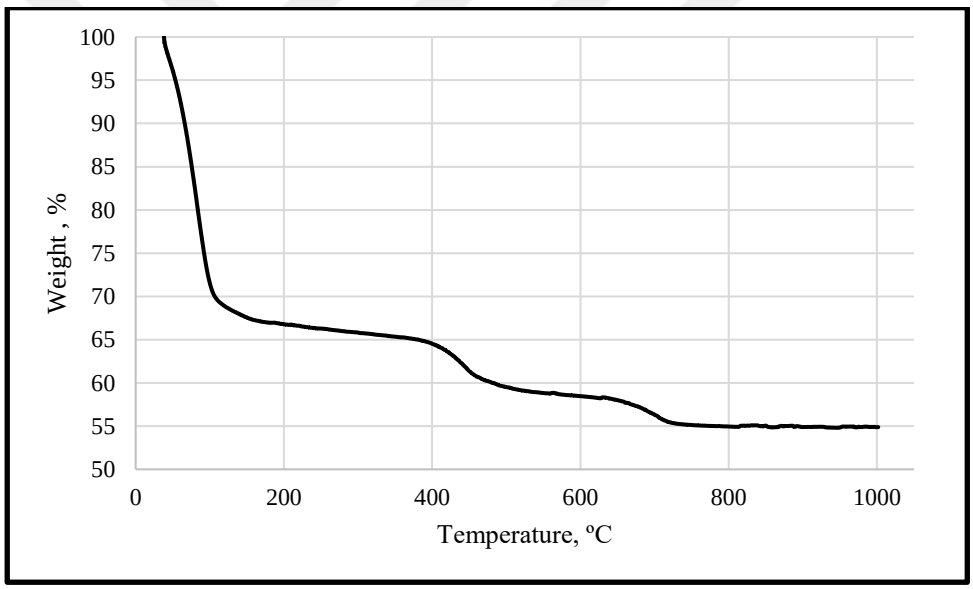

Figure B.48 TGA plot of lime-CC2 400 ºC-limestone powder paste at 7 days

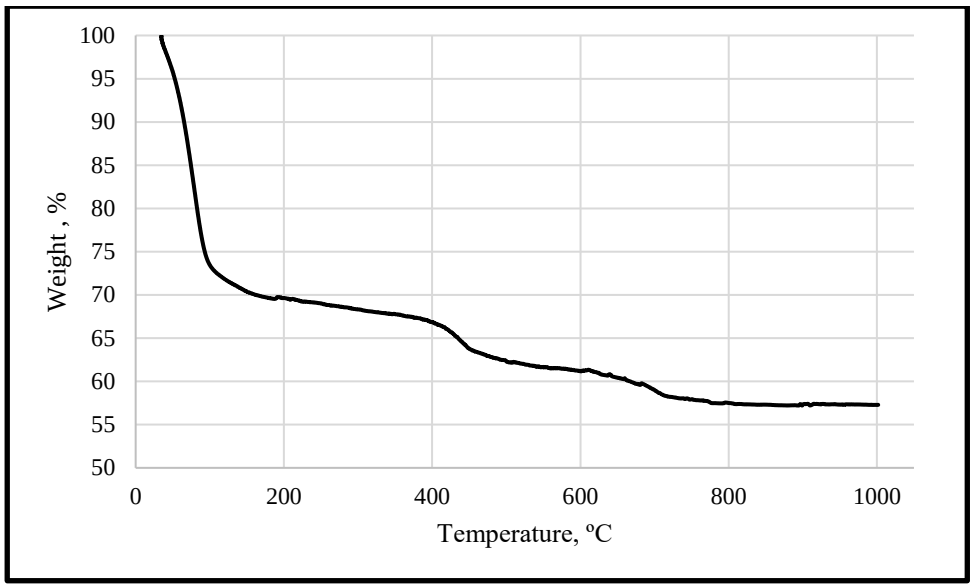

Figure B.49 TGA plot of lime-CC2 400 ºC-limestone powder paste at 28 days

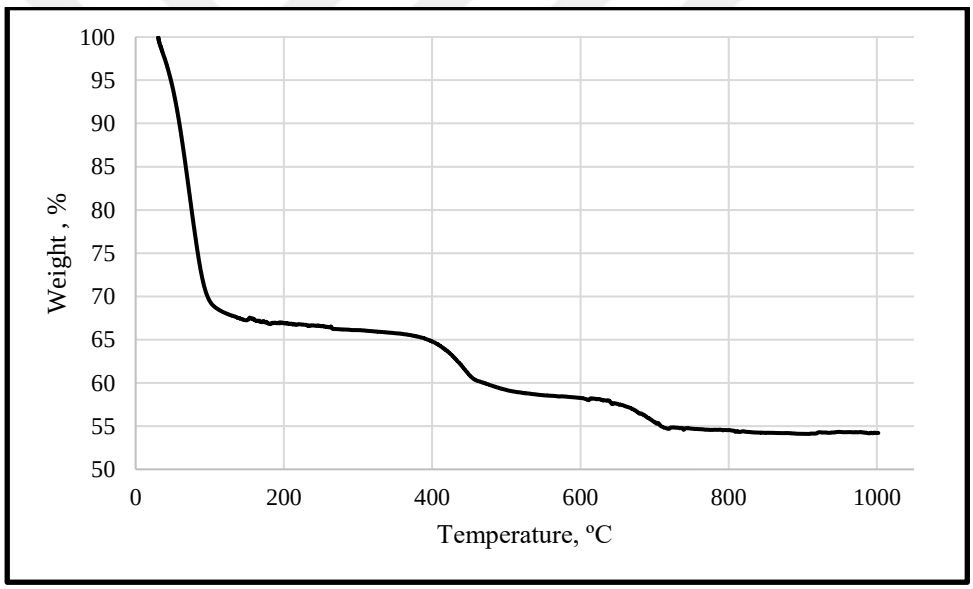

Figure B.50 TGA plot of lime-CC2 520 ºC-limestone powder paste at 3 days

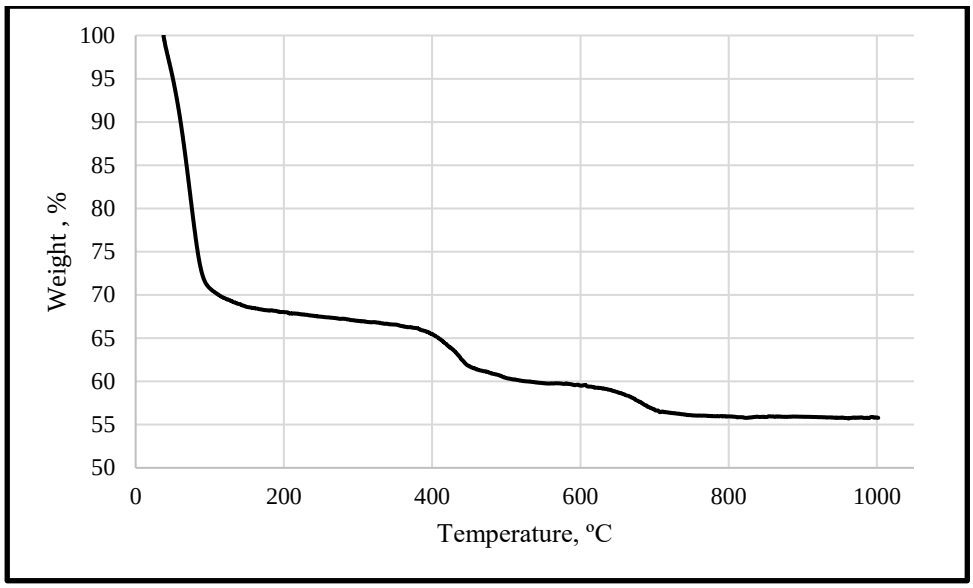

Figure B.51 TGA plot of lime-CC2 520 ºC-limestone powder paste at 7 days

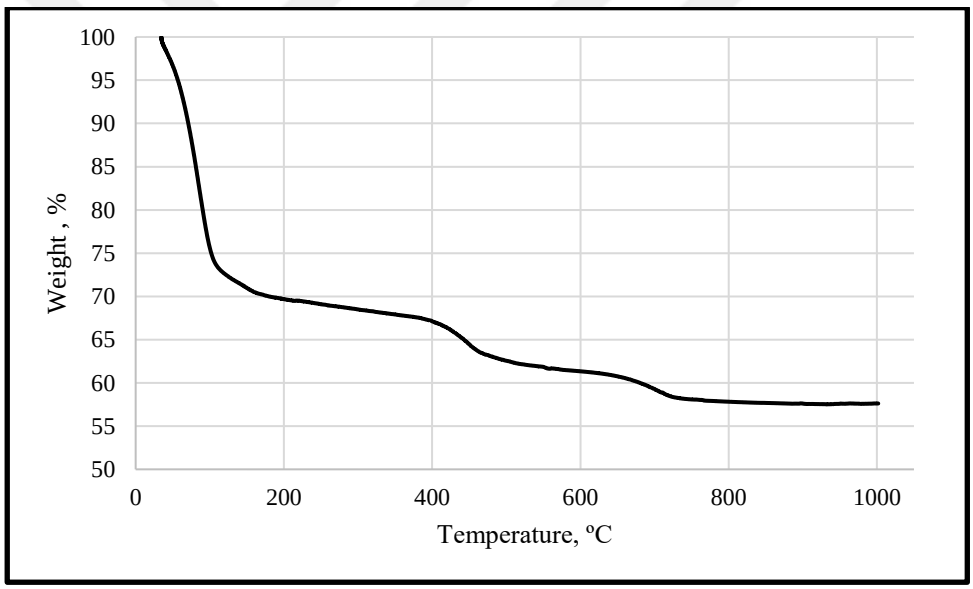

Figure B.52 TGA plot of lime-CC2 520 ºC-limestone powder paste at 28 days

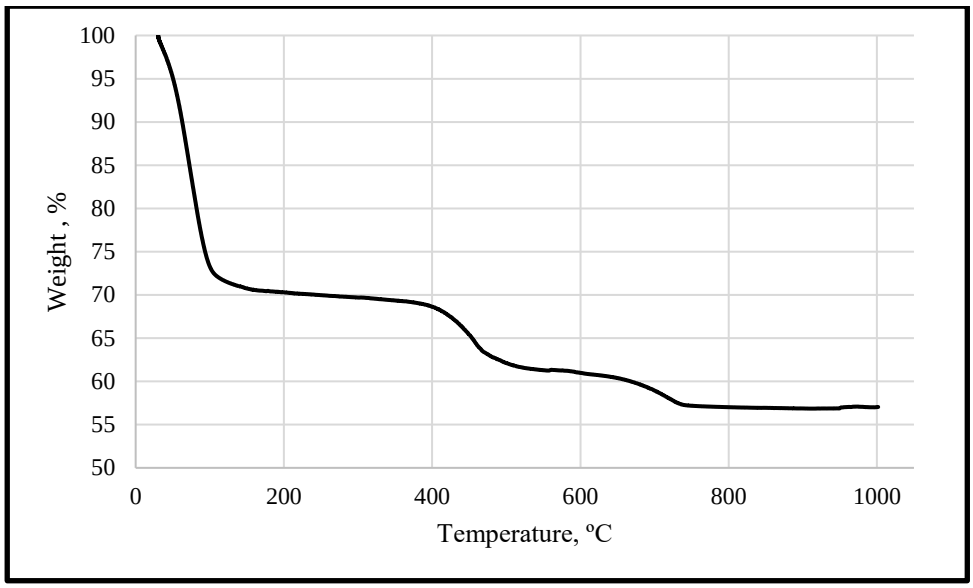

Figure B.53 TGA plot of lime-CC2 700 ºC-limestone powder paste at 3 days

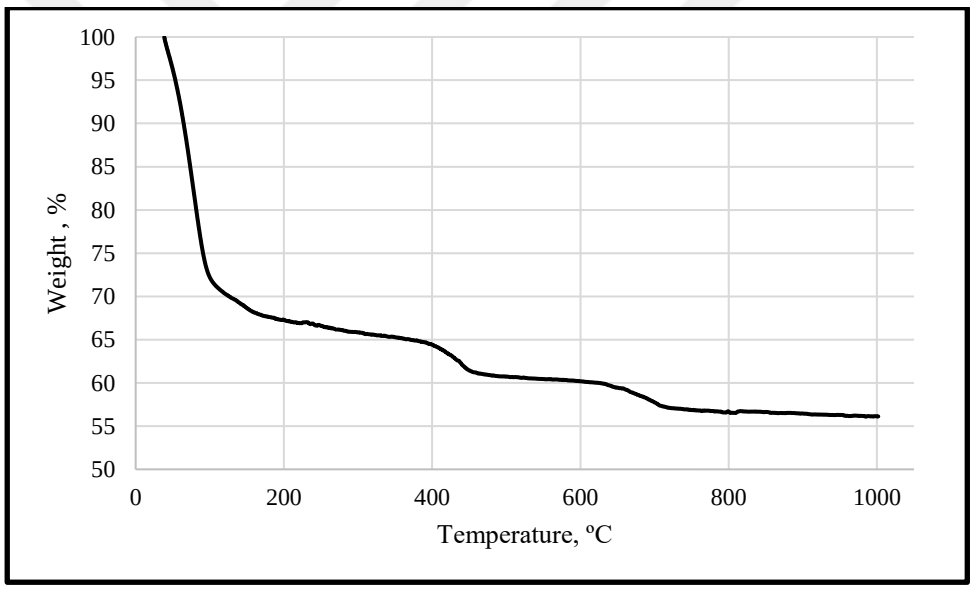

Figure B.54 TGA plot of lime-CC2 700 ºC-limestone powder paste at 7 days

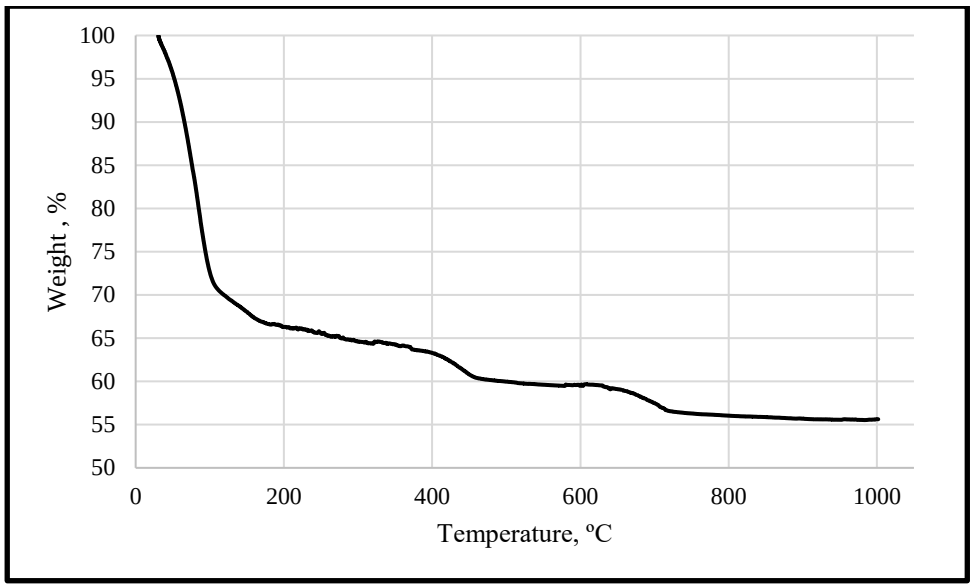

Figure B.55 TGA plot of lime-CC2 700 ºC-limestone powder paste at 28 days